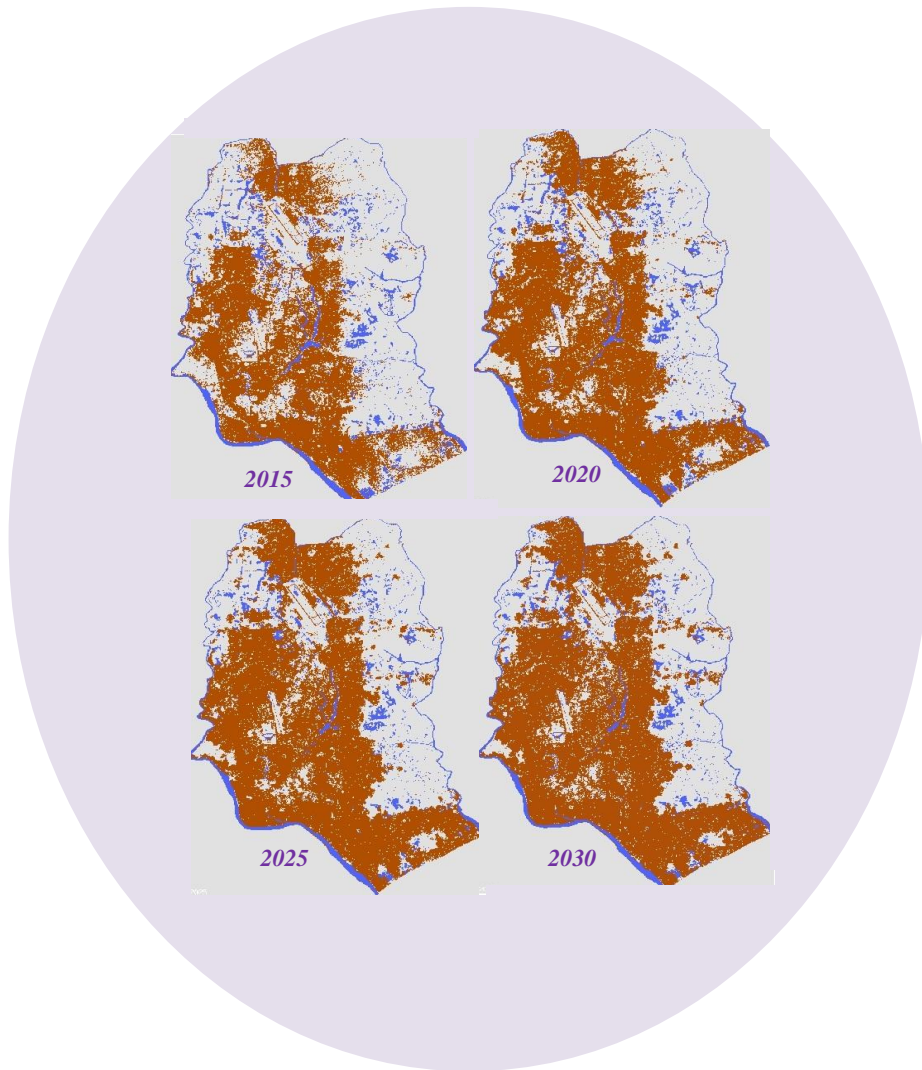**UNIVERSITY OF THESSALY**
FACULTY OF ENGINEERING
DEPARTMENT OF PLANNING AND REGIONAL DEVELOPMENT

<u>PhD Thesis</u>

Forecasting Urban Sprawl in Dhaka city of Bangladesh

2015 *2020*

2025 *2030*

By

Md. Monjure Alam Pramanik
Department of Planning and Regional Development
University of Thessaly

VOLOS, 2015

CERTIFICATE

The thesis titled "**Forecasting Urban Sprawl in Dhaka city of Bangladesh**"
submitted by Md. Monjure Alam Pramanik,
has been accepted as satisfactory in partial fulfillment of the requirement of the
degree of PhD in Planning and Regional Development 0f University of Thessaly.

BOARD OF EXAMINERS

1.   --------------------------------
   Dimitris Stathakis   Supervisor
   Assistant Professor
   Department of Planning and Regional Development
   University of Thessaly, Volos 38834.

2.   ----------------------------------
   Konstantinos Perakis   Member
   Professor
   Department of Planning and Regional Development
   University of Thessaly, Volos 38834.

3.   ------------------------------
   Elias Beriatos   Member
   Professor
   Department of Planning and Regional Development
   University of Thessaly, Volos 38834.

4.   --------------------------------
   Dimitrios Economou   Member
   Professor
   Department of Planning and Regional Development
   University of Thessaly, Volos 38834.

5.   --------------------------------
   Marie Noelle Duquenne   Member
   Associate Professor
   Department of Planning and Regional Development
   University of Thessaly, Volos 38834.

6.   ----------------------------------
   Vassilis Tselios
   Assistant Professor   Member
   Department of Planning and Regional Development
   University of Thessaly, Volos 38834.

7.   --------------------------------
   Christos Chalkias   External
   Associate Professor   Member
   Geographic Information Systems and Applied Geography
   Harokopio University, Athens.

CANDIDATE'S DECLARATION

It is hereby declared that neither this thesis nor any part of it has been submitted elsewhere for the award of any degree or diploma

----
Md.Monjure Alam Pramanik

Executive Summary

Dhaka, the capital of Bangladesh, is expected to be one of the five largest cities of the world by 2020 in terms of population. The rapid urban growth experienced in the city in the recent decades is one of the highest in the world. Urban expansion of Dhaka was slow in the 1950s, but strong growth followed the independence of Bangladesh in 1971. To understand Dhaka city growth dynamics and to forecast its future expansion by the year 2030, a self-modifying cellular automated Slope, Land use, Exclusion, Urban extension, Transportation and Hill shade - model (SLEUTH) has been used in this research using satellite images from 1989 to 2014. This model showed two interesting findings: (a) approximately an additional 20% of the metropolitan area will be converted into built-up land by 2030 (b) it will expand towards north and north-west direction in the future. The interpretation of depicting the future scenario as demonstrated in this research will be of great value to urban planners and decision makers, for the future planning of Dhaka.

Keywords: urban expansion; SLEUTH model; model calibration; growth prediction.

Σύντομη περίληψη

Η Ντάκα, η πρωτεύουσα του Μπαγκλαντές, αναμένεται να είναι μία από τις πέντε μεγαλύτερες πόλεις του κόσμου ως το 2020 σε πληθυσμό. Η ραγδαία αστική ανάπτυξη που βιώνει η πόλη τις τελευταίες δεκαετίες είναι από τις υψηλότερες στον κόσμο. Η αστική επέκταση της Ντάκα ήταν αργή στη δεκαετία του 1950, αλλά ισχυρή ανάπτυξη ακολούθησε την ανεξαρτησία του Μπαγκλαντές το 1971. Για να κατανοήσουμε τη δυναμική της ανάπτυξης της Ντάκα και να προβλέψουμε τη μελλοντική επέκτασή της μέχρι το έτος 2030, χρησιμοποιήθηκε το αυτοματοποιημένο μοντέλο πρόβλεψης SLEUTH (Slope, Land use, Exclusion, Urban extension, Transportation and Hill shade), αξιοποιώντας παράλληλα δορυφορικές εικόνες από το 1989 έως το 2014. Τα αποτελέσματα του μοντέλου μπορούν να συνοψιστούν ως εξής: (α) περίπου ένα επιπλέον 20% της μητροπολιτικής περιοχής θα μετατραπεί σε δομημένη περιοχή έως το 2030 και (β) η επέκταση θα λάβει χώρα σε βόρεια και βόρειο-δυτική κατεύθυνση. Τα εν λόγω αποτελέσματα, όπως αποδεικνύονται στην παρούσα έρευνα, θα αποτελέσουν χρήσιμη πληροφορία για τους πολεοδόμους και τους διαφόρους φορείς λήψης αποφάσεων που σχετίζονται με το μελλοντικό σχεδιασμό της Ντάκα.

Λέξεις-κλειδιά: αστική εξάπλωση, μοντέλο SLEUTH, βαθμονόμηση, πρόβλεψη ανάπτυξης.

Table of Contents

ii

iii

List of Tables

List of Figures

iv

Abbreviations and Acronyms

ANN	Artificial Neural Network
BBS	Bangladesh Bureau of Statistics
CA	Cellular Automata
DCC	Dhaka City Corporation
DEM	Digital Elevation Model
ETM+	Enhanced Thematic Mapper Plus (LANSDSAT'S sensor)
FAP	Flood Action Plan

v

GIF	Graphics Interchange Format
GIS	Geographic Information System
MT	Motorized Transport
NMT	Non Motorized Transport
SLEUTH	**S**lope **L**and **E**xcluded area **U**rban **T**ransportation **H**illshade
SRTM	Spatial Radar Topographic Mission
TM	Thematic Mapper (LANDSAT'S sensor)
USGS	United States Geological Survey

Acknowledgements

At the outset, all praises belong to the almighty 'Allah', the most merciful, the most beneficent to all the creatures and their dealings.

Finally, I would like to express my gratitude to my family members for their unaccountable tolerance, supports and encouragements all the way towards completing this research.

viii

Chapter 1: Introduction

1.1 Background of the research

Urban areas are the most dynamic regions on earth. Their size has been constantly increased during the past and this process will go on in the future. Especially in less developed countries a strong trend towards concentration of people in urban areas can be observed (Moeller, 2005). Monitoring urban growth and accordingly anticipating urban extent is always recognized as a dynamic issue for any urban planning decision making procedure. In the past 200 years, the world population has increased six times and the urban population has multiplied 100 times (Stalker, 2000).

Two centuries ago there were only two cities with a million inhabitants, London and Beijing (Desai and Potter, 2002). However, more than 293 cities have reached such population amounts within the developing world. The growth rate of these cities counted tenfold between 1950 and 1990. Cohen (2006), states that 50% of world population is now living in the cities, whereas it was only 3% in 1800. UN population division also forecast that by 2050, urban inhabitants will raise to 6.3 billion which is now counted to 3.2 billion.

Figure 1. The increase trend of urban population worldwide from 1950 to 2050
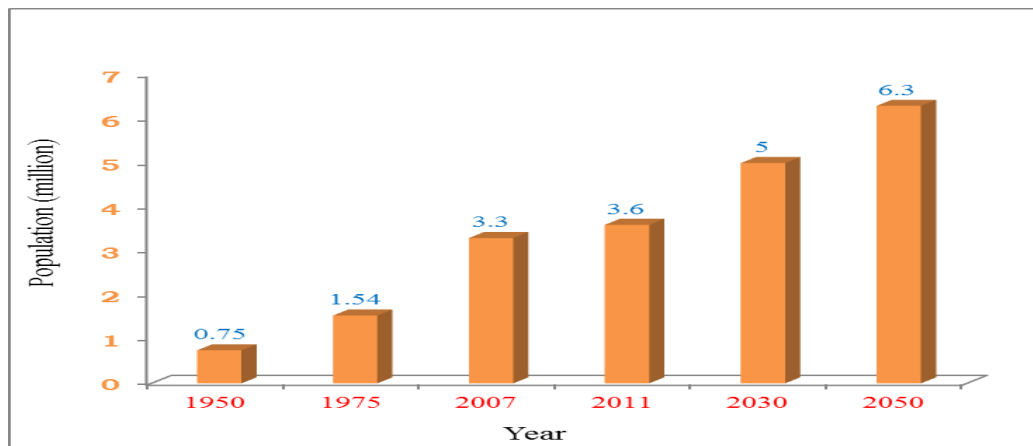
Source: World Urbanization Prospects: the 2014 Revision, United Nations

Figure 1 shows the increasing trend of urban population in all regions of the world from 1950 to 2050. Due to the increase in world population and the progressive departure of national economies from merely agricultural systems, cities have been undergoing a rapid and often uncontrolled growth. So, now urbanization is one of the most common

1

anthropogenic causes of the arable land loss, the destruction of habitats and the decline of natural vegetation cover. In the last few decades, land use/cover conversion, due to human activities, occurred more rapidly in developing countries than in the industrialized world. Modern technological revolution within developing nations already has taken place with lots of opportunities, but at the same time, developing nation decreases living conditions of urban inhabitants with all sorts of environmental degradation which directly impacted on sustainability and life of urban quality (Rana, 2010). So, rapid urbanization is now becoming a threat to the environment and sustainable development on a global level. Environmental degradation and booming populations in these cities are the burning issues of the present world in case of urbanization. In most of the developing countries, the respective governments fail to provide basic needs to inhabitants in the cities due to rapid growth of urban population and poverty.

Like other developing countries, Bangladesh has experienced rapid urbanization and Dhaka, the capital of Bangladesh, is also the outcome of spontaneous rapid growth. Presently, Dhaka is the 8th largest city in the world in terms of population. Its population exceeds approximately 15 million.

Figure 2. Growth of Dhaka city in terms of Population from 1950 to 2025

Source: World Urbanization Prospects: the 2014 Revision, United Nations

2
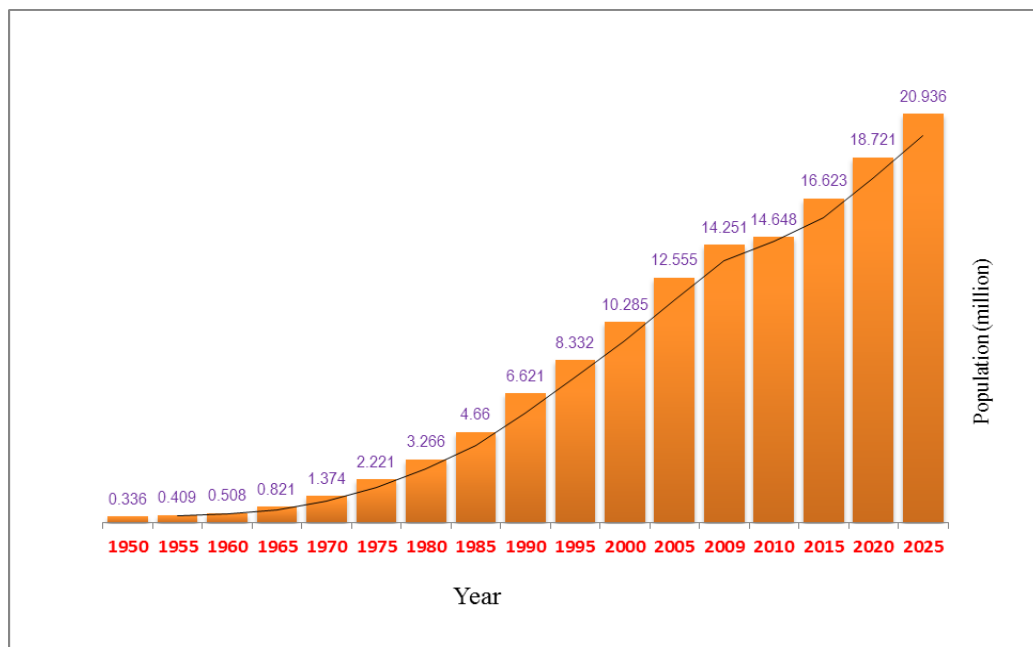
If this trend continues, it will be the 3rd largest city of the world by 2025 and the population will be more than 20 million (World Bank, 2007a) as shown in figure 2. On the other hand, in the process of urbanization, the physical characteristics of Dhaka city are gradually changing, as plots and open spaces have been transformed into built up areas, open squares into car parks, low land and water bodies into reclaimed built-up lands, *etc*. Dhaka is now attracting a significant amount of rural-urban migrants from all over the country due to better job opportunities, better educational, health and other daily life facilities (Islam, 1999). This kind of increasing and over population pressure is putting adverse impacts on Dhaka city, like unplanned urbanization, extensive urban poverty, water logging, growth of urban slums and squatters, traffic jams, environmental pollution and other socio-economic problems (World Bank, 2007a). If this situation continues, Dhaka might soon become an urban slum with degraded living standards for the city dwellers.

Thus, it is very important to project the future scenario of urban growth of Dhaka in order to understand how the city can expand. This may help the planners to carry out their planning more efficiently based on computer simulation methods in addition to their expertise.

In this case, land cover and land use change models are useful tools to analyze, understand and predict land cover changes and their consequences. Using these models, policy makers can analyze different scenarios of land use and land cover change and evaluate their effects, so models can support land use planning and policy (Veldkamp and Lambin, 2001).

A number of analytical and static urban models has been developed to explain urban expansion and evolving patterns rather than to predict future urban development. At present there is a significant number of urban models developed worldwide based on different theoretical underpinnings. Among them artificial neural networks (Pijanowski *et al.,* 2002; Stathakis and Vasilakos, 2006; Stathakis, 2009), statistical models (Cheng and Masser, 2003), multi-agent models (Benenson, 1998), fractal models (Batty *et al.,* 1989), UrbanSim (Waddell, 2002) cellular automata (Clarke *et al.,* 1997) are mentionable. They vary a lot in terms of their complexities, data requirements, spatial resolutions and temporal resolutions. It can be said that there is currently resurgence in urban modeling, primarily because new methods and data have made computer-based models functional

and useful tools for urban planning. This growth has been driven by two major factors: improved representation and modeling of urban dynamics; and increased richness of information in the form of multiple spatial data sets and tools for their processing (Herold *et al.*, 2003). Enhancements in the field of Geographic Information Science and Remote Sensing have now enabled this process to be more robust and effective.

Developing countries are lagging far behind in this case where unplanned urbanization and rapid growth of the cities are going on without any comprehensive decision making process. Applications of urban growth or land use change models are very limited in these cities primarily due to lack of resources and lack of detailed historical land use or socio-economic data. Poor documentation of historical data and lack of a unique mapping procedure is a common scenario in most of the developing countries.

Considering these constraints, a self-modifying cellular automated Slope, Land use, Exclusion, Urban extension, Transportation and Hill shade - model (SLEUTH) developed under project Gigalopolis of United States Geological Survey (USGS) has good potentiality to be transferred to developing countries. Among all the documented dynamic models, those based on Cellular Automata (CA) are probably the most impressive in terms of their technological evolution in connection to urban applications.

The study focus here is not the creation of a new model, but understanding and exploration of an existing dynamic model for problem solving in applied urban studies. This is built upon a self-modifying CA urban growth model namely SLEUTH originally developed by Keith Clarke at the University of California at Santa Barbara. Goldstein (2004) examines SLEUTH's main properties, which cause to be chosen by researchers. It runs with a series of growth rules that can modify the form of the growth. This study has monitored the urban growth of Dhaka City by remote sensing and also predicted the urban growth in a Cellular Automata (CA) based environment.

1.2 Objectives of the Study

The aim of this study is to evaluate the usefulness of urban prediction model. Specific objectives of this study can be specified as below:

1. Acclimate the SLEUTH Urban Growth Model for Dhaka city and its surroundings.

2. Simulate urban growth dynamics of the area using CA-based urban growth model.

3. Forecast urban sprawl of Dhaka city by the year 2030.

1.3 Scope of the Study

Worldwide already significant research has been done in the field of urban growth modeling based on different theories and techniques. But this kind of exercise is yet to be conducted in Bangladesh and very few examples are there from other developing countries. From this perspective, the present study has got a reduce tone to harness the theoretical and technical capabilities developed worldwide. The scopes of this study encircle around the simulation of the historical urban growth pattern of Dhaka Metropolitan Area. It is evaluated to what extent the urban growth pattern of the study area can be simulated in a Cellular Automata (CA) environment. Future growth scenarios for different planning contexts are also predicted here to identify their influences on the overall growth pattern of the study area.

1.4 Outline of the Dissertation

This thesis is divided into five sections, additional to these introductory remarks and the concluding chapter. The second chapter summarizes the theory and background of CA models applied to urban studies, with particular emphasis on the state of the automata, as well as other issues theoretically relevant to the modeling. The third chapter describes the study area, in terms of its extent and physical expansion and the input data of the model. It also summarizes the design of the model, as well as the calibration and prediction processes. Chapter four shows a discussion on the substantive results derived from model. Finally, a concluding section synthesizes the overall recommendations on the basis of output on the model.

A series of appendices provide an expanded view over specific technical issues. *Appendix A* shows the application of SLEUTH model in international cities of the world. *Appendix B* includes the snapshot of activities that will be affected for the future urban sprawl in Dhaka city. *Appendix C* comprises the picture of the existing traffic problem of Dhaka city because of rapid urbanization. *Appendix D* documents installation instructions of the SLEUTH model and *Appendix E* comprises the source codes that were used in coarse, fine and final calibration of the model.

Chapter 2: Urban Growth and Modeling

2.1 Introduction

In the field of urban planning, one of the important subjects of concern is to predict the trend of land use transition (Osaragi and Kurisaki, 2000). However, prediction without a scientific understanding of the system under study implies a degree of uncertainty due to the numerous unknown factors involved. Significant research on urban growth modeling and simulation has already been conducted worldwide. This chapter will demonstrate how the concept of urban dynamics has evolved and what approaches have been used to achieve better simulation and modeling. This chapter addresses some modeling and simulation principles. It also traces the origin and formulation of spatial models in urban studies. Later in this chapter, a clear illustration of the present time most convenient model cellular automata model is discussed elaborately.

2.2 Urban Growth Concept

Batty *et al*. (1999) believe complexity is the basic characteristic of urban systems. Many components act on each other within the city, land use, transportation, culture, population, policies, and economics. The relationships between each other are neither clear nor linear. Urban growth indicates a transformation of the vacant land or natural environment to construction of urban fabrics including residential, industrial and infrastructure development. It mostly happens in the fringe urban areas (Shenghe and Sylvia, 2002). This process can be regarded as the spatial representation of the economic structural shift of labour away from agricultural to industrial-based activities. Crucial to this shift are the output gains associated with resource transfers from the low-productivity agricultural sector to the high productivity industrial sector (Kam, 1994). From systematic view, urban growth may be divided into spontaneous and self-organization process (Wu, 2000). Spontaneous growth results in a homogeneous and sparse spatial pattern, which contains more random components, whereas self-organizational growth result in spatial agglomeration pattern, which is combined with more socio-economic activities (Cheng, 2003). Urban development consists of physical expansion and functional changes. The former refers to the change in space (transition from non-built-up to urban), the latter to the change in major activities (land uses). As a result, space and activity should be the basic

elements of any systems defined for understanding urban growth. Figure 3 tries to simplify the urban development process and locate the urban growth sub-process within this system.

Figure 3. Urban development processes
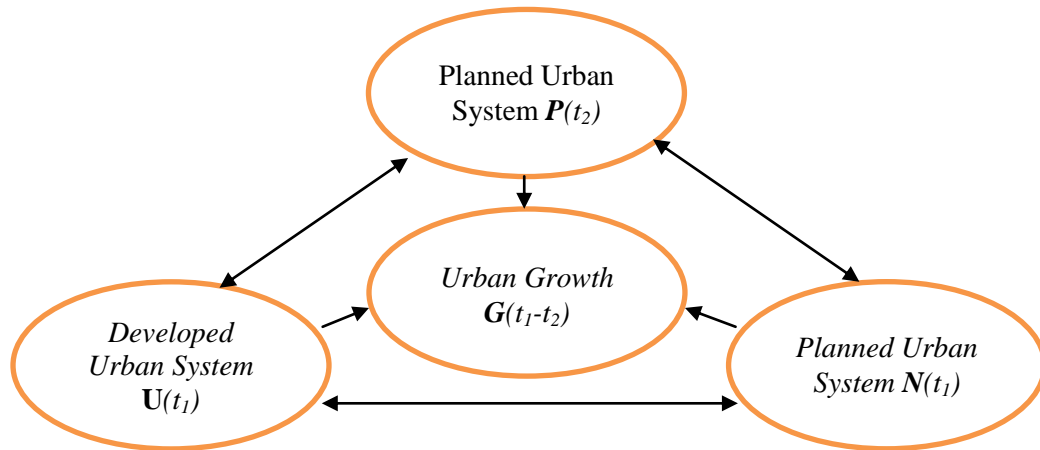
Source: Cheng, 2003

According to Cheng (2003), it is assumed that urban growth occurs in a specific period from time (t1) to (t2); apparently the evolution of urban growth is closely related to three systems (P), (U) and (N). (U) itself is a highly complex social and economic system, as the concentration of considerable urban activities present at time (t_1) shows. It offers current activities rather than space for urban growth to come. (N) is a typical physical and ecological system, including various ecological units (water body, deserts etc.) and agricultural land. It primarily provides possible opportunities and potential for urban growth in space instead of activities, until time (t_2). (P) is a spatial and conceptual system that results from a spatial planning scheme. It prepares organized space and activities for urban growth in the future. Under such an assumption, urban growth (G) can be defined as a system resulting from the complex dynamic interactions (only from t_1 to t_2) between the three systems (P, U and N). The thin arrows in figure 3 refer to the interaction between the three systems, and the thick arrows to the contributions to urban growth made by the three systems. System (P) contributes planning control and requirements to (G); system (N) contributes developable land, and system (U) contributes activities and stimulant factors to the growth of (G). A key to understanding urban growth is to understand the complex dynamic interactions. It may be assumed that the interaction is open, non-linear, dynamic and emergent.

2.3 Urban Growth Patterns

Patterns of urban morphological changes contemporary urbanization trends are quite likely the most significant since railroads and automobiles turned world cities inside out in the early twentieth century. Indeed, the resultant patterns from these trends differ significantly between the developed and developing countries according to varying factors, such as demographics, level of economic development and political structure. Yet, there are also many significant similarities among the underlying dynamics that shape these patterns (Perlman, 1990; Myllyla, 2001). Among the various factors that both derive from and are profoundly affected by these dynamics is the evolving urban spatial structure within which they operate (Knox, 1995; Cadwallader, 1996; Haack *et al.*, 1997; Clarke and Couclelis, 1999; Collins *et al.*, 2000). Therefore, an understanding of how urban morphological patterns change over time and space is critical to the understanding of a host of socioeconomic, natural and technological phenomena associated with the contemporary trends of urbanization (Batty and Longley, 1994).

In a study of the post-war growth era of British cities, Smailes (1966) identified two fundamental patterns of urban morphological change that seem to remain suitable for characterizing contemporary morphological change in urban areas, namely: *outward extension* and *internal reorganization or modification* (e.g. densification). The former refers to the spatial extent of a city's growth, resulting from such processes, as urban sprawl onto agricultural lands and wild habitats, and the expansion of residential land use at the urban fringe. The latter refers to the internal modifications that happen to the urban fabric as some of its existing elements deteriorate and new ones are introduced (Knox, 1995). In large cities, particularly in developing countries, the pace of internal morphological change tends to be much slower in comparison to the rapid change resulting from the outward extension of the city (Perlman, 1990; Knox, 1995; Bayat and Denis, 2000; Myllyla, 2001). Using Cairo as an example, Malik (1989) showed how the old city, previously inhabited by influential citizens, has now been left with a marginal economic and political influence, as those who could afford to move out have done so (Malik, 1989). What this indicates is that ongoing processes of urbanization make a context of change in which socioeconomic and demographic forces continuously interact with the urban fabric. Hence, the importance of such approaches adopted in this research is not only for describing the physical nature of urban change, but also for providing measures regarding

the rate and magnitude of that change, which can be utilized further in the study of urban growth phenomena.

2.4 Urban growth and urban sprawl

Urban sprawl and urban growth are not synonyms (Stathakis and Tsilimigkas, 2014). Urban sprawl is a type of urban growth but not the only one. Specifically, urban sprawl is a type of excessive and unplanned urban growth (Razin and Rosentraub, 2000). Sprawl is a non-compact, low-density development urban form, often exhibiting scattered, leapfrog, strip or ribbon structure, resulting in poor travel patterns (Ewing, 1994; Wassmer, 2000). Sprawl can take the form of single-use bedroom communities (Schneider and Woodcock, 2008). It can also take the form of parasitic retail development along the street network and near highway exits, attracted by increased accessibility (Torrens, 2008). A key observation is that the linkage between different land uses is poor due to excessive segregation (Ewing, 1994). Moreover, because sprawl is a process in time, it is sometimes described as a temporary condition (Frenkel and Ashkenazi, 2008). But this can only be true if suburbanization occurs within planned areas. Otherwise, unplanned sprawl has the further side effect of undermining future planning by establishing an irreversible status quo. In that case, sprawl might as well be a temporary condition but in the wrong direction (Stathakis and Tsilimigkas, 2014). Most but not all scientists agree that sprawl should be curtailed. Some question that compactness is either desirable or feasible as a goal (Breheny, 1997; Gordon and Richardson, 1997; Neuman, 2005). Recent advances in telecommunications certainly add an additional centrifugal force (Gordon and Richardson, 1997) although their impact might be exaggerated (Ewing, 1997). At the European Unions' policy agenda, however, urban sprawl is clearly considered parasitic (Torrens, 2008) and is explicitly mentioned as a problem. Sprawl in Europe is clearly a significant trend, but is often neglected (CEC 2006a). French cities, for example, have doubled their footprint in just 15 years (Kasanko *et al.*, 2006). However, the rates in different member states are diverse. The variation increased further after the enlargement that took place during the past decade to include several former communist countries in Central and Eastern Europe, with distinctively different planning systems and land markets (Stathakis and Tsilimigkas, 2014).

Sprawl is acknowledged to have several negative impacts in European Unions' territory. It contributes to high and unsustainable energy consumption rates because of increased levels of private transport (CEC, 1999, 2011) and heating demands (CEC, 2006b). Increased

energy demands result in air pollution (Grimm *et al.,* 2008). Chalkias *et al*. (2006) mentioned that the modern way of life in developing countries is conductive to environmental degradation in urban and suburban areas. One specific parameter for this degradation is light pollution due to intense artificial night lighting. On the other hand, Zhang *et al.* (2015) discussed that tranquility disturbance is profound in modern urban areas, suburban and rural areas also face the same problems due to urban growth, intense cultivation activities, transportation network expansion, etc.

Sprawl threatens cultural assets and landscapes and degrades the countryside (CEC, 1999, 2011). It is a land-consumptive pattern (Wilson *et al*., 2003), and soil is a non-renewable resource (CEC, 2006a). By increasing soil-sealing, it results to fragmentation or loss of natural habitats (biotopos) and ecological corridors (CEC, 1999, 2006b, 2011). Increased land consumption is also associated with the loss of prime farmland (high-quality arable land) and results in conflicting land uses (CEC, 1999, 2010). It makes provision of infrastructure and public services more costly (CEC, 1999).

2.4.1 Spatial forms of sprawl

Sprawl development consists of three basic spatial forms: low-density continuous sprawl, ribbon sprawl, and leapfrog development sprawl (Barnes *et al.,* 2001) that will be discussed in the sequel.

2.4.1.1 Low-density sprawl

Low density sprawl is the highly consumptive use of land for urban purposes along the margins of existing metropolitan areas. This type of development is supported by piecemeal extensions of basic urban infrastructures, such as water, sewer, power, and transportation.

Figure 4. Low-density sprawl – ribbon – leapfrog respectively
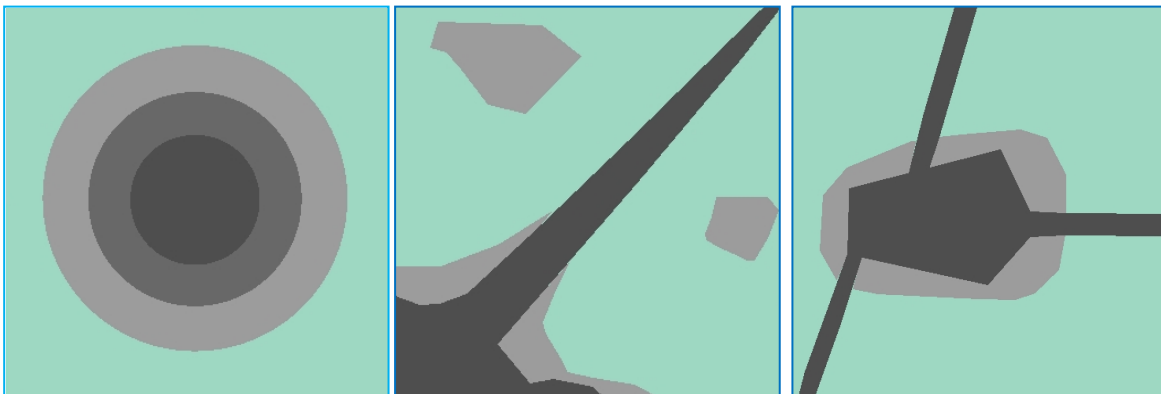
Source: Centre for Geographical Information Sciences (CGIS) at Towson University, 2010

2.4.1.2 Ribbon sprawl

Ribbon sprawl is development that follows major transportation arteries outward from urban cores. Lands adjacent to corridors are developed, but those without direct access remain in rural uses/covers. Over time, these nearby 'raw' lands may be converted to urban uses as land values increase and infrastructure is extended perpendicularly from the major roads and lines (Barnes *et al.,* 2001).

2.4.1.3 Leapfrog development

It is a discontinuous pattern of urbanization, with patches of developed lands that are widely separated from each other and from the boundaries, albeit blurred in some cases, of recognized urbanized areas. Leapfrog development sprawl is caused by various factors. Physical geography, such as rugged terrain, wetlands, mineral lands, or water bodies may preclude continuous development or make it prohibitively expensive. Other factors encouraging leapfrog sprawl are not necessarily physical: restrictive land-use policies in one political jurisdiction may lead development to 'jump' to one that is favorably disposed toward development or is less able to prevent or control it (Barnes *et al.,* 2001).

2.4.2 The role of urban economics in urban growth and sprawl

Usually when population rises in a metropolitan area it becomes increasingly more difficult to locate the same percentage of residential and business activity in its central places whose boundaries remain fixed. In addition, expansion of economic base (such as higher per capita income, increase in number of working persons) creates demand for new housing or more housing space for individuals (Boyce 1963; Giuliano 1989; Bhatta 2009). This also encourages many developers for rapid construction of new houses. Rapid development of housing and other urban infrastructure often produces a variety of discontinuous uncorrelated developments. Establishment of new industries in countryside may sometimes introduce urban sprawl if it is not properly planned. Industry requires providing housing facilities to its workers in a large area that generally becomes larger than the industry itself. The transition process from agricultural to industrial employment demands more urban housing. Single-storied, low-density industrial parks surrounded by large parking lots are one of the main reasons of sprawl. Industrial sprawl usually happens because land at the urban edge is cheaper.

So, economists in urban economics have long been interested in understanding the process of urbanization. The mono-centric city model of Muth (1969) and Mills (1972) is the corner stone of urban economics since its formulation. It is the first theoretical and still the dominant model in urban spatial structure. In its simplest form, the model described the city as a circular residential area surrounding a central business district in which all jobs are located. The model also uses a very simple idea – that people will pay a premium for sites that lead to lower commuting costs – to generate a complete model of the spatial structure of an entire city. As for example in the Figure 5, it is shown that some American cities named Indianpolis, Atlanta, Boston and Minneapolis, were primarily developed based on the mono-centric concept.

Figure 5. Application of mono-centric concept.

Indianpolis, IN

Atlanta, GA

Boston, MA

Minneapolis, MI
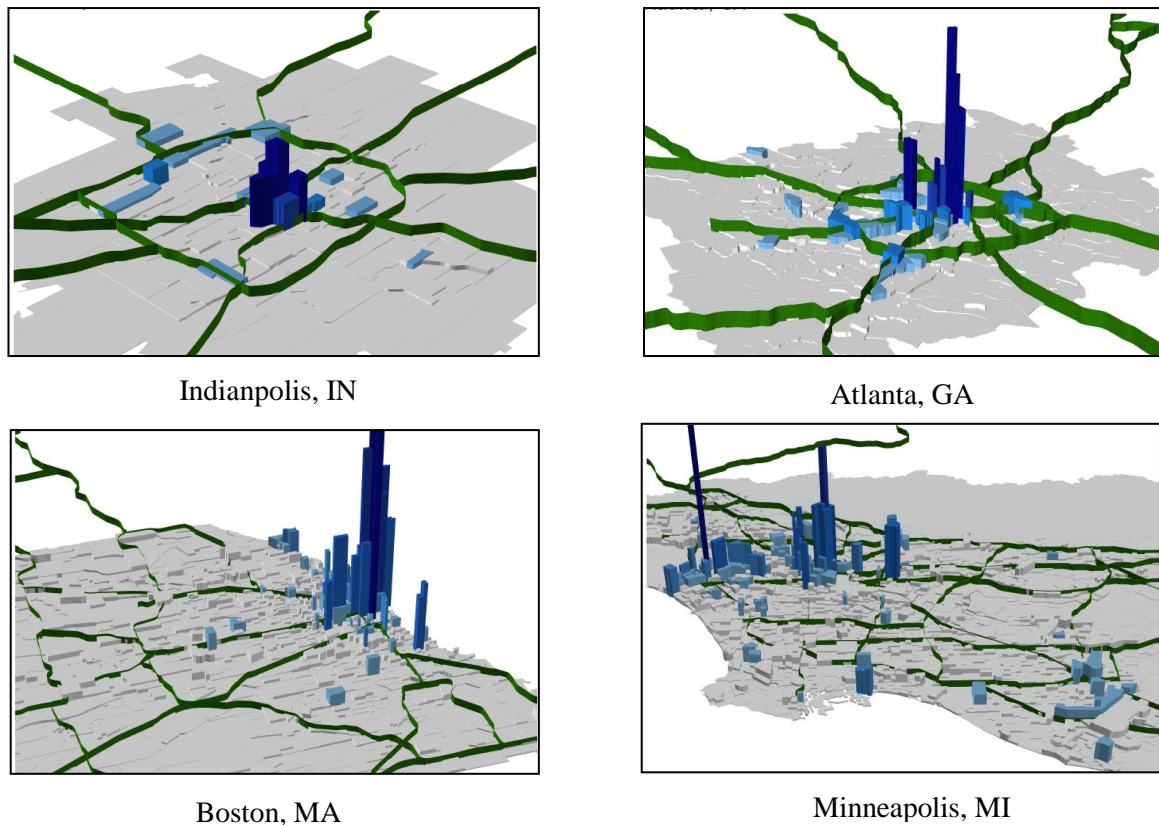
Source: Watanabe, 2012

The mono-centric model remained the most influential depiction of urban structure for at least two decades after the Second World War (1945). Although the assumptions are not literally accurate in all situations, they produce a mathematically tractable model with remarkable predictive power. Even modern urban areas tend to be dominated by the

traditional CBD. But a consensus appears to have developed that the mono-centric city model is no longer an accurate depiction of urban spatial structure. O'Sullivan's (2002) popular textbook perpetuates the notion that the mono-centric city model is designed to explain an old-fashioned city by listing as one of the assumptions "horse-drawn wagons," implying that the model does not apply to a modern city with cars. The model's failure is more serious in the suburbs because suburban data have never been explained well by the mono-centric city model.

However, in the mid to latter half of the 20th century, the mono-centric model became increasingly irrelevant in the face of:

- Decentralization of economic activities
- Increased mobility through new transport technologies
- Multiplicity of travel patterns and complex cross-commuting, and
- Changes in household structure and life style

It had become obvious over the years that the structure of many metropolitan areas diverged from the mono-centric model and that many daily trips expanded in clusters over a wide area outside the original CBD (Bertaud 2003). Many cities evolved from a mono-centric spatial structure into a polycentric city model. So, theoretical and empirical research in urban economics treats metropolitan areas as polycentric that is, having multiple employment centers with varying degrees of influence on urban spatial patterns.

Muller (1981) proposed a concept of the multi-centred metropolis, which showed that some suburbs had transformed into increasingly independent and self-sufficient urban entities beyond the older central city. These urban entities not only hold a rising share of the population of metropolises, but also accommodated increasing major economic activities, employment, and social, educational, cultural and entertainment services.

Additionally, Garreau (1991) put forward an idea of 'edge cities', a model of polycentric spatial structure usually located at major highway interchanges, to describe new suburban cities with office buildings and huge commercial infrastructures. Anas and Kim (1996) established a computable general equilibrium model to demonstrate the emergence of urban sub-centres resulted from multiple equilibrium. Hall (1999) supposed that the polycentric city focuses on the location of business and envisaged a new polycentric urban form emerging in many contemporary cities.

13

Fujita, Krugman and Venables (2001) developed a theoretical framework to describe the evolution of polycentric structure that had resulted from centripetal forces and the agglomeration of economic relationships between firms.

The polycentric city included six main elements:

- a traditional business core
- a secondary business core
- a tertiary business core or inner-city edge city;
- an outer edge city
- outermost edge cities and
- specialized concentrations

Hence, what some commentators see as an organized system of sub-centres, others see as an unorganized urban sprawl. In other words, what some people consider as a polycentric city, others conceptualise it as a dispersed city. Such distinction often depends on what criteria, thresholds and scale of observation are used as the basis of analysis. In the Figure 6, various types of urban spatial structures are shown,

Figure 6. The most common urban spatial structures.

The Monocentric Model
- Strong high density center with high concentration of jobs and amenities.
- Radial movements of people from periphery towards center

The Polycentric Model
- No dominant center, some sub centers.
- Jobs and amenities distributed in a near uniform manner across the built-up area.
- Random movement of people across the urban area.

The Composite Model
- A dominant center, some sub centers.
- Simultaneous and Random movement of people across the urban area.

The "urban village" Model
- People live next to their place of employment.
- People can walk or bicycle to work.
- This model exists only in the mind of planners; it is never encounted in real life.

Source: Adapted from Bertaud , 2003

One recent empirically based study from German urban regions based on data on commuter flows (German Census 1987 and German Social Security Statistics 2007) provides somewhat support for polycentric development. In their research they found that the polycentric city tends to be more travel-efficient when compared with a monocentric

city. A polycentric city's commuting volumes are much higher than that of a monocentric city. The finding of their research shows that average distance of commuters in polycentric cities of Stuttgart (13.5 km) and Frankfurt (16.4 km) is lower than that experienced in the monocentric cities of Munich (19.0 km) and Hamburg (20.8 km) in 2007 (Guth, Holz-Rau & Maciolek 2009). There is another case study in Istanbul based on available data from 209 traffic analysis zones which showed that the average commuting time decreased in all the zones due to highway improvements with suburban clustered employment growth (polycentric development) in Istanbul from 1985 to 1997 (Alpkokin et al. 2008).

Some recent study shows that the choice of a residential location cannot be reduced to "minimizing distance to work". Consumer preferences are complex. It is not possible to talk about "spatial mismatch" without knowing households and firms locational priorities. It is shown in Figure 7.

Figure 7. The choice of a residential location.

Residential location depends on a complex trade-off between conflicting preference which are unique to each household.
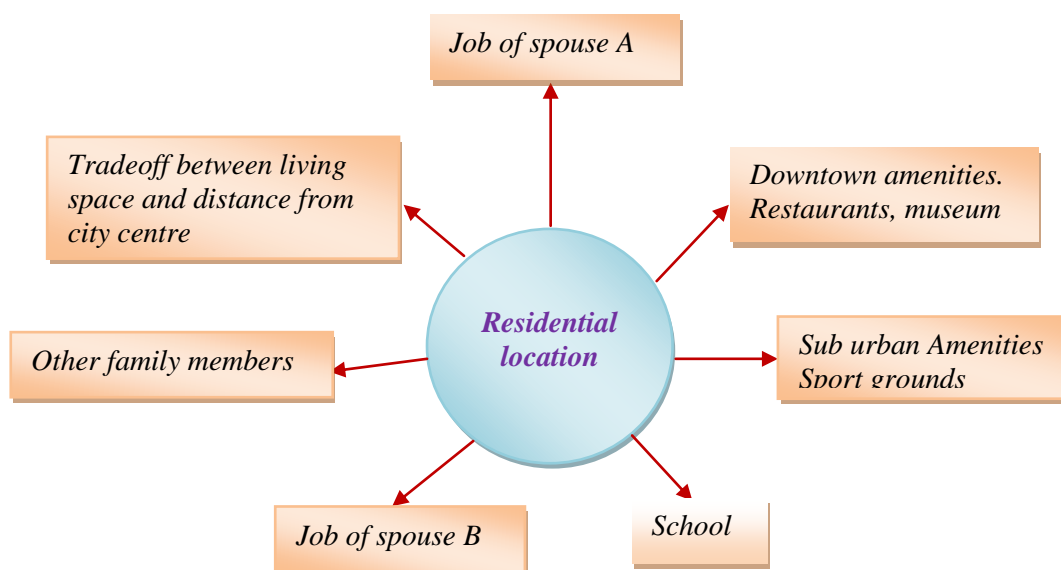
Most land use planner assume that there is only one preference: minimizing distance between job and residence

Source: Adapted from Bertaud , 2003

15

An alternative hypothesis comes from another study is that the growth of the suburbs has come about because people have fled the social problems of the inner city. As forcefully argued by Mills and Lubuele (1991) and Jackson (1985), central city problems may have led people to leave and seek solace in bucolic, socially controlled suburbs. At the individual level, this theory is irrefutable. Millions of Americans have surely been directly motivated in their move to the suburbs by the desire for a more attractive social milieu. Moreover, in the case of individual cities, such as Detroit, lack of downtown amenities has surely spurred suburbanization (as in Brueckner, Thisse and Zenou, 2000).

It is more or less demonstrated in all the studies that three fundamental forces have led to the spatial expansion of cities:

- The growth of population;
- The rise in household incomes and
- The decline in the cost of commuting.

It is also revealed that in reality no city is purely mono-centric or purely polycentric; most cities are a mix of the two modes with one mode being the dominating mode.

2.5 Urban Dynamics Modeling and Simulation

Urban modeling history is closely related to the understanding of urban systems. In the beginning cities were considered as one kind of natural and social phenomena, instead of an interrelated system. So with the influence of this kind of understanding, urban models were built in a static or descriptive way. Generally, these models rarely contain the capacity for prediction. They were formulated in an analogous and conceptual method. The typical this kind of models is Burgess' Concentric Zone model, Hoyt's sector model and Harris, Ullman's multiple-nuclei model (Candau, 2002; Torrens, 2000). Even though the von Thünen model is simplistic and was created in a time before the era of factories, highways, and even railroads, it is still an important model in urban studies. The Von Thunen model is an excellent illustration of the balance between the cost of land and transportation. The price of land decreases with increasing distance from a city. The farmers of the Isolated State try to maximize profit by balancing the cost of transportation and land, and produce the most cost-effective product for market.

Figure 8. Some typical historical models.

1 Central business district
2 Wholesale, light manufacturing
3 Low-class residential
4 Medium-class residential
5 High-class residential
6 Heavy manufacturing
7 Outlying business district
8 Residential suburb
9 Industrial suburb
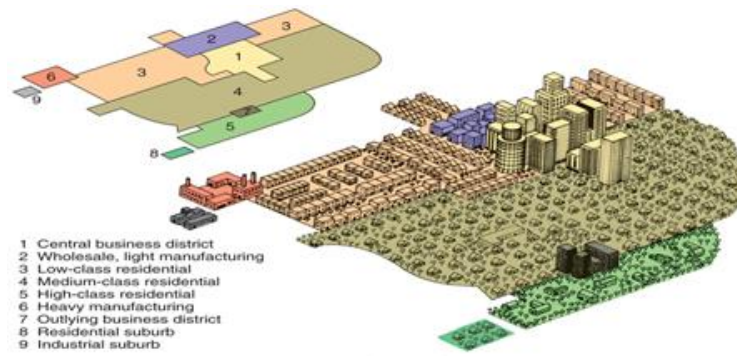
Multiple nuclei model
(Harris and Ullman 1945)

- Central city
- Intensive farming / dairying
- Forestry
- Extensive field crops
- Ranching / animal products
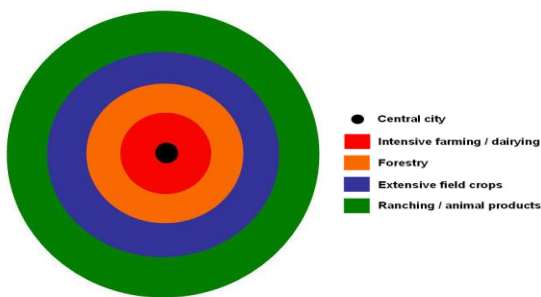
Von Thunen model model
(Johann Heinrich von 1826)

1 Central business district
2 Zone of transition
3 Zone of independent workers' homes
4 Zone of better residences
5 Commuter's zone
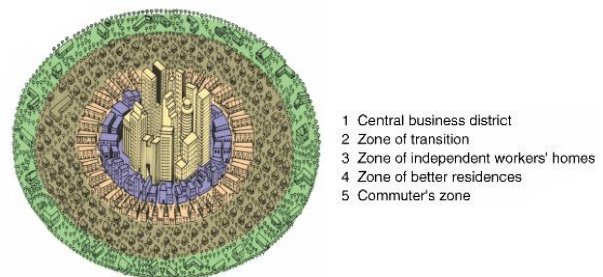
Concentric zone model
(Ernest Watson Burgess 1925)

KEY

- City
- Town
- Market Town
- Village

Boundaries
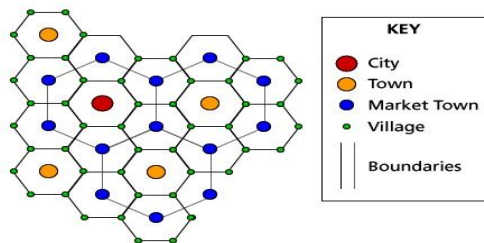
Centre place model
(Walter Christaller 1933)

- CBD
- Factories/Industry
- Low class residential
- Middle class residential
- High class residential
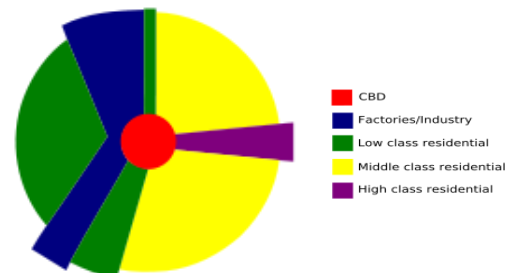
Sector model
(Homer Hoyt 1939)

Source: University of Illinois at Urbana-Champaign (UIUC), 2006 and Candau, 2002

Unlike the von Thunen approach, Burgess offers a descriptive rather than analytical account of these urban dynamics (Candau, 2002). It is proposed that a city's land use may be classified as a series of concentric zones and that the city grows by expanding these zones outward. Central Place Theory was devised by geographer Walter Christaller. This theory is concerned mainly with the arrangements of cities providing wholesale, retail, service, and administrative functions to a population. It also tries to explain the number, size, spatial distribution, and hierarchical arrangement of cities. Hoyt (1939) was able to improve upon Burgess' Concentric Zone model by advancing the Sector Theory of urban

17

land use. The model suggests that, over time, high quality housing tends to expand outward from an urban center along the fastest travel routes. Multiple Nuclei Theory, which was advanced by C.D. Harris and E.L. Ullman (1945) is based on the fact that many towns and nearly all large cities have many nuclei that serve as centers of agglomerative growth rather than a simple CBD around which all urban activity revolves.

With the further understanding of urban phenomena, cities were no longer considered as one kind of phenomena, but more of complex systems. Static, descriptive and explanatory models were not suitable for explaining and reflecting the essence of urban phenomena, and thus the need for models that consider urban dynamics appeared.

Urban modeling bloomed in the late 1950s and throughout the 1960s in both the USA and Western European countries, e.g. the Lowry model was designed in 1964 and first introduced into the process of urban planning by using aggregated data. However, with the massive transformation from an industrial to an informational economy, urban modeling gradually faded away as a dominant planning and decision-making paradigm in the late 1970s and through most of the 1980s. Modeling techniques from the 1960s to the 1980s were dominated by spatial, static, linear, cross-sectional, deterministic approaches, such as regression analysis, mathematical programming, input output analysis and even system dynamics. They proved inadequate to reflect the complex, dynamic and non-linear factors inherent in urban systems or subsystems (Lloyd-Jones and Erickson, 1997), and were of limited value in supporting planning decision-making. So, at present time, the time and space dimensions need to be incorporated into the urban modeling process.

Urban dynamics modeling has gradually moved from theories based on static centralized approaches, to spatio-temporal based theories. Models are now accounting for the complexity exhibited by urban processes, forms and systems. Current urban simulation approaches are taking advantage of progress in information technology, data availability and complex theories to address the criticisms raised by previous urban dynamics modeling attempts. Advances in remote sensing and geographic information science played a great role for introducing new spatial modeling approaches, such as artificial neural networks (Pijanowski *et al.,* 2002; Stathakis and Vasilakos, 2006; Stathakis, 2009), statistical models (Cheng and Masser, 2003), multi-agent models (Benenson, 1998) and fractal models (Batty *et al.,* 1989), UrbanSim (Waddell, 2002) cellular automata (Clarke *et al.,* 1997).

UrbanSim is a rapidly evolving integrated transportation land-use model ("integrated model" hereafter) that has been under development since 1996 by the research team of Paul Waddell at the University of Washington. It has been distributed on the web since 1998, with regular revisions and updates from www.urbansim.org. It has received a fair bit of attention in the academic and grey literatures. With respect to population, it operates at the level of individual households. With respect to employment, it operates at the level of individual jobs or establishments. Compared to most other integrated models that operate at the level of much larger traffic analysis zones, this characteristic of UrbanSim allows a much finer-grained approach to urban modeling. However, the data requirements for an operational UrbanSim model are large. Moreover, the complexity of model preparation, estimation and calibration may seem very onerous (Patterson and Bierlaire, 2010).

Among all documented dynamic models, cellular automata (CA) probably are the most used in urban growth modeling in terms of their flexibility, their simplicity in application, their close ties to remote sensing data and geographic information system (Torrens, 2000).

2.6 CA-based modeling

The concept of Cellular Automata (CA) was first introduced by Johann Louis von Neumann in 1948. The purpose was modelling biological self-reproduction (Wolfram, 1983). At the same time Stanislaw Marcin Ulam suggested the same idea by introducing the concept of "Cellular Spaces" map (Maerivoet and Moor, 2005). Therefore, both of them are considered to be the developers of this CA concept (Kier *et al.,* 2005).

Game of Life: In the seventies, John Horton Conway made a popular application called "Game of Life" based on CA concept. This was a kind of simulation game map (Maerivoet and Moor, 2005). The Game of Life, invented by John Conway, was the first and still most popular CA today. It is played on an infinite two-dimensional rectangular grid of square cells. Every cell interacts with its eight neighbours, which are the cells that are horizontally, vertically, or diagonally adjacent. At each step in time, the transitions that occur are- 1) Any live cell with fewer than two live neighbours dies, as if caused by under-population, 2) Any live cell with two or three live neighbours lives on to the next generation, 3) Any live cell with more than three live neighbours dies, as if by

19

overcrowding and 4) Any dead cell with exactly three live neighbours becomes a live cell, as if by reproduction (National Taiwan University, 2012)

Figure 9. Rules for the cellular automation game 'Life'.

Each cell has 08 neighbours

If an occupied cell has 0 or 1 neighbours, it dies (loneliness)

If an occupied cell has 4 to 8 neighbours, it dies (overcrowding)

If an occupied cell has 2 or 3 neighbours, it survives to the next generation

If an unoccupied cell has 3 occupied neighbours, it becomes occupied (birth)
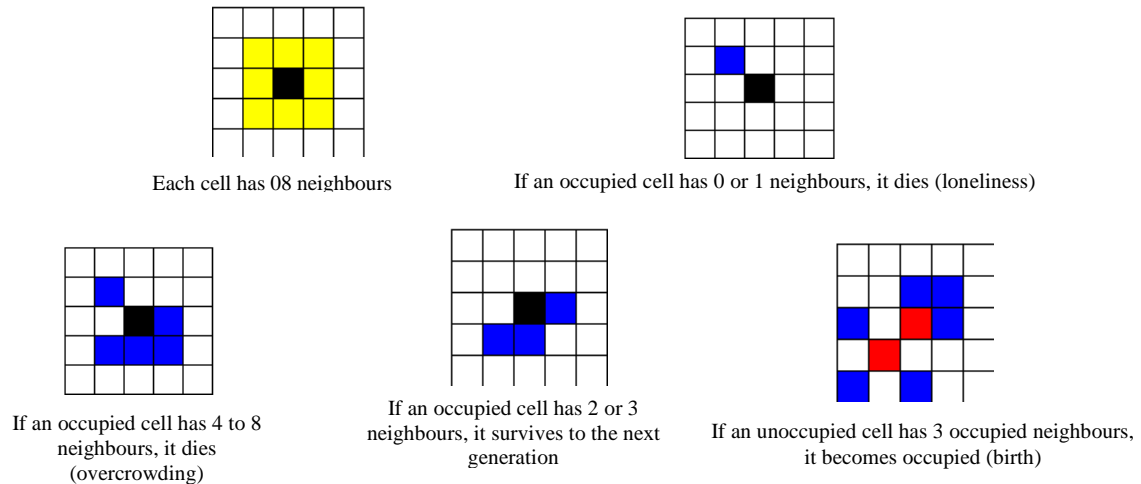
Source: Adapted from Gardener, 1970
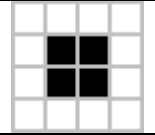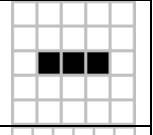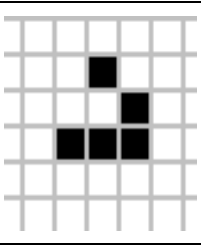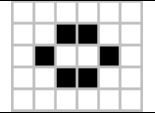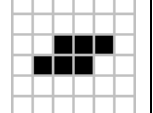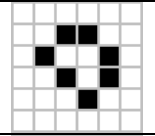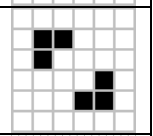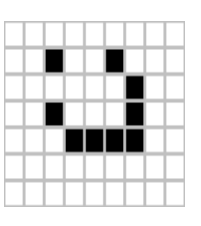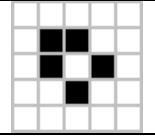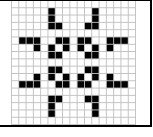
The initial pattern constitutes the *seed* of the system. The first generation is created by applying the above rules simultaneously to every cell in the seed—births and deaths occur simultaneously, and the discrete moment at which this happens is sometimes called a *tick* (in other words, each generation is a pure function of the preceding one). The rules continue to be applied repeatedly to create further generations.

Examples of patterns:

The earliest interesting patterns in the Game of Life were discovered without the use of computers. The simplest static patterns ("still lifes") and repeating patterns ("oscillators"—a superset of still lifes) were discovered while tracking the fates of various small starting configurations using graph paper, blackboards, physical game boards and the like. During this early research, Conway discovered that the R-pentomino failed to stabilize in a small number of generations. In fact, it takes 1103 generations to stabilize, by which time it has a population of 116 and has fired six escaping gliders (these were the first gliders ever discovered).

Many different types of patterns occur in the Game of Life, including still lifes, oscillators, and patterns that translate themselves across the board ("spaceships"). Some frequently occurring, examples of these three classes are shown in Figure 10, with live cells shown in black, and dead cells shown in white.

Figure 10. Different types of pattern that occur in the game of life.

Source: National Taiwan University, 2012

This concept was originated in computer science, but now it is being used by other disciplines like urban planning, geography, mathematics, physics, natural science, transportation, and biology etc. (Singh, 2003). CA has also been used to better understand and predict urban growth (Santé *et al.,* 2010).

2.6.1 What are Cellular Automata?

According to Torrens (2000), "An automaton essentially comprises a finite state machine that exists in some form of tessellated cell-space". Stephen Wolfram (1983) defined CA as follows: "Cellular automata are simple mathematical idealizations of physical systems in which space and time is discrete, and physical quantities take on finite set of discrete values" reproduction (Wolfram, 1983). Cellular automata have been defined as simple dynamic spatial systems where the state of each cell in an array depends on the previous state of the cells within a neighbourhood, according to a set fixed rules (Barredo *et al.,* 2003).

2.6.2 The Elements of Cellular Automata:

The components that comprise an elementary cellular automaton are as follows (Torrens, 2000):

a)   The physical environment or the space represented by an array of cells, on which the automaton exists (its lattice)

b)   The cell in which the automaton resides that contains its state(s)

c)   The neighbourhood around the automaton

21

d) Transition rules that describe the behaviour of the automaton

e) The temporal space in which the automaton exists

These elements have been described in brief to better understand the concept of CA:

a) The Cell Space: The cell space (lattice) is composed of individual cells. In an elementary CA, the lattice is one-dimensional (Figure 2.4). This is a linear string of cells called an elementary cellular automaton map (Maerivoet and Moor, 2005). But it can be *n*-dimensional. CA lattices can be of infinite proportions with any dimension. In most cases, lattices are defined in a regular fashion: grid squares, triangles, hexagons, torus (ring-shaped surface) etc. (Figure 11). Figure 11 and Figure 12 have been adopted from (Torrens, 2000) and (Maerivoet and Moor, 2005) respectively.

Figure 11. One-Dimensional Cellular Automata.
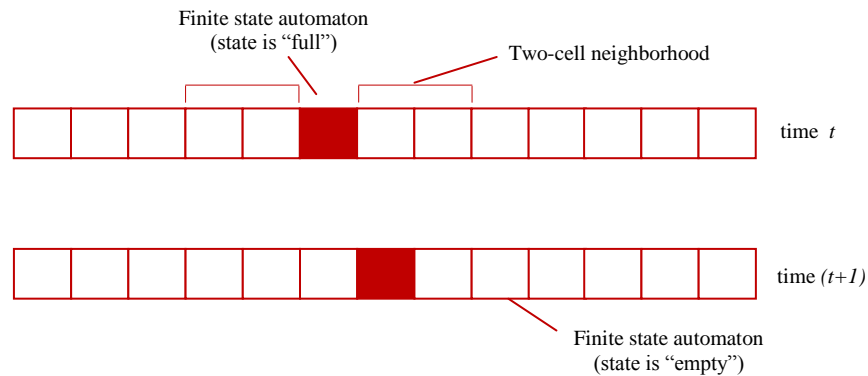
Source: Torrens, 2000

Figure 12. Two-Dimensional Cellular Automata Grid: [a] Rectangular, [b] Triangular, [c] Hexagonal and [d] Torus map.
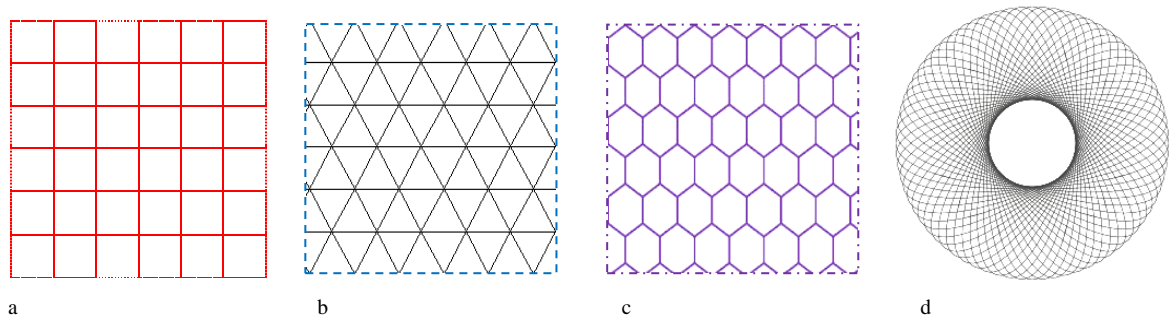
Source: Maerivoet and Moor, 2005

b) The Cell States: Each cell in the lattice can exist in a number of distinct states, which define the occupancy of the cell. The cell can be empty or contain a specific ingredient (e.g. molecule, particle, organism, land use etc.) (Kier, *et al.,* 2005). A cell's state is typically represented by an integer (binary state), but it can also have a continuous range of values map (Maerivoet and Moor, 2005). Recently, the idea of variegated cell, in which each edge can have its own independent rules for interacting with each other, has been introduced. Examples of some types of variegated cells are shown in Figure 13 (Singh, 2003).

Figure 13. Examples of Variegated Cells: (a) Two different types of edges with different rules, (b) Three different types of edges with different rules and (c) Four different types of edges with different rules.

(a)   (b)

(c)
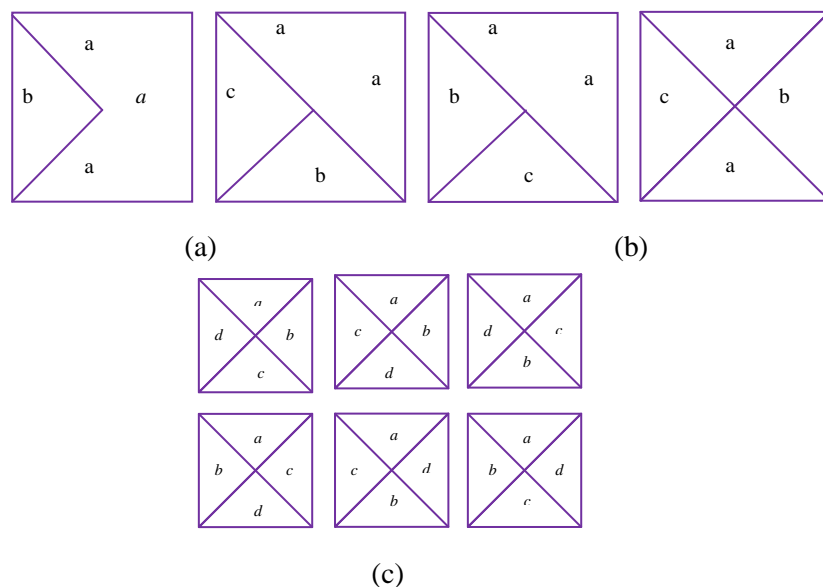
Source: Singh, 2003.

c) The Cell Neighbourhood: The movements/actions of an ingredient on the lattice are governed by some rules. These rules depend on the nature cells in close proximity to the ingredient. This proximity environment of a cell is called neighbourhood (Kier *et al.,* 2005). In one-dimensional cellular automata (1D lattice), each cell has two neighbours, while in a 2D rectangular lattice there are several possibilities map (Maerivoet and Moor, 2005).

The most common neighbourhood in 2D CA is called "von Neumann Neighbourhood" with a radius of 1 there are four adjacent cells including the cell itself. This neighbourhood for a cell, A, refers to the four B, cells adjoining its four faces. One more popular example is "Moore Neighbourhood" referring to the eight B cells completely

surrounding cell A. Another useful neighbourhood is "extended von Neumann Neighbourhood", where the four C cells lying just beyond the four B cells of von Neumann Neighbourhood are included. All the examples are shown in Figure 14 (Kier *et al.,* 2005).

Figure 14. Two-Dimensional CA Neighbourhoods: (Left) the von Neumann Neighbourhood, Middle) the Moore Neighbourhood and (Right) the extended von Neumann Neighbourhood of cell A.
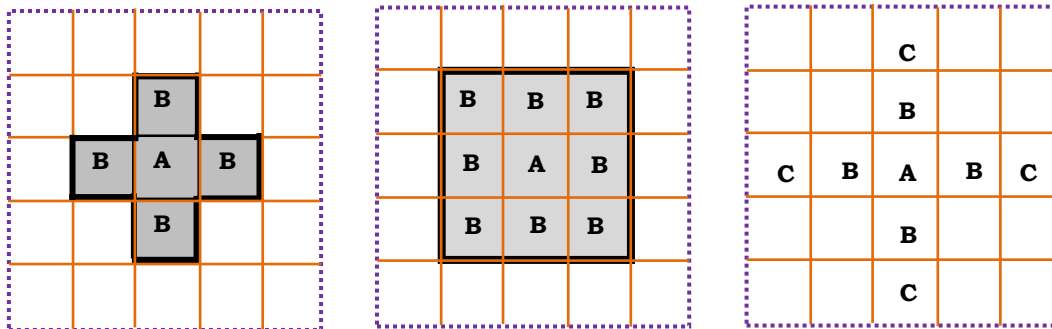
Source: Kier *et al.,* 2005.

d) The Transition Rules: A transition rule (also called function) acts upon a cell and its neighbourhood, such that the cell's stage changes from one discrete time to another (i.e. the system's iterations). The same rule is subsequently applied to all the cells in parallel map (Maerivoet and Moor, 2005). These rules are the heart of CA that guides its dynamic evolution (Singh, 2003). Transition rules influence the probability that an ingredient (e.g. land cover type) will transform to a different ingredient during iterations of the simulation (Kier *et al.,* 2005). For example suppose:

Case 1: If $P_T(AB) = 1.0$, then the transition A→B is certain to occur.

Case 2: If $P_T(AB) = 0.0$, then the transition A→B will never occur.

Case 3: If $P_T(AB) = 0.5$, then during each iteration, there will be a 50% change that the transition A→B will occur.

Case 1 and Case 2 are called "Deterministic CA Model", as there are no possibilities for different outcomes. Case 3 is considered as 'Stochastic (Probabilistic) CA Model' since it allows different outcomes, like the ingredient might remain unchanged or it might transform to a different state.

e) The Temporal Space: A CA evolves at sequence of discrete time steps. The temporal evolution of cells destroys the independence of initial cell states (Torrens, 2000). At each

step, the cells are updated simultaneously based on transition rules.

 Mathematical Notation of Cellular Automata: A CA model represents discrete dynamic system consisting of four elements map (Maerivoet and Moor, 2005):

$$CA = (\mathcal{L}, \Sigma, \mathcal{N}, \delta)$$

Where, L = the discrete lattice or the physical environment

Σ = the set of possible states, where each ith cell of the lattice at time step t has a state

$\sigma_i(t) \in \Sigma$ $N_s(r) = \{(i_1, i_2) / dist((i_1, i_2)) < r\}$

N = the neighbourhood of a cell automaton, which is defined as all cells that fall within a radius $r \in N$ around the actual cell. It denotes the idea of neighbourhood template (the proximity environment of a cell) (Soltani, 2004).

Where $N_s(r)$ = the relative index of all neighbours of a particular cell, δ = the local transition rule, which is denoted as follows (Maerivoet and Moor, 2005):

$$\delta : \Sigma^{|\mathcal{N}|} \longrightarrow \Sigma : \bigcup_{j \in \mathcal{N}_i(t)} \sigma_j(t) \longmapsto \sigma_i(t+1)$$

It shows that the state of the ith cell at the next time step $t+1$ is computed by δ based on the states of all the cells in its neighbourhood at the current time step t.

Here, $N_i(t)$ = the associated neighbourhood with i^{th} cell at time t

$|N|$ = the number of cells in the neighbourhood

The local transition rule is given by a rule table where given the sizes of Σ and N, the total number of possible rules equals map (Maerivoet and Moor, 2005):

$$\left| \Sigma^{\Sigma^{\mathcal{N}}} \right|$$

Where each of the $|\Sigma^{N}|$ possible configurations of a cell's neighbourhood is mapped to the number of possible states a cell can be in. Now considering the ordered set of all the states of all cells collectively at time step t, a CA's global configuration can be denoted as follows map (Maerivoet and Moor, 2005):

$$\mathcal{C}(t) = \bigcup_{j \in \mathcal{L}} \sigma_j(t)$$

Now applying the local transition rule to all the cells in the CA‟s lattice, the next configuration of the CA can be computed by its induced global map (Maerivoet and Moor, 2005):

$$ G : \Sigma^{\mathcal{L}} \longrightarrow \Sigma^{\mathcal{L}} : \mathcal{C}(t) \longmapsto \mathcal{C}(t+1) $$

In brief, the standard CA can be generalized as follows :

$$ S^{t+1} = f(S^t, N) $$

Where, S = the set of all possible states of the cellular automata; N = a neighbourhood of all cells providing input values for the function f and f = a transition function that defines the change of the state from t to $t+1$

2.6.3 Application of CA for Urban Growth Modeling

Early proposals for the use of CA in urban modeling tended to stress their pedagogic use in demonstrating how global patterns emerge from local actions (Almeida *et al.,* 2002). But increasingly models have been proposed which depart from the basic elements (Couclelis, 1985; Tobler, 1979). Strict CA follows highly localized neighborhoods where change takes place purely as a function of what happens in the immediate vicinity of any particular cell. Action-at-distance is forbidden, for it is argued that the intrinsic dynamics which generates emergent phenomena at the global level is entirely a product of local decisions which have no regard to what is happening outside their immediate neighborhood (Batty, 2000). Early models such as Tobler's (1970) model of Detroit and Couclelis's (1989) model of developer behaviour in Los Angeles were pedagogic in this spirit, yet the attractiveness of the approach which grew alongside the enormous interest in GIS, has eventually led to a flurry of more practical applications to urban problems. In this, the strict adherence of CA to the most local of neighborhood is inevitably relaxed, and the models that have emerged are best called cell-space—CS models rather than CA (Albin, 1975).

White and Engelen (1993) developed a CA to model the spatial structure of urban land use over time. They found that for realistic parameter values, the model produces fractal or bi-fractal land use structure for the urbanized area and for each individual land use type. They also found that the cellular approach makes it possible to achieve a high level of spatial detail and realism and to link the results directly to general theories of structural evolution.

Wu (1996) developed a linguistic CA based simulation approach. He integrated CA with heuristically defined transition rules to simulate land use conversions in the rural-urban fringe of a fast growing metropolis. He applied fuzzy set theory to capture the

uncoordinated land development process. An innovative feature of this integrated approach lies in its definition of transition rules through a 'natural language interface', thus being more realistic and transparent.

O'Sullivan and Torrens (2000) focused on the difficulties with the representation of human systems, and suggest that many modifications to simple CA introduced in modeling cities are responses to these problems. They propose a two-pronged approach to research. First, for operational model-building many variations on the CA theme are required and should be welcomed; and second theoretically motivated variations of the CA formalism are required so that the possible effects on model dynamic behavior may be more systematically explored.

Almeida *et al.* (2002) proposed a structure for simulating urban change based on estimating land use transitions using elementary probabilistic methods, which draw inspiration from Bayes' theory and the related 'weights of evidence' approach. These land use change probabilities drive a CA model based on eight cells Moore neighborhoods implemented through empirical land use allocation algorithms. The model framework was applied to a medium-sized town, Bauru, in the west of Sao Paulo State, Brazil. They showed how various socio-economic and infrastructural factors can be combined using the weights of evidence approach which enabled them to predict the probability of changes between land use types in different cells of the system. These modeling experiments support the essential logic of adopting Bayesian empirical methods, which synthesize various information about spatial infrastructure as the driver of urban land use change.

Liu and Andersson (2004) examined the impact of the degree of temporal dynamics on the behaviour of an urban growth model which is based on a modified Markov random field and probabilistic cellular automata. Experimental results from this case study suggested that the degree of temporal dynamics does have an important impact on the urban morphology produced by the model. Too much or too little dynamics could both lead to unrealistic patterns. However, the impact seems to vary for processes with different levels of change intensity. In the case of a process with moderate changes, the impact of temporal dynamics is also moderate. For a process with high change rate, the degree of temporal dynamics affects the model output significantly.

CA systems are especially suitable for urban modeling for some reasons:

• CA as a tool for urban modeling implies inputs and outputs in a qualitative and cartographic form, which is for urban planners, more preferable than numerical representations.

• CA can be linked with GIS, for better analysis and interpretation of the modeling process outputs and results.

• The working mechanism of CA is relatively simple, because it concludes mainly in the transition rules between one state and another of a cell, which depends on the state of the cell itself and its neighboring cells.

2.6.4 Application of SLEUTH Model

The majority of SLEUTH applications have been for urban forecasting or for integrated modeling of urban growth with some other social or physical process model or planning effort. The application of SLEUTH to the San Francisco Bay area by Clarke *et al.,* (1997) was the first major application of the model to a metropolitan region. In this research, the historical urban extent was determined from cartographic and remotely sensed sources from 1850 to 1990. Using this information, coupled with transportation and topographic data, animations of the spatial growth patterns were created, statistics describing the spatial growth were calculated, and the model was used to predict future urbanization.

In addition to modeling extant urban regions, SLEUTH has been used as a tool for theoretical investigations of urban processes. Bierwagen's (2003) dissertation focused on simulating generic urban forms and examining the connectedness in the landscape in order to assess the viability of different urban growth forms on butterfly habitat.

Goldstein *et al.* (2004) compared using SLEUTH for the "back casting" of urban extent with spatiotemporal interpolation. Backcasting starts with defining a desirable future and then works backwards to identify policies and programs that will connect the future to the present. As a back casting tool, SLEUTH has been used extensively, most notably in Herold *et al.* (2003), where the use of landscape metrics in the historical development of an urban region is presented, and by Goldstein *et al.* (2000), where historical urban-wildfire conflicts are investigated While early applications of SLEUTH focused solely on the modeling of urban growth, the coupling of the Deltatron model, the portion that simulates land use change, increased the model's ability to represent multi-attribute landscape

change over time. Candau and Clarke (2000) document this sub-model, and its use for modeling land use change in the MAIA (Mid-Atlantic Integrated Assessment) region of US Environment Protection Agency (EPA). Much like Clarke *et al.* (1997), the paper is documentation on how the land use changes CA model (Deltatron) functions.

In any application of SLEUTH, one of the most time consuming processes is the calibration. While briefly discussed in Clarke *et al.* (1997) and in Clarke and Gaydos (1998), Silva and Clarke (2002) present a more refined focus on the calibration of SLEUTH during the application of the model to Lisbon and Porto, Portugal. The paper presents four key findings from the application: (1) SLEUTH is a universally portable model that may not only be applied to North American cities, but to European and international cities as well; (2) increasing the spatial resolution and detail of the input datasets makes the model more sensitive to local conditions; (3) using a multistage 'Brute force' calibration method can better refine the model parameters to find those that best replicate the historical growth patterns of an urban system; and (4) the parameters deriving from model calibration may be compared between different systems, and the interpretation may provide the foundation for understanding the urban growth processes unique to each urban system.

The work of Silva and Clarke in documenting the calibration process of SLEUTH in their application of the model to Lisbon and Porto provided a basis for the work of others applying SLEUTH (Jantz *et al.,* 2003; Yang and Lo, 2003; Dietzel and Clarke 2004), and made those applications more robust through a better understanding of the calibration process Most recently an important advance has been made in the use of SLEUTH; coupling model outputs with other spatiotemporal models to provide greater insight into problems dealing with future urbanization. Some of these applications involved the coupling of SLEUTH outputs with social modeling efforts, while others rest more in the domain of physically-based modeling. Claggett *et al.,* (2004) were successful in coupling SLEUTH with the Western Futures Model (Theobald, 2001). By doing so, they demonstrated the ability of SLEUTH to move beyond just providing a spatiotemporal picture of urban growth, but actually categorizing the growth into different classes of 'development pressure' based on forecasted population growth. Working almost in parallel, Leão *et al.,* (2004) coupled SLEUTH outputs with a multi-criteria evaluation of landfill suitability (Siddiqui *et al.,* 1996) in order to determine zones around Porto Alegre City (Brazil) where future land would not be urbanized, yet was suitable for landfills.

Arthur (2001) coupled SLEUTH to an urban runoff model in Chester County, Pennsylvania. Cogan *et al.* (2001) compared using SLEUTH outputs with the California Urban Futures model (Landis, 1994) to assess stresses on biodiversity. Lin *et al*. (2008) applied a framework to the SLEUTH with the Conversion of Land Use and its Effects (CLUE-s) model using historical SPOT images to predict urban sprawl in the Paochiao watershed in Taipei County, Taiwan. These researches demonstrate that SLEUTH can be successfully coupled with other models displaying the potential of the model to be incorporated into a wide array of applications ranging from urban development to environmental assessment and beyond.

SLEUTH has been used for exploratory visualization as well. Acevedo and Masuoka (1997) presented the general methodologies used to create 2-D and 3-D animations of the Baltimore-Washington DC region. Candau (2000) presented the possible ways of visualizing the uncertainty of the location of urban growth in a simulated landscape. Aerts *et al.* (2003) continued this thread by experimenting with subjects about their understanding of the uncertainty of the forecasted urban growth in a section of Santa Barbara using two different techniques. While the myriad of visualization techniques has expanded since SLEUTH's introduction, the understanding and interpretation of simulation forecasts is still a nascent research topic, especially given the accessibility of modern visualization techniques to stakeholders.

Oguz *et al.* (2007) used the SLEUTH urban growth model, closely coupled with a land transition model, to simulate future urban growth in the Houston metropolitan area, one of the fastest growing metropolises in the United States during the past three decades. The model was calibrated with historical data extracted from a time series of satellite images. Prior to the work of Oguz, Sangawongse *et al.* (2005) integrated remotely sensed images and Geographical Information Systems (GIS) data into the SLEUTH model to analyze land −use/land- cover dynamics in Chiang Mai city of China and its vicinity. Figure 15 shows worldwide SLEUTH application. Details are shown in *Appendix A*.

Figure 15. Worldwide SLEUTH application.

Source: Adapted from Project Gigalopolis, 2014d

2.7 Details of the urban growth SLEUTH Model

The urban growth model SLEUTH, uses a modified Cellular Automata (CA) to model the spread of urbanization across a landscape (Clarke *et al.,* 1997). Its name comes from the GIS data layers that are input into the model - Slope, Land use, Exclusion layer (where growth cannot occur), Urban, Transportation, and Hill shade. It is a program written in programming language C running under UNIX that uses the standard GNU C compiler (gcc) and may be executed in parallel. The urban growth model is the main component of SLEUTH and this study will utilize it for simulating the growth dynamics of Dhaka. The core model can be used without this module. The number of newly urbanized cells, generated in the core model, is the driver for land use transition. However, the Deltatron-module generates only non-urban land use transition (Clarke, 1997). Complete documentation and downloadable code of this model can be found at the Project Gigalopolis website: www.ncgia.ucsb.edu/projects/gig.

In an effort to more realistically portray urban growth, some of the formalisms of simple CA have been relaxed in SLEUTH (Candau, 2002). Like a standard CA, SLEUTH begins with an initial set of conditions, after that some transition rules are applied. Here the initial conditions are defined by some input image data. The input data serve as layers of information that create a non-homogenous cellular space and influence cell transition

31

suitability (Candau, 2002). Some growth parameters affect the transition rules sequentially. These growth parameters may be altered at the end of each time step by the self-modification behavior of SLEUTH. Calibration using the input image data produces these growth parameters which can be applied for predicting future growth scenario of the concerned urban area. This section discusses the data requirement, urban growth process, calibration and forecasting procedure of SLEUTH.

2.7.1 Data Requirement for SLEUTH

a) Slope: Topography, in general terms, creates the most basic definition of area available for urban development. Because of ease of development, flat grounds are the easiest to build upon. Lands get less suitable as slope increases, and eventually become impossible to develop due to structural infeasibility. The point where structures are no longer built due to slope constraints is defined as CRITICAL_SLOPE. Usually in SLEUTH, cells on a slope greater than 21% are called CRITICAL_SLOPE (Watkis, 2008).

b) Land-use: Land-use classes additional to urban may be modeled in SLEUTH. This is an optional input.

c) Exclusion: Areas not available to urbanization are included in the exclusion layer. Water bodies, parklands, and national forest are all good examples of commonly excluded land use types. The exclusion layer is not necessarily binary and may include levels, or probabilities, of growth resistance.

d) Urban: This is a binary classification: urban or non-urban. How "urban" is defined is application dependent. Methods used in the past include digitizing city maps and aerial photographs; thresholding remotely sensed images or block densities from census data. For calibration, the earliest urban year is used as the seed, and subsequent urban layers, or control years, are used to measure several statistical best fit values. For this reason, at least four urban layers are needed for calibration: one for initialization and three additional for a least-squares calculation.

e) Transportation: A transportation network can have an important role in a city's developing structure. Due to increased accessibility, urban corridors tend to reach out from the city core along modes of transportation. The transportation infrastructure expands with city growth. To include the dynamic effect of transportation in calibration, several road layers that change over time are desirable. SLEUTH is initialized with the earliest road layer. As growth cycles, or "time", pass and the date for a more recent road layer is

reached, the new layer is read in and development proceeds. The roads are not necessarily binary, but may be weighted to simulate one section of road's greater attractiveness to urbanization relative to another section of road.

f) Hillshade: A gray scale background image gives context to the spatial data generated by the model. It is useful for describing location and scale as well as topography. This layer is not an active input for model simulation, but can greatly assist the visual examination and analysis of model output image.

2.7.2 Image Processing

SLEUTH requires an input of five types of gray scale GIF image files (six if land use is being analyzed). For all layers, 0 is a nonexistent or null value, while $0 < n < 255$ is a "live", or existing, value. The model requires all input layers to have a consistent number of rows and columns.

Format standards for all data types are as follows:

• Grayscale GIF images

• Images are derived from grids in the same projection

• Images are derived from grids of the same map extent

• Images the same resolution (row and column count is consistent)

• Images follow a certain naming convention

Similar to other predictive models, this model requires some input data in order to initiate the simulation. All layers should be checked for agreement; urban areas should not be present in locations defined as undevelopable in the excluded layer. Following is a summary of the required input data (Figure 16).

Figure 16. SLEUTH model Input data – illustrative.

Slope	Urban
Derived from a Digital Elevation Model. DEM cell values must be percent not slope degree. *Pixel value range 0-100*	*The urban extent for the start year, or seed, is used to initialize the model and is the basis for the CA driven urban growth. Pixel value range: binary*
Land use	**Transportations Roads:**
Land use images should represent a unique land class *Pixel value range 0-255*	*Required to model road influence growth. Pixel value range: binary* *0: non-road* *0<n<256- road rank*
Excluded	**Hill shade**
Defines all locations that are totally or partially resistant to urbanization. *Pixel value range : 0-255*	*To give spatial context to urban extent data.*

Source: Adapted from Project Gigalopolis, 2014a.

2.8 Basic working mechanism of the model

A CA system usually consists of four basic elements: Cells, set of states (occupied/free, on/off,…). Neighborhoods defined by cells, Rules and Time periods. Cells are the smallest units which must manifest some adjacency or proximity**.** Cells can be pixels from raster images. The cell state is updated considering the close environmental situations and states, not only a particular theoretical rule (Automata).

The state of a cell can change according to transition rules which are defined in terms of neighborhood functions. This transition between one pixel state to another takes place in discrete time steps according to fixed rules (Wolfram, 1983). Neighbourhoods can be configured in several ways: agglomerations of adjacent distance-defined cells and clusters of cells (Figure 17).

Figure 17. Neighborhoods configuration.
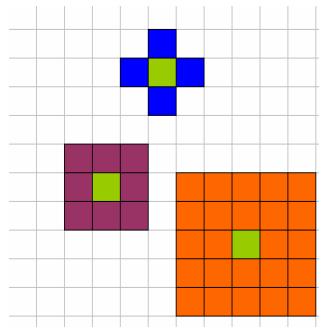
Source: Wolfram, 1983.

Figure 18. SLEUTH growth cycles.
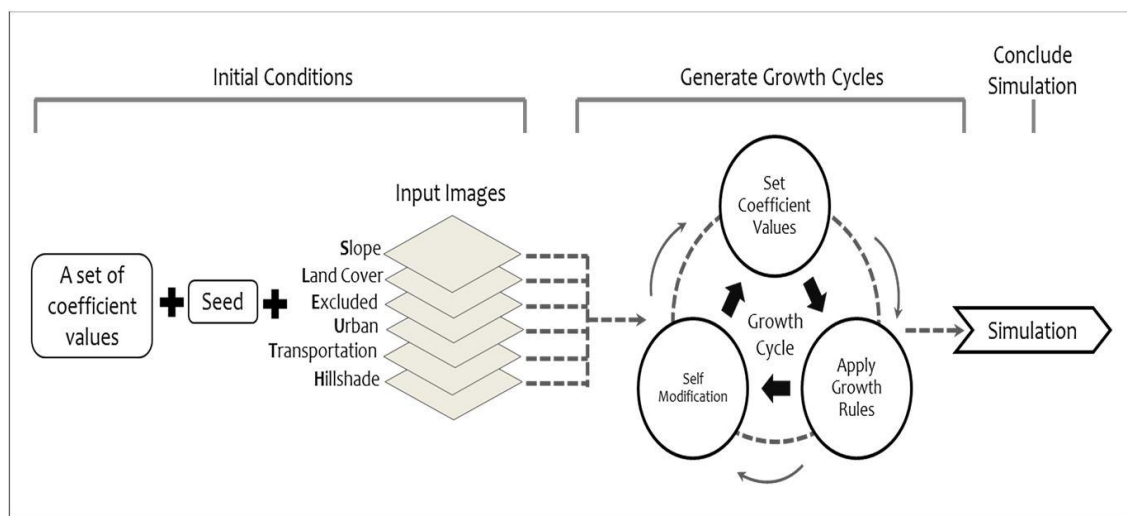
Source: Chaudhuri and Clarke, 2014

Each time step in a model could be called cycle or iteration or generation (Figure 18). A simulation is just a sum of Cycles that determine a simulation for a specific time period. SLEUTH is composed of 2 modules. One is Urban Growth Model which predict on how an urban area will grow (extension and development) and predict the land cover change and another is land use/cover transition model (Alive/dead cells). Every Growing Cycle in SLEUTH is based on 1) Rules: they will allow the model to develop following certain patterns, using the assigned coefficients. 2) Coefficient: set by the user every time but acquired using statistical methods, represent the metrics of a concrete behaviour (probability, frequency).

Five coefficients, or parameters, affect how the growth rules are applied. First, diffusion coefficient determines the overall depressiveness of the distribution both of single grid cells and in the movement of new settlements outward through the road system. Second, breed coefficient determines how likely a newly generated detached settlement or road

35

influenced settlement is to begin its own growth cycle. Third, the spread coefficient controls the amount of outward 'organic' expansion takes place within the system. Fourth, the slope resistance coefficient influences the likelihood of settlement extending up steeper slopes. Finally, the road gravity coefficient has the effect of attracting new settlements onto the existing road system if they fall within a given distance of the road and thus develop near the transportation network.

The UGM model works with 4 basic growth dynamics, Spontaneous Growth, New Spreading Centers, Edge Growth, and Road-Influenced Growth. Firstly, Spontaneous growth (Figure 19) simulates urbanized pixels by random and it is controlled by diffusion coefficient. This type of growth models the development of urban settlements in undeveloped areas. Spontaneous growth simulates the random urbanization of single pixels, which has the potential to capture low-density development patterns and is not dependent on proximity to existing urban areas or the transportation infrastructure. The overall probability that a single non-urbanized cell in the study area will become urbanized is determined by the dispersion coefficient.

Figure 19. Spontaneous growth.
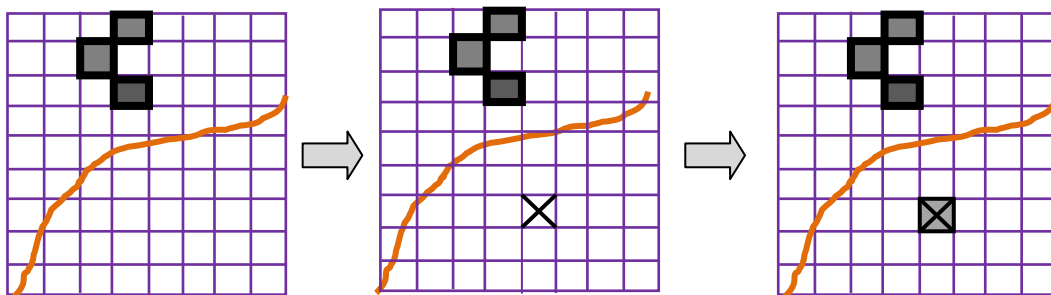
Source: Project Gigalopolis, 2014f

Secondly, new spreading center growth (Figure 20) determines whether any of the new spontaneously urbanized cells will become new urban spreading centers by the breed coefficient. This type of growth permits isolated cells to become new urban spreading centers for further outward expansion. New spreading center growth models the emergence of new urbanizing centers by generating up to two neighboring urban cells around areas that have been urbanized through spontaneous growth. The breed coefficient determines the overall probability that a pixel produced through spontaneous growth will also experience new spreading center growth

36

Figure 20. Spreading center growths.
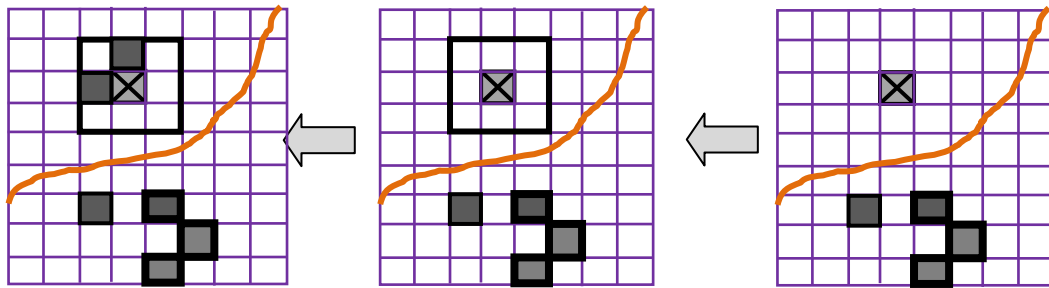
Source: Project Gigalopolis, 2014c

Thirdly, edge-growth (Figure 21) simulates growth that stems from existing urban centers. It is controlled by the spread coefficient, which influences the probability that a non-urban cell with at least three neighbors will become urbanized. This type of growth promotes the expansion of established urban cells to their surroundings. Only undeveloped cells that have at least three urban neighbors and pass the spread coefficient and slope resistance tests become a new urban location. Newly urbanized clusters can experience edge growth, which simulates outward growth from the edge of new and existing urban centers. Edge growth is controlled by the spread coefficient, which influences the probability that a nonurban cell with at least three urban neighbors will also become urbanized.

Figure 21. Edge growth.
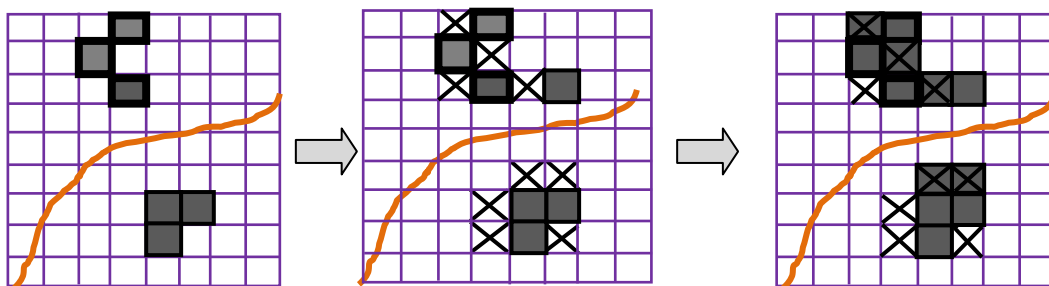
Source: Project Gigalopolis, 2014b

Actually, the urbanization is the sum of the four types of growth: spontaneous, diffusive, organic, and road-influenced. The growth rules are applied sequentially during each cycle (year), and are controlled by five coefficients (factors), namely: diffusion, breed, spread, slope resistance, and road gravity (Clarke, 1997).

SLEUTH's functionality termed "self-modification" (Figure 22) allows the growth coefficients to change throughout the course of a model run and which is intended to

simulate more realistically the different rates of growth that occur in an urban system over time (Clarke *et al.,* 1997). When the rate of growth exceeds a specified critical threshold, the growth coefficients are multiplied by a factor greater than one, simulating a development `boom' cycle. Likewise, when the rate of development falls below a specified critical threshold, the growth coefficients are multiplied by a factor less than one, simulating a development `bust' cycle. Without self-modification, SLEUTH will simulate a linear growth rate. In SLETUH, the growth rate is computed by comparing the number of new cells urbanized to the total existing urban area during a single time period.

Figure 22. SLEUTH model self-modifying conditions.

Rapid Growth
Greater than Critical number of hectare/year
Diffusion is multiplied by a constant <1.0
Spread is multiplied by a constant <1.0
Breed is multiplied by a constant <1.0

Normal Growth
Between Rapid and Little or No growth
If average slope <10% , increase speed
Road gravity increases by percent road
Slope resistant increases by 0.2*percent urban

Little or No Growth
Annual growth rate is less than a critical value
Diffusion is multiplied by a constant <1.0
Spread is multiplied by a constant <1.0
Breed is multiplied by a constant <1.0

Source: Project Gigalopolis, 2014d

Critical high and critical low growth thresholds, respectively, defined by the model, will initiate an increase or decrease in diffusion, breed, and spread coefficients. An increase in the diffusion, breed, and spread coefficients represents the tendency of an expanding urban system to grow even more rapidly. A decrease in the diffusion, breeds, and spread coefficients causes growth to slow.

The other two self-modification rules affect the road gravity coefficient and the slope resistance coefficient. The road gravity coefficient is increased as the road network enlarges, representing increased accessibility to the area. The slope coefficient is decreased as the percentage of land available for development decreases, allowing expansion to move up steeper slopes.

Under self-modification, the coefficient values during a model run increase most rapidly in the beginning of a growth cycle, when many cells are open for urbanization, and decrease

as urban density increases in the region and expansion declines (Clarke & Gaydos, 1998). Both growth rules and self-modification rules are the core of the model.

They reflect the universal understanding of the process of urbanization, but, to be successfully used, they need to be refined to the locale. To describe the behavior of the system correctly and predict its possible futures, the model needs to be calibrated (Silva & Clarke, 2002).

2.9 Sleuth Calibration Approach

2.9.1 Fitting Historical Data

A major tenet of SLEUTH application is: by calibrating how a region has changed in the past, a reasonable forecast of future change can be made (Clarke *et al.,* 1997). Following this assumption, the model is calibrated by fitting simulated data to historical spatial data. SLEUTH is initialized with the earliest data (signifying the date furthest in the past) and growth cycles are generated. It is assumed that one growth cycle represents one year. As growth cycles complete, "time" passes. Dates where historical data exist are referred to as control years. When a completed cycle has a corresponding control year, an image of simulated data is produced and several metrics of urban form are measured and stored in memory.

2.9.2 Monte Carlo Averaging

Monte Carlo averaging reduces dependence upon initial conditions and stochasticity. When a coefficient set has completed a defined number of Monte Carlo simulations, the metric values stored to memory are summed and divided by the number of Monte Carlo iterations. These averaged values are then compared to the control data metrics and linear regression, and best-fit statistics are calculated.

2.9.3 SLEUTH Brute Force Calibration

By running the model in calibration mode, a set of control parameters is refined in the sequential "brute-force" calibration (Silva and Clarke, 2002), although other methods of calibration, including the use of genetic algorithms, have been suggested and tested (Goldstein, 2004). SLEUTH utilizes five coefficients that may range independently between zero and 100. This poses a large set of possible solutions and a daunting number of computer processing unit (CPU) cycles required to explore the multidimensional coefficient space (Candau, 2002). Brute force calibration reduces the number of solution sets but still search the range of solutions. Instead of executing every permutation of possible coefficient sets, each parameter range is examined in increments. For example, the

range {0-100} may be stepped through in increments of 25 resulting in the values {0, 25, 50, 75, 100} or 55 simulations being implemented in order to cover the range. In this way, the model may be calibrated to the data in steps, successively narrowing the range of coefficient values. Generally, this process is accomplished in three phases here referred to as *coarse*, *fine* and *final* (Candau, 2002).

2.9.3.1 Coarse Phase

In the initial, coarse phase of calibration, the entire range $(0 - 100)$ of the five coefficients is explored using large increments (e.g.; for each coefficient, value = {0, 25, 50, 75, 100}) and a small number (5) of Monte Carlo iterations are used.

2.9.3.2 Fine Phase

Using the best-fit values found in the control_stats.log file produced in the coarse calibration phase, the range of possible coefficient values is narrowed. Ideally, the ranges will be narrowed so that increments of 5 - 10 may be used while still only using about 5-6 values per coefficient (e.g.; for a single coefficient, value = {25, 30, 35, 40, 45, 50}) and a larger number of Monte Carlo iterations are used (8).

2.9.3.3 Final Phase

Using the best-fit values found in the control_stats.log file produced in the fine calibration phase, the range of possible coefficient values is narrowed. Ideally, the ranges will be narrowed so that increments of 1 - 3 may be used while still only using about 5-6 values per coefficient (e.g.; for a single coefficient, value = {4, 6, 8, 10, 12}) and a larger number of Monte Carlo iterations are used (10).

2.10 Determining Goodness of Fit

Results from each of the calibration phases are examined to determine the goodness of fit for each parameter set. Narrowing of the parameter set can be based on a variety of different goodness of fit measures (Jantz *et al.,* 2003 and Yang and Lo, 2003); no sole metric has been shown to be the most effective. Traditionally the Lee and Sallee (1970) metric has been used to determine which parameter sets best describe the replication of the historical datasets. Lee-Sallee is the ratio of the intersection and the union of the simulated and actual urban areas, but others including the compare statistic, and population statistics have been used. Dietzel and Clarke (2007) found that the OSM (optimal SLEUTH metric, the product of the compare, population, edges, clusters, slope, X-mean, and Y-mean metrics) will provide the most robust results for SLEUTH calibration. Table 1 describes the 13 metrics that can be used to determine the goodness of fit of model calibration; they

have a value range of 0 to 1, with 1 being a perfect fit. After determining the parameter set that best fits the historical data, a range of values around that set of parameters is selected and the calibration is run again. The goodness of fit of the second calibration is evaluated, and an even narrower range of parameters is selected. The best fitting parameters from this third calibration are then the parameters used in forecasting urban growth and land-use change.

Table 1. Some of the indices for evaluation of the calibration results in the SLEUTH modeling.

Index	Description
Product	A composite index which is the result of all scores multiplied together
Compare	Comparison of modeled final urban extent to real final urban extent
r2	Population Least square regression score of modeled urbanization compared with actual urbanization for control years
Edge r2	Least square regression score for modeled urban edge count compared with actual urban edge count for control years
R2cluster	Least square regression score for modeled urban clustering compared with known urban clustering for control years
Leesalee	A shape index, a measurement of spatial fit between the modeled growth and the known urban extent for control years
Average slope R2	Least square regression of average slope for modeled urbanized cells compared with average slope of known urban cells for control years
X-r2	Center of gravity[x]: Least square regression of average x values for modeled urbanized cells compared with average X values of known urban cells for control years
Y -r2	Center of gravity[y]: Least square regression of average y values for modeled urbanized cells compared with average y values of known urban cells for control years

Source: Silva and Clarke, 2002

2.11 Forecast Methodology of SLEUTH

SLEUTH forecasts rely on replicating growth trends from the past (Candau, 2002). Once a coefficient set is found that can best describe how urban change has occurred over time, these values are used to forecast future growth. The calibration process produces initializing coefficient values that best simulate historical growth for a region. However, due to SLEUTH's self-modification qualities, coefficient values that initialize the model for a date in the past may be altered by the simulation end date. Therefore, for forecast run initialization, the coefficient values at the simulation end date are used to initialize a new simulation into a future date. Using the best coefficients derived from calibration to run a large number of Monte Carlo simulations will produce a single set of averaged coefficients for the simulation end date. Using the Best Solution Set (BSS) parameters derived from the simulation end date, a forecast run may be initialized (Candau, 2002). For the image data,

41

the most recent urban layer (the one that defined the calibration end date), the most recent transportation layer, and the exclusion and slope layers used in calibration, in addition to the background hill shade are used to initialize a forecast run. Growth rules are then applied to the data for a defined number of years. Forecasts are run in Monte Carlo fashion with 100 or more iterations. In addition to generating annual urban growth probability maps, a log of coefficient and metric values may be written to a file as output. The growth control coefficients have values that can range from 0 to 100, and each of their initial values can be derived through model calibration. These values evolve during the course of model runs as a function of a second hierarchy of growth rules that cause the model to ''self-modify''. The self-modification rules control the rate of growth to more realistically simulate how urban development occurs over time (e.g., to prevent linear growth and to simulate the Scurve-type growth rate typical of urban expansion). Specifically, critical threshold values are set so that unusually high or low growth rates lead to either a slowing down or a speeding up of urban expansion through slight alteration of the dispersion, spread, and breed growth-control parameters. The Total process can be shown (Figure 23) in the following diagram:

Figure 23. How model works.
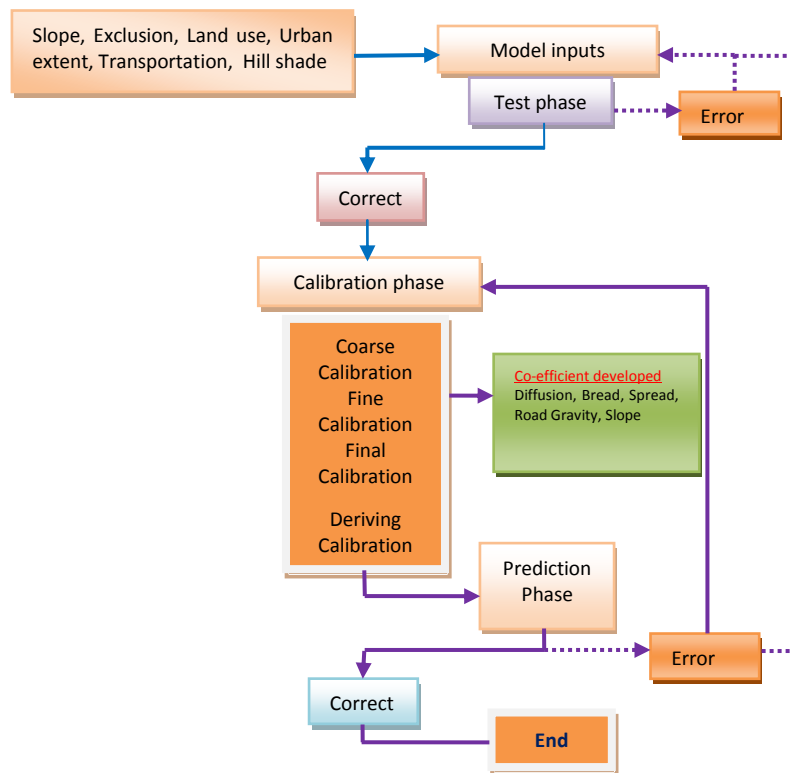
Source: Candau, 2002

42

2.12 Limitations of SLEUTH

SLEUTH, being open-source, has attracted numerous applications throughout the world and it has been successfully applied over the last 15 years to simulate land use change and predict urban growth. But the model is not beyond some limitations:

a) Time Consuming: At the calibration stage the model requires to run continuously more than 07 days to complete the process.

b) Resource demanding: The model requires minimum duo processor with 2 GHz speed and 1 GB of RAM. The better the processor and RAM, the better the model run. If the processor and RAM are low, the model takes long time to function. Additionally, in order to run the model in a Linux based operating system, gcc (GNU C compiler) is obligatory and in a window operating system Cygwin complier is essential. GIS and remote sensing software and photo processing software are also required to make the input data of the model.

c) Scale sensitivity: The model has scale sensitivity. Jantz *et.al.* (2003) found that the overall spatial accuracy at the pixel scale was quite high (93.1%), at the regional level. However, when it was applied at the local level or very small areas (only areas where change was predicted or observed roughly 22% of the study area), the overall accuracy dropped to 19%.

d) Data to be set subjectly: Preparation of input data for the model is very subjective. All the layers should be papered in the same resolution, same extent and same projections. If they are not same the model will not run. All the input layers must be converted into gray scale (GIF) image format.

e) Parameters to be set subjectly: After each calibration, SLEUTH scenario need to be changed for getting best fit parameter and here spatial caution is required to set the range of the co-efficient.

f) Predictability: The model produces better result by using short span (may be 20 years or less) data than long span data (Jantz *et.al.,* 2003 and Candau, 2002). So, the user must make wise use.

g) Resolution sensitivity: Normally, to save time in coarse calibration the resolution of the each layer is converted into one-fourth resolution, in fine calibration it is converted into half resolution and in final calibration full resolution of the layer is

43

used. But if in all 03 calibration stages, the full resolution is used, it produces better result especially in the flat area. But it worth the time.

With increasingly efficient computational infrastructure, new generations of geospatial data and, more interdisciplinary applications, these limitations can be addressed successfully in the near future. Despite these considerations, the researchers found SLEUTH to be a useful tool for assessing the impacts of alternative policy scenarios.

Chapter 3: Forecasting urban sprawl in Dhaka city using SLEUTH

3.1 Introduction

Dhaka, a city of history and heritage of nearly 400 years, is the administrative capital of the People's Republic of Bangladesh. During the last four decades this city and its surrounding region has recorded phenomenal growth in terms of both population and area. At present it is one of the fastest growing metropolises in the world. The study area for this research is Dhaka City Corporation (DCC) and its surrounding impact areas shown in Figure 24.

Figure 24. The gray rectangle corresponds to the study area (axes show geographic latitude and longitude in degrees).
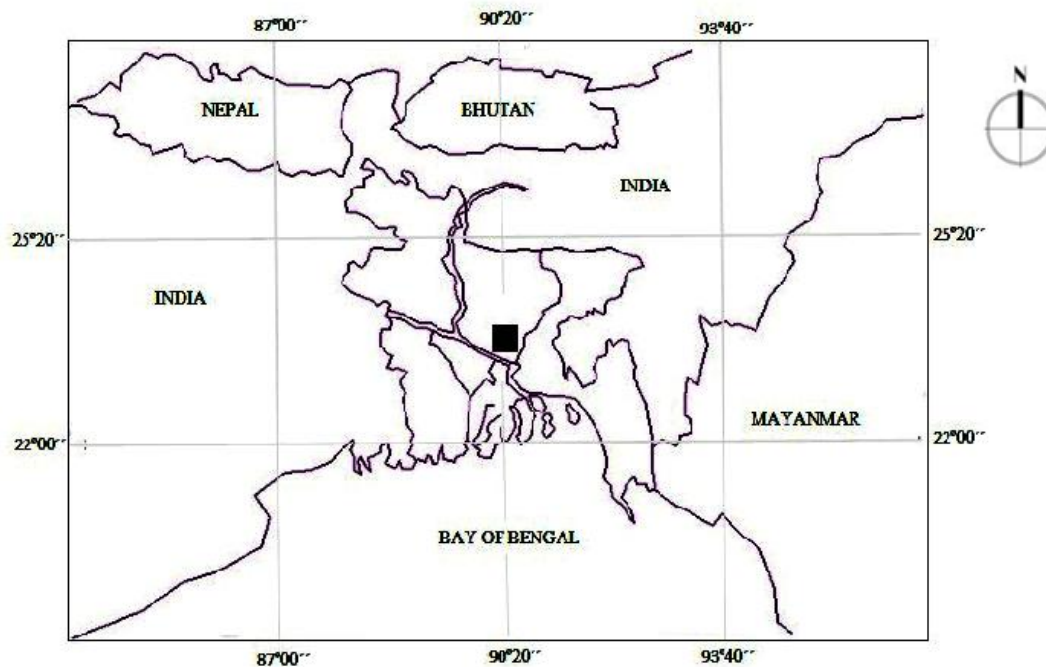
Source: Adapted from maplandia.com, 2005

The study area is located in the central place of Bangladesh. The study area covers the oldest core part of Dhaka city (old Dhaka), the planned areas and even the unplanned new generation areas that are called 'Informal Settlements'. This area has great probability to be completely urbanized growth in near future based on the current trend of rapid urbanization. Topographically, the area is completely flat with surface elevation ranging from 1 to 14 m. Most urban areas are located at elevations ranging from 6 to 8 m (JICA, 1992). The city is surrounded by four rivers: the Buriganga, Turag, Tongi and the Balu, which flow to the south, west, north and east respectively. The average rainfall of this area

45

is high. The city has a humid sub-tropical monsoon climate and receives approximately 2000 mm of rainfall annually, more than 80% of which falls during the monsoon season from June to September. The occurrence of heavy monsoon rainfall combined with flood water run-off from the rivers surrounding the city mean that Dhaka is very prone to monsoon flooding.

3.2 Physical Expansion of Dhaka City:

Different physical and socio-economic issues have guided the development process of Dhaka. Political importance and trade played significant roles in the city's expansion in different time periods.

Figure 25. Urban growth of Dhaka city in terms of area over the years.

Pre Mughal (1205-1610)   Mughal (1620-1757)

British (1758-1947)   Pakistan (1947-1971)   Bangladesh (1971 onward)
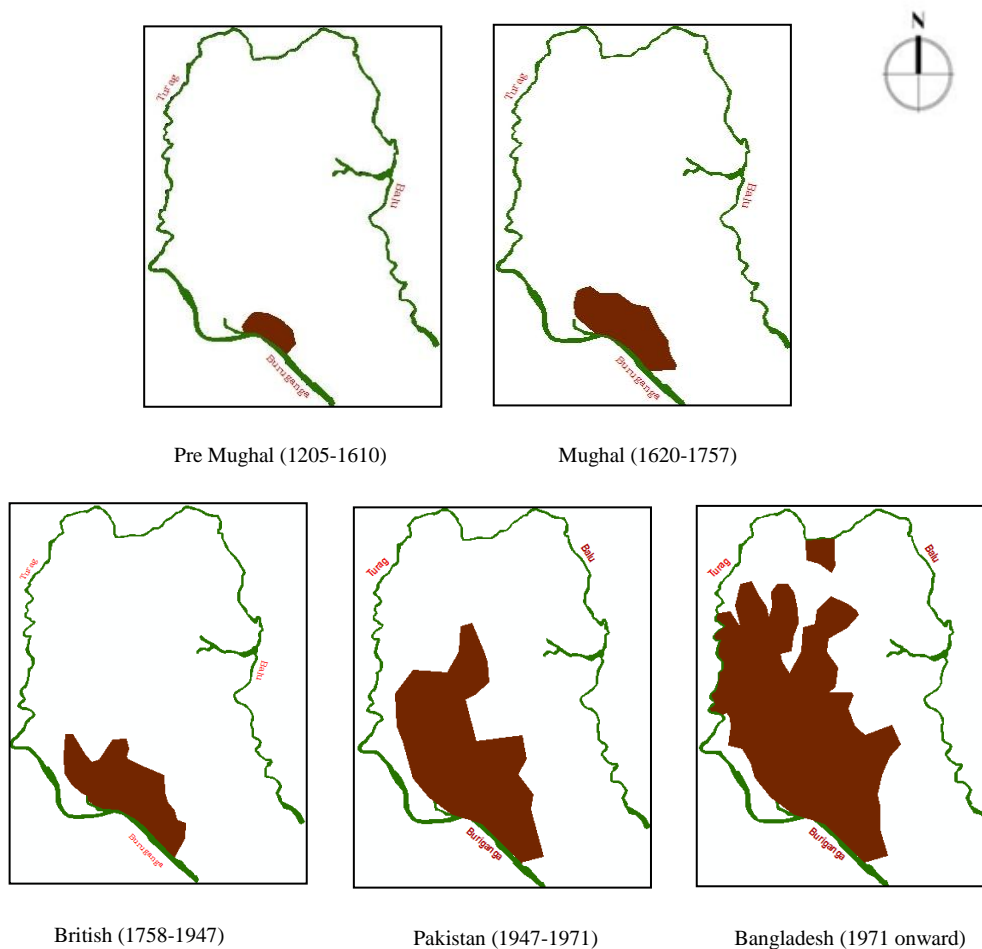
Source: Shankland Cox Partners, 1981

This section briefly describes the growth and expansion of the city in five major periods: pre-Mughal, Mughal, British (1764-1947), Pakistan (1947-1971) and Bangladesh (after 1971). In Figure 25, the increasing growth trend of Dhaka City in terms of area over time

is shown in Figure 25. In the pre-Mughal and Mughal period (1205-1757) the area was only 10 sq. km, the British (1758-1947) and Pakistan period (1947-1971) the area was 22 and 85 sq. km respectively (Chowdhury *et al.,*1989*)* and now in the Bangladesh period the area of greater Dhaka is 1530 sq.km (World Bank, 2007b).

3.3 Modeling Urban Growth in Dhaka city using SLEUTH

In this research, SLEUTH model was used to capture the rate and location of expected future urban growth patterns for Dhaka city and surrounding area. There will be three phases in order to implement that process. These three phases outline the workflow for modeling the expected future urban growth pattern on the study area, where each phase build upon the output of the previous one. The four phases for the research structure are outlined as follows:

Phase I, Historic Data Preparation and Input for the Model. The historic data required for the calibration phase, simulation (1989-2014), and future prediction phases, are prepared according to the model inputs' technical requirements.

Phase II, Model Calibration and Growth parameters Initialization. The model is calibrated with the prepared input data. During calibration, a set of growth parameters are derived, in order to maximize the model's ability to match the rate of growth and also perform well in terms of spatial fit.

Phase III, Future Growth Prediction. Using the calibration coefficients derived for this area, forecasts are made for Dhaka city and surrounding area till 2030. Forecasts are initialized with the extent of urban development in 2005 as represented in 30 meters resolution images.

3.3.1 Input data preparation

This study utilized data from various sources, including GIS digital data, satellite images and topographic maps. The input data required by the SLEUTH model includes Slope, Land use, Exclusion, Urban extent, Transportation and Hill shade. Data preparation depends greatly on GIS and remote sensing techniques, for example, data conversion, reclassification and data import/export.

The data preparation, calibration and prediction procedures followed here were mostly derived from the project Gigalopolis and different previous works on SLEUTH model. This study utilized data from various sources and topographic maps. The satellite data

47

for the study area were developed from the USGS website and topographic maps from Survey of Bangladesh. SLEUTH model required data on Slope, Land use, Exclusion, Urban Extent, Transportation and Hill shade. These are discussed below:

3.3.1.1 Slope

Topography, in general terms, creates the most basic definition of area available for urban development. Because of ease of development, flat expanses are the easiest to build upon. Lands get less hospitable as slope increases, and eventually become impossible to develop due to structural infeasibility. Slope data was derived from the Digital Elevation Model (DEM) of Shuttle Radar Topographic Mission (SRTM). SRTM is maintained by NASA. It provides digital elevation data (DEMs) for over 80% of the globe at a spatial resolution of 90 m.

3.3.1.2 Exclusion layer

The exclusion layer shows the area where urban growth would not occur without formal interventions. In this study, the excluded areas were identified as rivers, canals, airports, the zoo, botanical gardens, national monuments and parks which are not extensive. These areas occupy roughly 5% of the total city area.

3.3.1.3 Urban Extent layer

For calibration, at least four urban layers are required in order to calculate best-fit statistics (Jantz et al., 2003, Candau, 2002). Four historical urban maps were used for 1989, 1999, 2009 and 2014 (Figure 26). The urban extents for the study area were extracted from satellite images as follows (Table 2):

Table 2. Details of LANDSAT Satellite Images.

Date Acquired (Day/month/year)	Sensor	Quality (100% Cloud Free)
13/02/1989	Landsat 4-5 Thematic Mapper (TM)	7
24/11/1999	Landsat 7 Enhanced Thematic Mapper Plus ETM+)	9
26/10/2009	Landsat 4-5 Thematic Mapper (TM)	9
24/03/2014	Landsat 8 Operational Land Imager (OLI)	9

Source: USGS, 2014

LANDSAT path 137 row 44 covers the whole study area. Map projection of the collected satellite images is Universal Transverse Mercator (UTM) within Zone 46 N– Datum World

48

Geodetic System (WGS) 84 and the pixel size is 30 meters. The study area is selected by choosing the same geographic position of all 7 bands for the same time period. This helps to maintain the same number of rows and column.

Figure 26. LANDSAT images of Dhaka city

| 1989 | 1999 | 2009 | 2014 |

Source: USGS, 2014
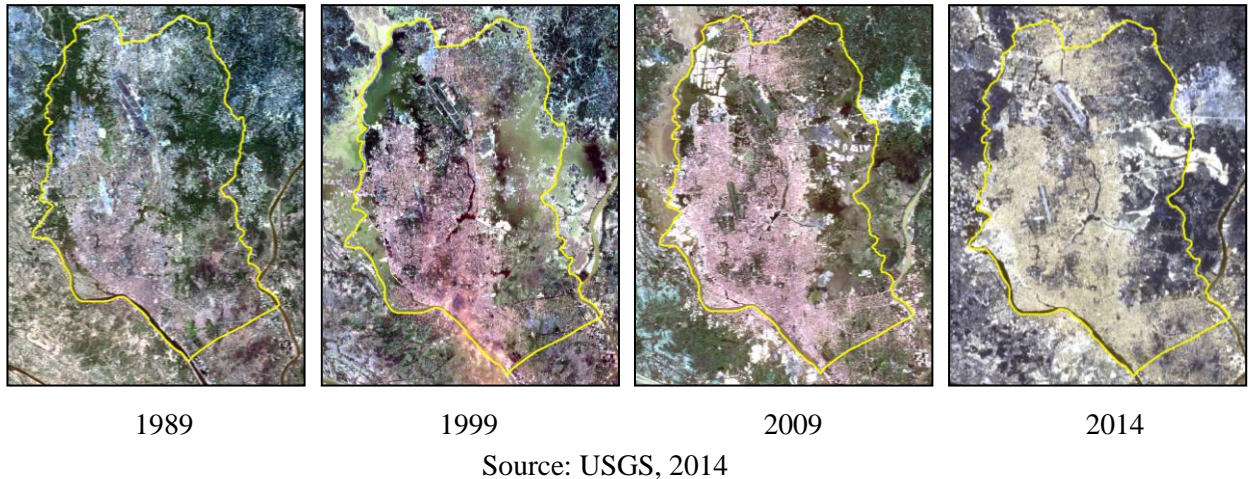
This layer is the most important input of the model, so in preparing this layer special caution and attention was applied. Urban areas were derived by classifying LANDSAT imagery. To produce an accurate classification, the images were classified into five classes by supervised classification (Figure 27). Subsequently, these classes were reclassified into built and non built classes with maximum likelihood classification (Figure 28). Maximum likelihood classification assumes that the statistics for each class in each band are normally distributed and calculates the probability that a given pixel belongs to a specific class. Each pixel is assigned to the class that has the highest probability (that is, the maximum likelihood). The details of built and non-built classes are shown in Table 3.

Table 3. Details of built and non-built classes.

Major land classes	Detail sub classes	Description
Built-up Area	Built-up Area	All residential, commercial, industrial areas, settlements and transportation infrastructure.
Non Built Area	Water Body	River, permanent open water, lakes, ponds, canals and reservoirs
	Vegetation	Trees, shrub lands and semi natural vegetation: deciduous, coniferous, and mixed forest, palms, orchard, herbs, climbers, gardens, inner-city recreational areas, parks and playgrounds, grassland and vegetable lands.
	Low Land	Permanent and seasonal wetlands, low-lying areas, marshy land, swamps, mudflats, all cultivated areas including urban agriculture; crop fields and rice-paddies.
	Fallow Land	Fallow land, earth and sand land in-fillings, construction sites, developed land, excavation sites, solid waste landfills, open space, bare and exposed soils

Source: Own elaboration

49

Figure 27. Classification of the area into five classes

1989   1999   2009   2014
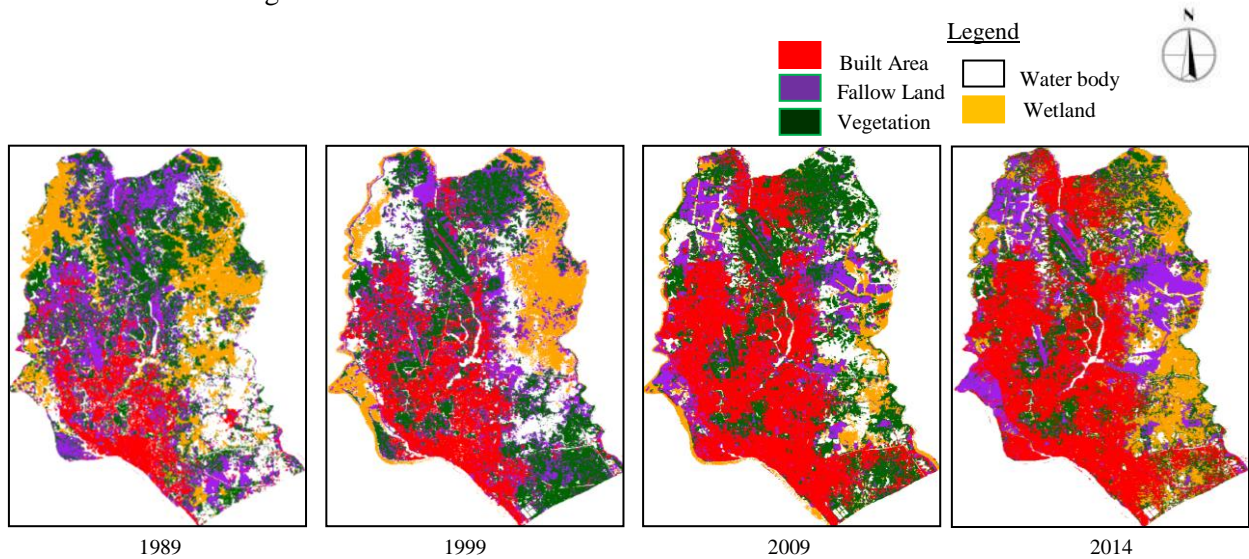
Source: Own elaboration

Figure 28. Reclassification of the area into two classes
(built and non-built).

1989   1999   2009   2014
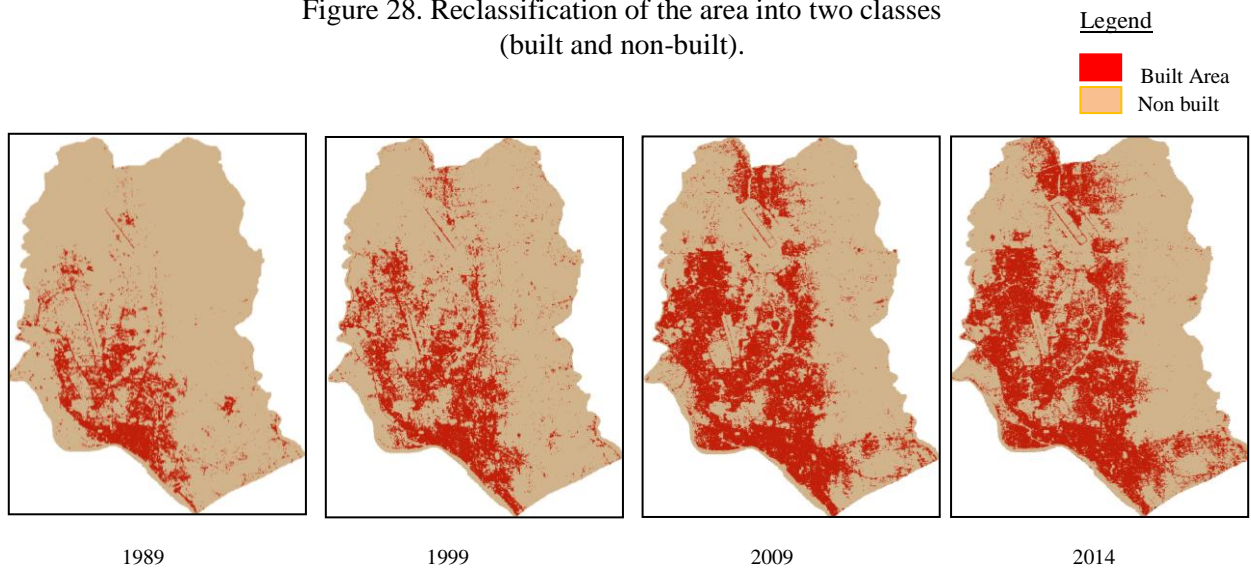
Source: Own elaboration

The accuracy was tested more than twice by kappa statistics using stratified random sampling from two classes (60 samples from each class). The result was satisfactory. In all instances, the kappa statistic showed very high score for each year as shown in Table 4.

50

Table 4. Year wise Classification Error Matrix.

Year	Classified Data	Reference Data (Number of samples=120)		
		Built-up Area	Non Built-up Area	Row Total
1989	Built Area	58	02	60
	Non Built Area	00	60	60
	Column Total	58	62	120
1999	Built Area	57	03	60
	Non Built Area	01	59	60
	Column Total	58	62	120
2009	Built Area	60	00	60
	Non Built Area	03	57	60
	Column Total	63	57	120
2014	Built Area	60	00	60
	Non Built Area	01	59	60
	Column Total	61	59	120

Source: Own elaboration

Table 5 shows classification accuracy per year.

Table 5. Classification accuracy per year.

Year	Class name	Reference Totals	Classified Totals	Number Correct	Producer Accuracy	User Accuracy	Kappa for each category	Overall Kappa statistics	Over all classification accuracy
1989	Built Area	58	60	58	100.00%	96.67%	0.93	0.96	98.33%
	Non Built Area	62	60	60	96.67%	100.00%	1.00		
1999	Built Area	58	60	57	98.28%	95.00%	0.90	0.93	96.67%
	Non Built Area	62	60	59	95.15%	98.33%	0.96		
2009	Built Area	63	60	60	95.24%	100.00%	1.00	0.95	97.50%
	Non Built Area	57	60	75	100.00%	95.00%	0.90		
2014	Built Area	61	60	60	98.36%	100.00%	1.00	0.98	99.17%
	Non Built Area	59	60	59	100.00%	98.33%	0.96		

Source: Own elaboration

3.3.1.4 Transportation layer

Four historical transportation layers were used for the years 2014, 2009, 1999 and 1989. The road network 1989, 1999 and 2009 were digitized from various transportation network maps of Dhaka city acquired from Survey of Bangladesh. The road network of 2014 was digitized from Google Earth.

3.3.1.5 Land use layer

An optional input to the SLEUTH model is land use. As already shown in Table 2, the LANDSAT images were firstly classified into five land classes in the process of preparing the urban extent layer. This land use layer has not been used in the model because it corresponds to the de facto land use on the ground that has limited role in restricting urban sprawl in the area. Formal (de jure) land use plans are not available for this region.

3.3.1.6 Image processing

All of the data layers were projected to the UTM (Universal Transverse Mercator) projection system. All the maps were resampled to 30 meter resolution raster files. All of the data layers had 636 columns and 864 rows. In Figure 29 and table 6, at a glance all input layers of the model are shown.

Figure 29. SLEUTH input layers Source.

Hill shade   Slope Layer   Exclusion layer

Land use layer

1989   2014

Transport layer

1989   1999   2009   2014

Urban layer

1989   1999   2009   2014

Source: Own elaboration

53
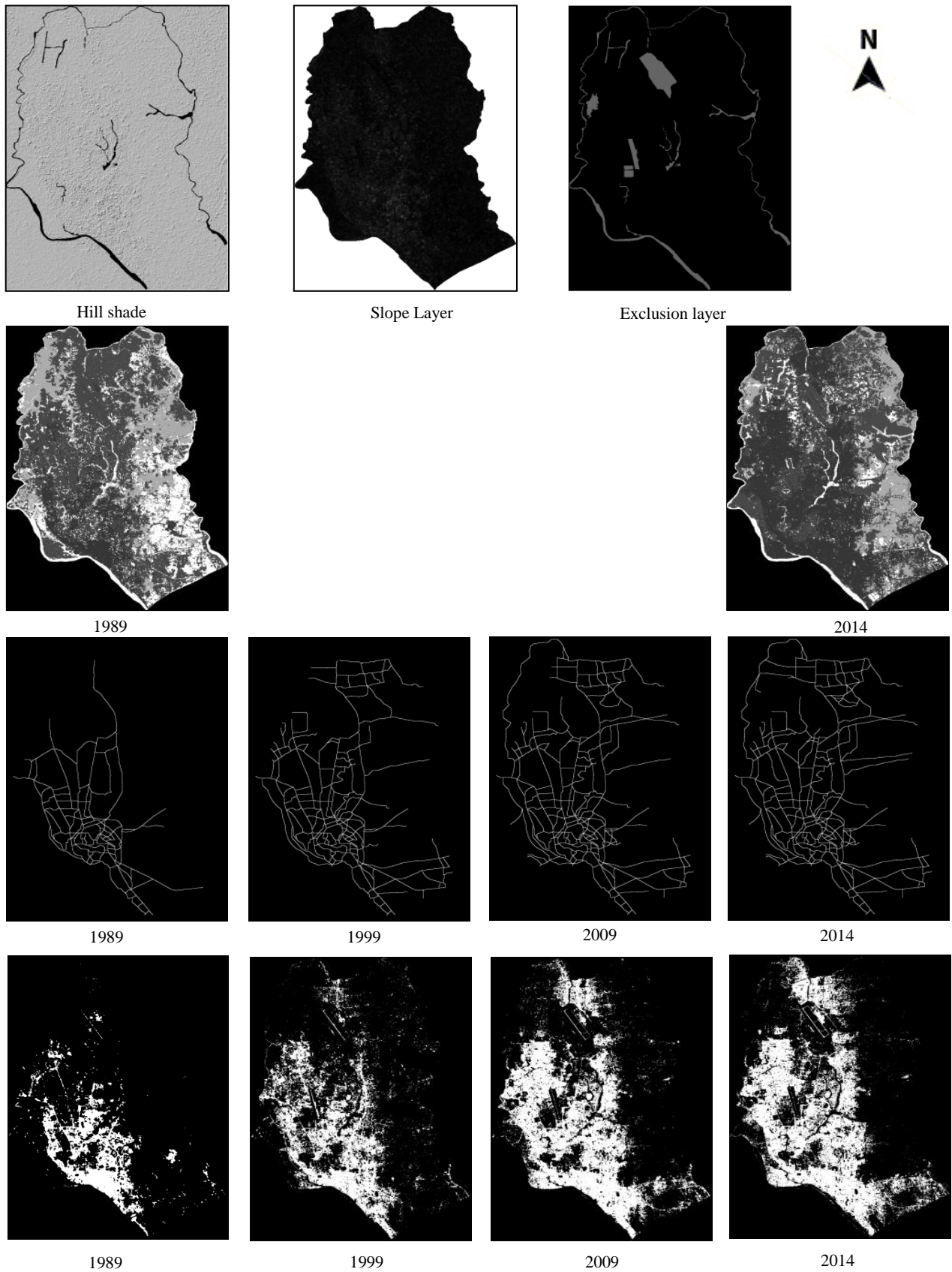
Table 6. The Study area SLEUTH's model input data description.

Layer Description	Year	Source	Format	Naming Convention
Slope	-	Produced from USGS DEM	Raster	dhaka.slope.gif
Excluded	-	(Rivers, canals, airports, the zoo, botanical gardens, national monuments and parks) vector derived from paper map	Raster(converted from vector data)	dhaka.excluded.gif
Urban extent	1989	Classified from Satellite images	Raster	dhaka.urban.1989.gif
	1999			dhaka.urban.1999.gif
	2009			dhaka.urban.2009.gif
	2014			dhaka.urban.2014.gif
Transportation (Roads)	1989	Produced from paper map	Raster (converted from vector data)	dhaka.roads.1989.gif
	1999	Produced from paper map		dhaka.roads.1999.gif
	2009	produced from paper map		dhaka.roads.2009.gif
	2014	produced from Google earth		dhaka.roads.2014.gif
Hill shade	-	Produced from USGS DEM	Raster	dhaka.hillshade.water.gif

Source: Own elaboration

3.3.2 Model Calibration and Growth parameters Initialization:

The main function of this model is to help the researcher determine the best fit parameters of five growth coefficients that can effectively model the growth during historic time period. As SLEUTH calibration is done in a Monte Carlo Brute Force fashion, the wide parameter space is gradually narrowed down step by step and the best fit coefficients are determined at the end. It is particularly done to reduce the total time period for calibration. This chapter discusses the calibration results of SLEUTH for Dhaka Metropolitan Area. The source code of the model was obtained from the Gigalopolis website. This study used the SLEUTH3.0beta_p01 version of the model.

Different researchers have used different metrics to determine the best fit coefficients. Some have used the product metric (which is simple multiplication of all other metrics); some have used Lee-Salle metric (ratio of the intersection and the union of the simulated and actual urban areas). This study has utilized the recent findings of Dietzel and Clarke (2007). They proposed Optimal SLEUTH Metrics (OSM) to identify the best fit coefficients. OSM is the product of the compare, population, edges, clusters, slope, X-mean, and Y-mean metrics. At the end of each calibration, OSM for each of the coefficient sets are calculated and based on the OSM the best fit coefficients are selected. For each coefficient the minimum value is taken as '_start' value and the maximum value is taken as the '_stop' value. '_Step' value is determined considering adequate interval between the '_start' and '_stop' value.

3.3.2.1 Coarse Calibration

It is the first stage of the SLEUTH calibration. Here parameter space is sparsely defined upon the whole parameter space (0-100). Five monte_carlo_iterations were mentioned in the scenario.log file including the coefficients as shown in Table 7.

Table 7. Input coefficients for coarse calibration.

Coefficient ranges	Coefficients				
	Diffusion	Breed	Spread	Slope	Road
_ Start	0	0	0	0	0
_ Step	25	25	25	25	25
_ Stop	100	100	100	100	100

Source: Own elaboration

3.3.2.2 Fine Calibration

Outputs of the coarse calibration were used to execute the fine calibration. The end of coarse calibration is control_stats.log file shown as Table 8.

Table 8. Coefficient selection from coarse calibration output.

Run	Product	Compare	Pop	Edges	Clusters	Cluster Size	Leesalee	Slope	%Urban	Xmean	Ymean	Rad	Fmatch	Diff	Brd	Sprd	Slp	RG	OSM
229	0.06504	0.71664	0.95757	0.88678	0.99152	0.86074	0.39093	0.97269	0.95867	0.63557	0.99737	0.96072	0.56413	1	25	100	1	100	0.37203439
225	0.06127	0.70596	0.9561	0.8862	0.92078	0.83855	0.392	0.9705	0.95748	0.67486	0.99993	0.95912	0.5627	1	25	100	1	1	0.360703089
232	0.05368	0.68193	0.94809	0.90402	0.96837	0.77264	0.3899	0.96593	0.9506	0.64368	0.99976	0.95239	0.55939	1	25	100	25	50	0.3518197
576	0.04986	0.70145	0.94271	0.90448	0.96911	0.7347	0.39062	0.96464	0.94593	0.65105	0.94709	0.94762	0.56213	1	100	75	1	25	0.344760687
329	0.05076	0.69376	0.94548	0.89847	1	0.75222	0.39007	0.96555	0.94837	0.63628	0.94241	0.94993	0.56275	1	50	75	1	100	0.341214996
109	0.0552	0.66073	0.95283	0.90087	0.97003	0.83247	0.38966	0.96742	0.95483	0.63693	0.98047	0.95613	0.56086	1	1	100	25	100	0.332374591
206	0.04711	0.63446	0.94042	0.92176	0.935	0.73627	0.38831	0.95949	0.9446	0.67128	0.99925	0.94472	0.5579	1	25	75	25	25	0.330958767
82	0.04736	0.62427	0.94466	0.91389	0.9994	0.73789	0.388	0.96156	0.94826	0.63735	0.99993	0.94829	0.55734	1	1	75	25	50	0.330069381
352	0.0552	0.73011	0.95426	0.88162	0.90919	0.85665	0.39107	0.97172	0.95574	0.63715	0.92257	0.95804	0.56419	1	50	100	1	50	0.318987201
577	0.04709	0.70529	0.94499	0.89537	0.9946	0.75	0.38974	0.96638	0.94782	0.6295	0.88104	0.94981	0.56255	1	100	75	1	50	0.31811579

Source: Own elaboration

Here the OSM for each of the coefficient sets are calculated and then the whole table is sorted in descending order of OSM. A portion of this table for both of the model framework In that table the first 10 parameter sets are taken as the best fit parameter combinations. Observing the results of the coefficients of that table the coefficient values necessary to execute the fine calibration were determined. Table 9 shows the input coefficients for the fine calibration of the model framework which were determined from the output of the coarse calibration. For fine calibration 8 monte_carlo_iterations were mentioned in the scenario.log file.

55

Table 9. Input coefficients for fine calibration.

Coefficient ranges	Coefficients				
	Diffusion	Breed	Spread	Slope	Road
_ Start	0	0	75	0	0
_ Step	5	20	5	5	20
_ Stop	20	100	100	25	100

Source: Own elaboration

3.3.2.3 Final Calibration

Final calibration was executed using the outputs of the fine calibration. In this stage the parameter space is narrowed down further. Selection of best fit coefficients here followed the procedure discussed in the previous section. Table 10 shows a portion of the metrics generated in the control_stats.log file in the output directory at the end of fine calibration of the model frameworks. Here also the metrics are sorted in the descending order of the OSM.

Table 10. Coefficient selection from fine calibration output.

Run	Product	Compare	Pop	Edges	Clusters	Cluster size	Leesalee	Slope	%Urban	Xmean	Ymean	Rad	Fmatch	Diff	Brd	Sprd	Slp	RG	OSM
620	0.05935	0.72539	0.95334	0.89135	0.9978	0.78283	0.39047	0.97094	0.95497	0.65031	0.97105	0.95712	0.56335	1	40	100	5	40	0.377108
401	0.05969	0.71745	0.95623	0.88769	0.99795	0.78382	0.39099	0.97165	0.95752	0.64206	0.99313	0.9595	0.56305	1	20	100	1	100	0.376544
412	0.06042	0.70736	0.95552	0.88693	0.99143	0.80207	0.39097	0.97127	0.95693	0.64695	0.99745	0.95887	0.56368	1	20	100	10	80	0.372506
632	0.0571	0.70744	0.9542	0.89002	0.99775	0.76697	0.39081	0.97094	0.95573	0.64283	0.98934	0.95805	0.5621	1	40	100	15	40	0.370156
584	0.06255	0.72107	0.95382	0.88842	0.98582	0.83755	0.39154	0.97122	0.9554	0.64439	0.98051	0.95754	0.56404	1	40	95	5	40	0.369639
806	0.0635	0.72485	0.95171	0.89124	0.99496	0.85473	0.3908	0.97005	0.95352	0.64658	0.96286	0.95593	0.56455	1	60	95	10	40	0.36943
402	0.06388	0.703	0.95817	0.88813	0.99931	0.85412	0.39138	0.97237	0.95925	0.63822	0.99324	0.96103	0.56256	1	20	100	5	1	0.368494
292	0.06118	0.6994	0.95509	0.88734	0.99778	0.82506	0.39129	0.97113	0.95657	0.64137	0.99969	0.95849	0.56128	1	20	85	1	80	0.368253
413	0.06021	0.7109	0.95603	0.88426	0.97534	0.81337	0.39046	0.97177	0.95734	0.64699	0.99576	0.95947	0.56246	1	20	100	10	100	0.366971
491	0.05275	0.68956	0.94703	0.89826	0.996	0.72959	0.39046	0.96635	0.94961	0.6538	0.9914	0.95171	0.5599	1	40	80	15	100	0.365953

Source: Own elaboration

Input coefficients for the final calibration (Table 11) are determined from this table. First 10 parameter sets are identified as the best fit parameter combinations and coefficients are determined according to that. The minimum coefficient value is used as the _start value and the maximum coefficient value is used as the _stop value. The _step values are determined in such a way that the _start value can reach the _stop value after 5-7 intervals. For final calibration 10 monte_carlo_iterations were mentioned in the scenario.log file.

Table 11. Input coefficients for final calibration.

Coefficient ranges	Coefficients				
	Diffusion	Breed	Spread	Slope	Road
_ Start	0	20	80	0	40
_ Step	5	8	4	3	12
_ Stop	20	60	100	15	100

Source: Own elaboration

56

3.3.3 Historic growth pattern simulation

The calibration process produces initializing coefficient values that best simulate historical growth for a region. However, due to SLEUTH's self-modification qualities, coefficient values at the start_date of a run may be altered by the stop_date. For forecast initialization, the stop_date values from the best calibrated coefficients are desired.

Table 12 Coefficient selection from final calibration output.

Run	Product	Compare	Pop	Edges	Clusters	Cluster size	Leesalee	Slope	%Urban	Xmean	Ymean	Rad	Fmatch	Diff	Brd	Sprd	Slp	RG	OSM
361	0.06578	0.71887	0.95528	0.88501	0.99731	0.84653	0.39108	0.97103	0.95669	0.65328	0.9989	0.95872	0.564	1	28	96	1	52	0.38407
552	0.06433	0.71548	0.95367	0.88844	0.9877	0.83656	0.39132	0.97073	0.95529	0.65617	0.99997	0.95738	0.56341	1	36	92	6	40	0.38137
298	0.06199	0.71217	0.95516	0.8864	0.99538	0.81246	0.39113	0.97161	0.95658	0.65199	0.99489	0.95875	0.56228	1	28	88	3	88	0.37826
325	0.06172	0.71791	0.95463	0.88536	0.99999	0.81028	0.39109	0.9713	0.95612	0.64697	0.9917	0.95823	0.56215	1	28	92	1	52	0.37813
404	0.0644	0.71751	0.95643	0.88602	0.99294	0.84176	0.39074	0.97188	0.95768	0.64425	0.99912	0.95973	0.56401	1	28	100	3	64	0.37769
360	0.06322	0.71525	0.95559	0.88352	0.97466	0.83039	0.39158	0.97119	0.95697	0.65879	0.99991	0.95893	0.56268	1	28	96	1	40	0.37654
379	0.06148	0.71425	0.95455	0.88759	0.97569	0.81418	0.39122	0.97111	0.95605	0.65175	0.99952	0.95816	0.56412	1	28	96	9	52	0.37352
374	0.06047	0.7159	0.95516	0.88427	0.99538	0.80328	0.39139	0.97149	0.95659	0.63884	0.99783	0.95864	0.56268	1	28	96	6	64	0.37273
447	0.05468	0.69757	0.94763	0.89513	0.99979	0.74025	0.39076	0.96681	0.95018	0.65401	0.99502	0.95191	0.5615	1	36	80	6	76	0.3722
508	0.06456	0.71545	0.95593	0.88708	0.99157	0.85414	0.39145	0.97252	0.95722	0.6434	0.98781	0.95952	0.56537	1	36	88	1	88	0.37183

Source: Own elaboration

Using the best coefficients derived from the final calibration stage and running SLEUTH for the historical time period produces a single set of stop_date coefficients to initialize forecasting. However, due to the random variability of the model, averaged coefficient results of many Monte Carlo iterations produces a more robust forecasting coefficient set.

Best calibrated coefficients were selected from the output of the final calibration (Table 3.6) following the procedure discussed in previous two sections. In this case only the first coefficient set is selected based on the performance of the OSM. Table 13. shows that for model diffusion value 1, breed value 28, spread value 96, slope resistance value 1 and road gravity of 52 produces the optimum OSM of 0.384.

These are the starting coefficient values that produced the optimum goodness of fit to the control layers. But SLEUTH through its self-modification characteristics change these values. For deriving the forecasting coefficients, another calibration run was conducted with the data using these best fit coefficients (shown in Table 13) with 110 Monte Carlo iterations.

57

Table 13. Input coefficients for identifying the forecasting coefficients.

Coefficient ranges	Coefficients				
	Diffusion	Breed	Spread	Slope	Road
Start	1	28	96	1	52
_ Step	1	1	1	1	1
_ Stop	1	28	96	1	52

Source: Own elaboration

Calibration run for deriving the forecasting coefficients produced the output presented in Table 14. These are the edited versions of the avg.log file produced through the calibration run with the best coefficients of final calibration. It shows that all of the coefficients have changed from 1999 to 2014.

Table 14. Output showing the self-modification nature of SLEUTH.

Year	Area	Xmean	Ymean	diffus	spread	breed	slp_res	rd_grav	grw_rate
1999	60100.51	257.37	575.09	1.09	100	30.62	1	53.03	2.89
2009	77518.86	266.73	574	1.21	100	33.83	1	54.61	2.27
2014	86268.63	271.86	573.61	1.27	100	35.55	1	55.56	2.02

Source: Own elaboration

The stop_date coefficients of 2014 are the final coefficients that are used for further growth prediction of the study area (Table 15).

Table 15. Forecasting Coefficient Derived through Calibration.

diffus	spread	breed	slp_res	rd_grav
1	100	36	1	56

Source: Own elaboration

During final calibration, statistics were produced for best fit parameters for the Dhaka city. They have a value range of 0 to 1, with 1 being a perfect fit. Most of the statistics for best fit parameters of the simulation results of Dhaka present high values of fit, indicating the ability of the model to reliably replicate past growth (Figure 30).

This suggests that future growth predictions can also be used with confidence. There was a high match for the amount of urban cells and clusters and the shape of urban edges between the simulated and control years (Figure 30).

58

Figure 30. Statistics of the best fit parameters (index) for modeling Dhaka city expansion.
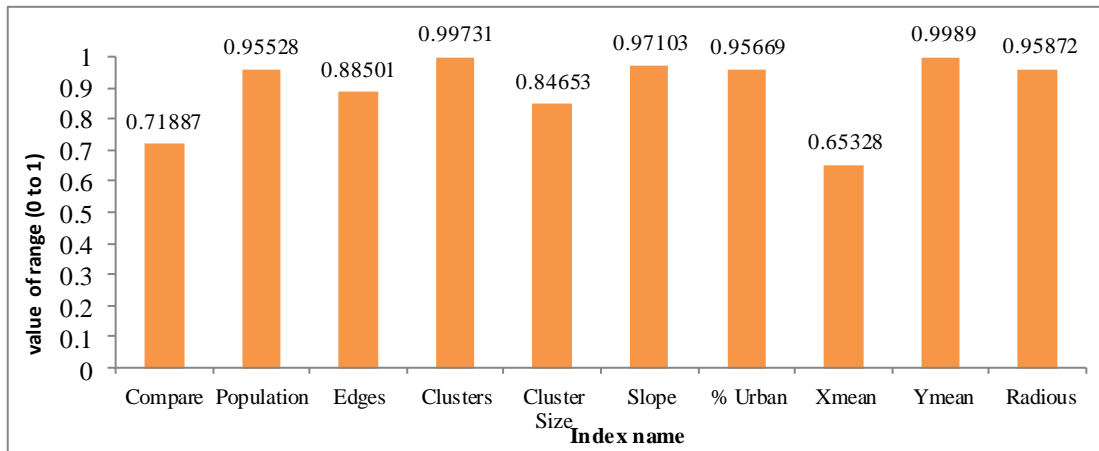
Source: Own elaboration

3.3.4 Urban growth prediction

Best fit coefficients derived through the calibration process were applied for predicting future growth scenario of the study area. It is done through the prediction mode of the SLEUTH model. The scenario.log file was updated for this purpose where the calibrated forecasting coefficients were mentioned in the PREDICTION_*_BEST_FIT flag (where * indicate the name of the coefficient). 110 MONTE_CARLO_ITERATIONS were used for the prediction runs for getting the optimum result which was also indicated in the scenario.log file. This study used a prediction time duration from the year 2015 to 2030. At first, the original input images were used for the prediction run to find out the growth if the present trend of development continues in the prediction time period. Figure 31 shows the urban extent provability map of 2015, 2020, 2025 and 2030 of Dhaka Metropolitan Area in cumulative percentage. Here the blue color indicates water, black color indicates exiting urban area and other colors indicate various degree of probability of future urban extent

59

Figure 31. Urban extent probability map (2015-2030) in cumulative percentage.

2015   2020

2025   2030

Source: Own elaboration

Legend:
- water (blue)
- urban existing (black)
- 70-100%
- 40-70%
- 0-40%

60
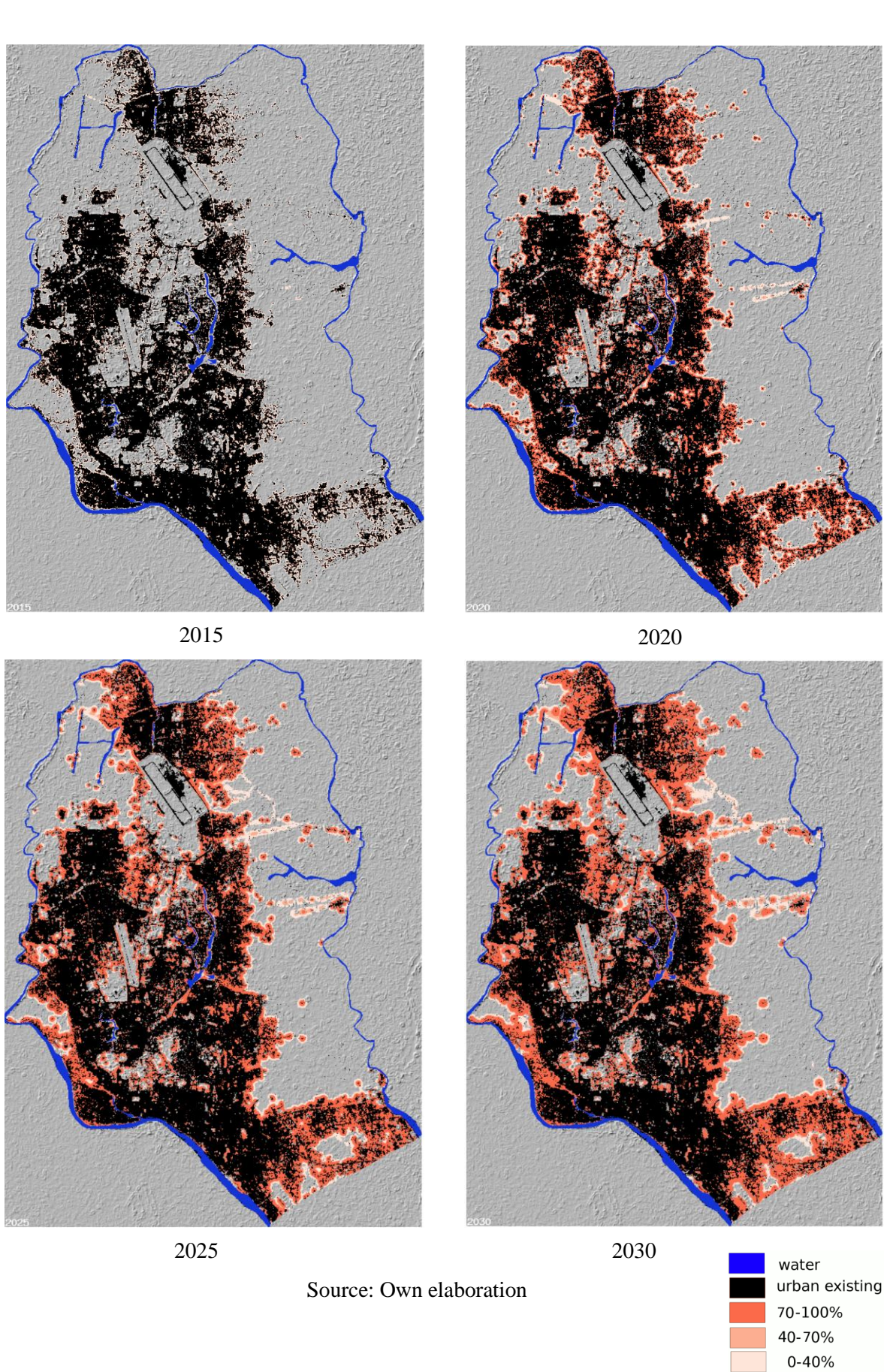
Chapter 4: Result and Discussions

The result of model calibration is shown in Figure 32. It reflects the high score in spread parameter (100) that indicates the high probability of urbanization outward of the existing urban centers.

Figure 32. Best fit parameters for forecasting.
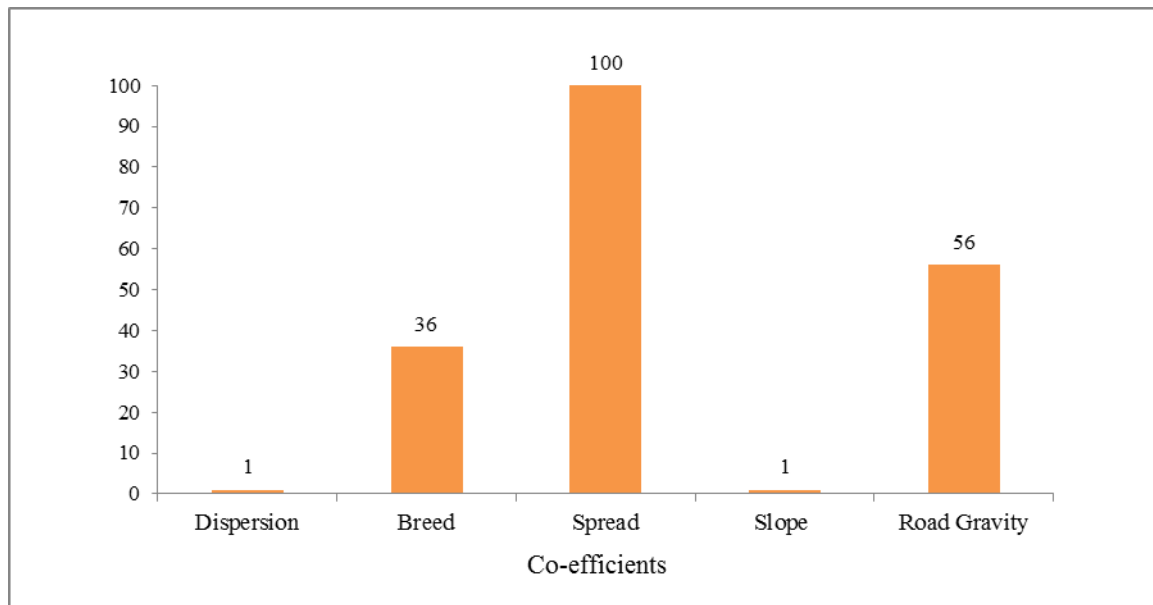
Source: Own elaboration

Another high score of road gravity (56) shows that urban growth has been affected by road networks significantly. Also, the breed parameter (36) scoring third position among the coefficients indicates a considerable probability of establishment of new urban centers. The score for slope resistance is almost negligible verifying that topography is obviously not a limiting factor for urban sprawl in Dhaka city. Finally, the low diffusion co-efficient shows that Dhaka city has a compact form of growth, with its main urbanization taking place near the existing urban areas and urban cores. This is a very interesting finding of the research.

In reality, the logic behind this compact form is that transportation of Dhaka is of poor quality; there is insufficient provision of appropriate transport modes and inadequate infrastructure. A study on Dhaka city's transport pattern (Mannan and Karim, 2001) says that the number of all vehicles per 100,000 population of Dhaka city is only 2,630 vehicles, among them about 2,195 are non- motorized vehicles. Motor vehicle (Bus, car and jeep) density for the Dhaka metropolitan is about 7 per 1,000 whereas the EU has 487 cars per 1000 inhabitants (European Automobile Manufactures Associations, 2012). Most of the

inhabitants of Dhaka city are dependent either on foot or on low cost non-motorized vehicle. Over 50% of trips involved walking alone and rickshaws (Figure 33), the non-motorized vehicle in the metropolitan area account for over 40% of passenger trips and only about 10% of trips involved motorized public transport service. Across all modes of transport average trip lengths for Non Motorized Transport (NMT) is about 1.3 km (36 minutes) and for motorized transport is 9 km (45 minutes) (Mannan and Karim, 2001).

Figure 33. The non-motorized slow moving vehicle rickshaw is on the road of Dhaka city.

Source: Guardian, 2015

So, there is a great reliance on non-motorized transport with limited range and capacity. It is also mentionable that the majority of the city's population is low-income. This low income people comprise more than 50% of total population of Dhaka city (Mannan and Karim, 2001). Because of the low income population and of the poor condition of the city's transit system, the non-motorized rickshaw has proved a popular mode of transport. This slow and low-capacity carrier has contributed little to urban expansion, as its slowness ensures that people commute less, and confine their journeys to locations in close proximity. All these have encouraged an increasingly compact city.

A Figure 34 shows in a graph the increasing trend of urban expansion from 2014 to 2030 in terms of acreage.

Figure 34. Increasing trend of urban expansion 1and urban population of Dhaka city (2014-2030).
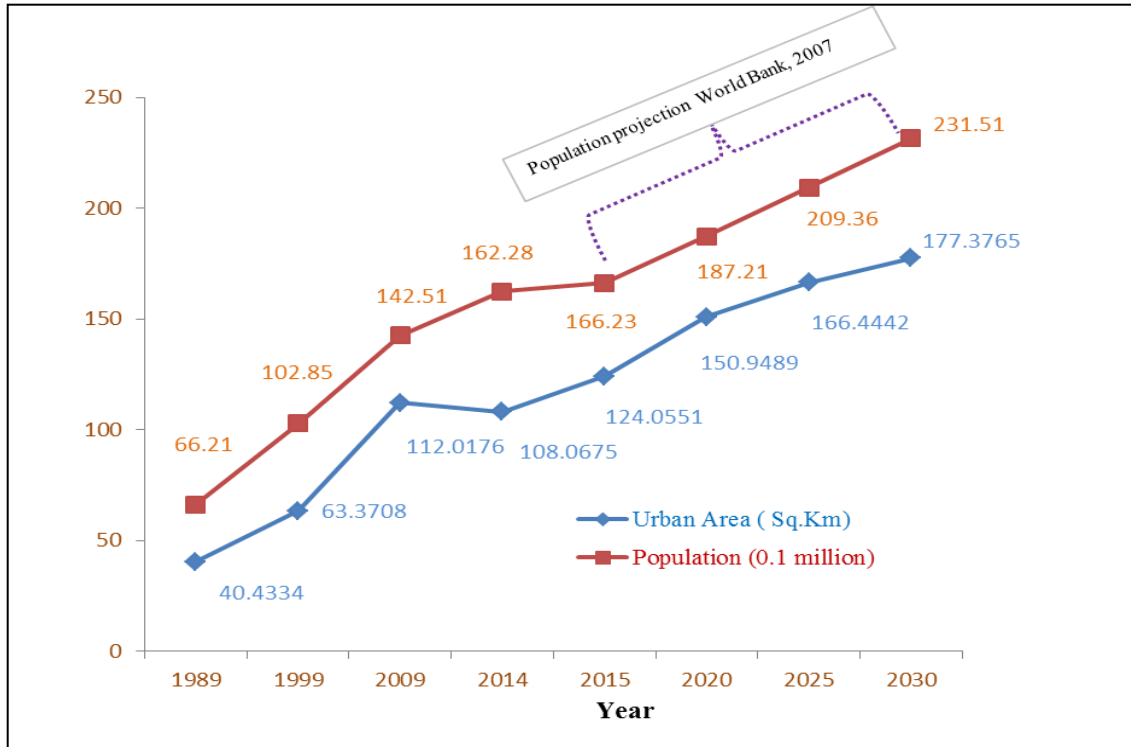
Source: Own elaboration and the World Urbanization Prospects: the 2014 Revision, United Nations

It is evident in this graph that urban extend is highly correlated with population. Here the co-relation score shows very high ($r^2 = 0.99$).

Another interesting finding is that the model predicts that the city will expand towards north-south direction. This is useful for policy makers that can be getting an idea about cities future expansion direction.

A final finding is that in the year 2030 some activities will be affected directly or indirectly in the fringe area of Dhaka city by land take. Among them agriculture, fisheries, recreation, flood control etc. are mentionable. It is clearly shown in Figure 35 that approximately 20% of the present urban fringe area will be converted to built-up. In Figure 36, flood-prone areas are overlaid to the probability map of 2030. The flood-prone zone has been digitized from a map of the Bangladesh Centre for Advanced Studies showing flooded areas during the 1998 flood (Cox, 2012). This severe flood affected two-thirds of the country and made 30 million people homeless. It is evident in Figure 36 that a lot of the foreseen urbanization pressure is within the flood-prone areas.

Figure 35. Mostly affected areas are shown in circle due to future urban expansion.
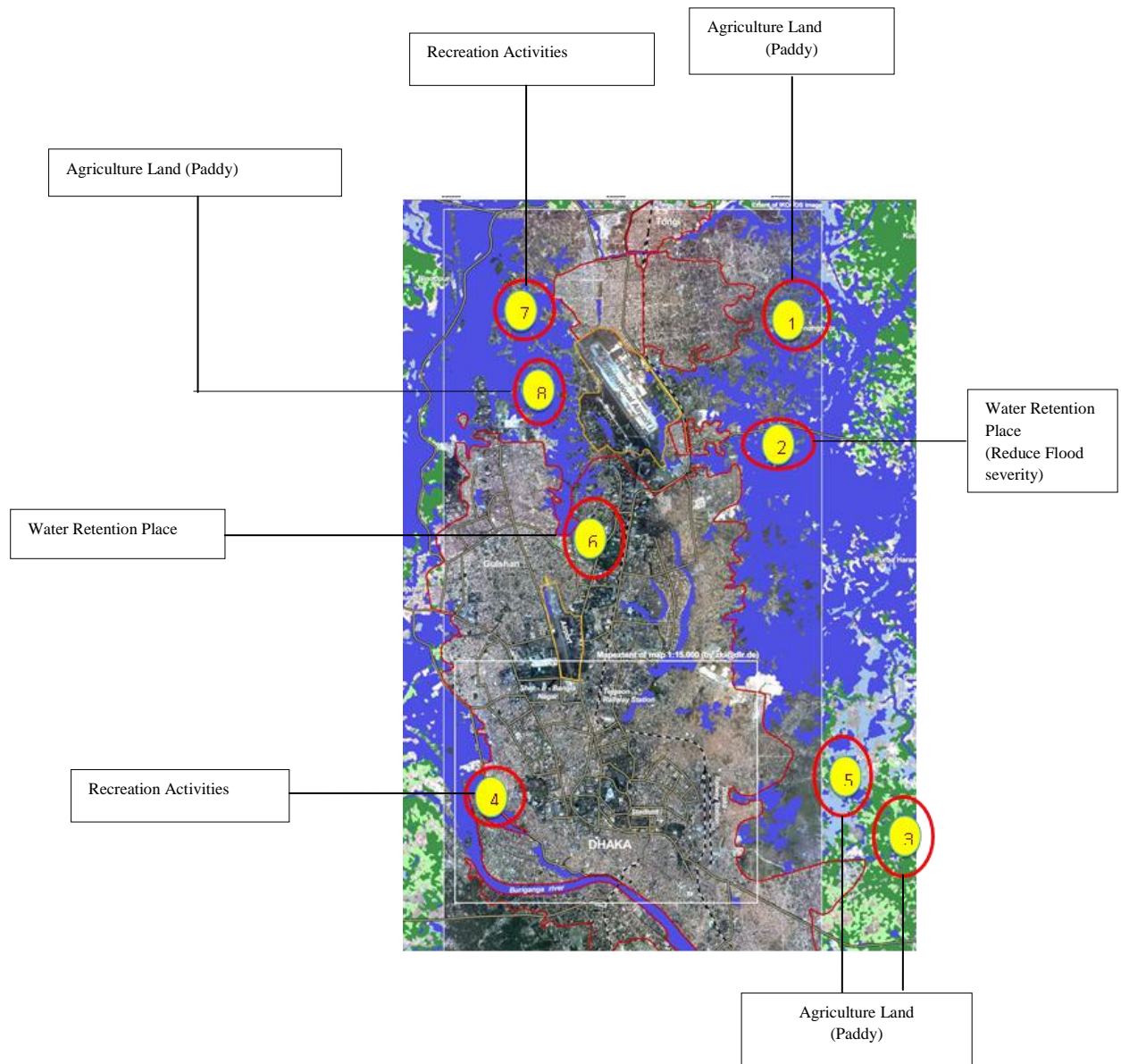
Source: Own elaboration

Figure 36. Flood-prone areas overlaid to the urban extend probability map for 2030.
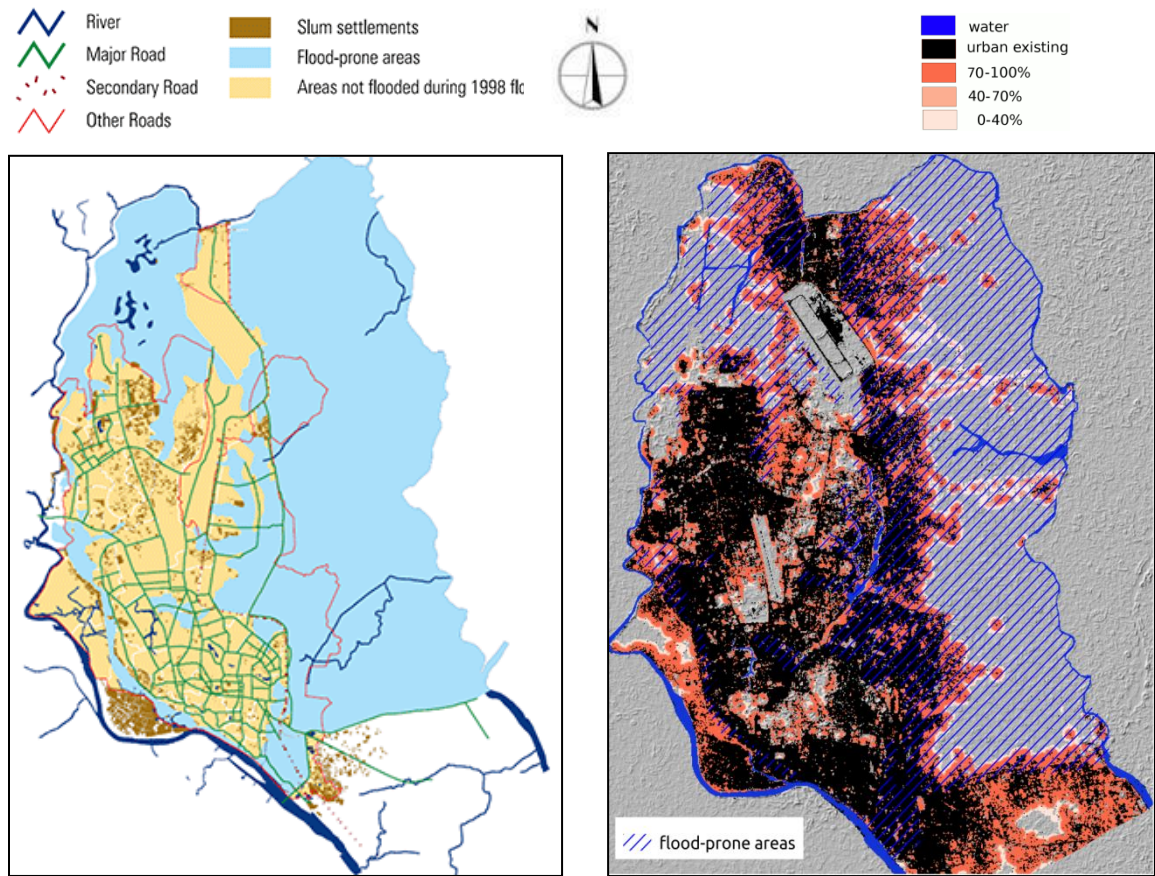
Source: Own elaboration and Cox, 2012.

Chapter 5: Concluding remarks

Urban growth and land use change models are already being applied for planning decision making in industrialized countries. As an integrated part of planning Decision Support System (DSS), urban models are now also proved to be an effective mean for public participation in urban and regional planning. But in developing countries, the application of urban models is very scarce and planning decision making process is lagging far behind here than those of the industrialized countries. The application of SLEUTH in developing countries like Bangladesh is unique in multiple ways. Cities such as Dhaka expand rapidly and are unplanned, while local data and know-how of planning models are limited. In that respect, SLEUTH is a very suitable approach, because it can efficiently model urban growth dynamics in a relatively straightforward manner, using a relatively minimal input dataset. Input data can currently be created even when local datasets are limited. In specific, land cover data can be derived from the LANDSAT sensor series, globally, for the past forty years. Digital Elevation Data are obtained from SRTM or similar semi-globally available datasets. The transportation network can be based on on-line databases such as Google maps or OpenStreetMap.org and completed with conventional historical locally available maps. It is quite important, especially for developing countries, that SLEUTH is provided at no cost, while sufficient examples exist in the literature to aid newcomers in the field. This context shows why local planning authorities can indeed be equipped with such models. Another factor contributing to the uniqueness of applying SLEUTH in Dhaka is that the process of urbanization is very different compared to industrialized parts of the globe. For example, in the time-frame of this study (1989-2014) the population of Europe (EU28) has increased by 6.5%, whereas in Bangladesh the increase for the same period is almost 50%. In terms of car ownership, which clearly affects road gravity in the model, merely one in a thousand inhabitants in Dhaka owns a car when non-motorized vehicles are excluded (Mannan and Karim, 2001), whereas for Europe this is almost one in two.

Overall, in the case of Dhaka, SLEUTH provided a very useful insight not only of the magnitude of future expansion but most importantly of its spatial pattern. This insight is crucial to maintain sustainable urbanization and control population density by balancing between population growth and urban expansions. Additionally, the prediction of the spatial pattern of the pressure for urbanization can be combined with flooding plans and

models as the area suffers from catastrophic floods during the rainy season that cause severe damage. Subsequently, expansion can be relaxed towards safer areas where water and drainage management plans can be prepared to continue the natural flow of water. Conversely, pressure for expansion in areas at risk can be anticipated based on SLEUTH's output and controlled so that land can be preserved for water runoff to reduce the over-flowing and flooding. A policy regarding Satellite cites or multiple development centres should be formulated around Dhaka city to reduce the pressure of internal migration to Dhaka.

References

European Automobile Manufacturers Association (2014) *The Automobile Industry Pocket Guide 2014-15*. Brussels: ACEA Communications department, pp. 68-72.
Available at: http://www.acea.be/uploads/publications/POCKET_GUIDE_2014-1.pdf [Last access 10 March 2015].

Acevedo, W. and Masuoka, P. (1997) "Time-series animation techniques for visualizing urban growth". *Computers and Geosciences,* **23** (4)**,** pp. 423-435.

Aerts, J.C.J.H., Clarke, K.C. and Keuper, A.D. (2003) "Testing popular visualization techniques for representing model uncertainty". *Cartography and Geographic Information Science,* **30** (3), pp. 249-261.

Albin, P.S. (1975) *The analysis of complex socio-economic systems*. Lexington, MA: Lexington Books.

Almeida, C.M., Monteiro, A.M.V., Camara, G., Soares-Filho, B.S., Cerqueira, G.C. and Pennachin, C.L. (2002) "Modeling urban land use dynamics through Bayesian probabilistic methods in a cellular automaton environment". In *Proceedings of the 29th International Symposium on Remote Sensing of the Environment*. Buenos Aires, Argentina, 8–12 April.

Alpkokin, P., Cheung, C., Black, J. and Hayashi, Y. (2008) "Dynamics of clustered employment growth and its impacts on commuting patterns in rapidly developing cities". *Transportation Research Part A: Policy and Practice*, **42** (3), pp. 427-444.

Anas, A. and Kim, I. (1996) "General equilibrium models of polycentric urban land use with endogenous congestion and job agglomeration". *Journal of Urban Economics*, **40** (2), pp. 232-256.

Arthur, S.T. (2001) *A satellite based scheme for predicting the effects of land cover change on local microclimate and surface hydrology*. PhD thesis. Department of Meteorology, Pennsylvania State University.

Barnes, K.B., Morgan J.M., Roberge, M.C. and Lowe, S. (2001) *Sprawl development: Its pattern, consequences and measurements*. Towson, MD: Centre of Geographic Information Sciences, Towson University.

Barredo, J.I., Kasanko, M., McCormick, N. and Lavalle, C. (2003) "Modelling dynamic spatial processes: Simulation of urban future scenarios through cellular automata". *Landscape and Urban Planning*, **64** (3), pp. 145-160.

Batty, M. (2000) "Geocomputation using cellular automata". In: Openshaw, S. (ed.) *Geocomputation*. London: Taylor & Francis, pp. 95-126.

Batty, M., Longley, P. and Fotheringham, S. (1989) "Urban growth and form: Scaling, fractal geometry and diffusion-limited aggregation". *Environment and Planning* A, **21** (11), pp. 1447-1472.

Batty, M. and Longley, P. (1994) *Fractal cities: A geometry of form and function*. London: Academic Press.

Batty, M., Xie, Y., and Sun, Z. (1999) "Modelling urban dynamics through GIS-based cellular automata". *Computers Environment and Urban Systems*, **23** (3), pp. 205-233.

Bayat, A. and Denis, E. (2000) "Who is afraid of ashwaiyyat?: Urban change and politics in Egypt". *Environment and Urbanization*, **12** (2), pp. 185-199.

Benenson, I. (1998) "Multi-agent simulations of residential dynamics in the city". *Computers Environment and Urban Systems*, **22** (1), pp. 25-42.

Bertaud, A. (2003) "The spatial organization of cities: Deliberate outcome or unforeseen consequence?" In World Bank (ed.) *World development report 2003*: *Dynamic development in a sustainable world*. Washington: World Bank.

Bhatta, B. (2009) "Modeling of urban growth boundary using geoinformatics". *International Journal of Digital Earth*, **2**(4), pp. 359-381.

Bierwagen, B. (2003) *The effects of land use change on butterfly dispersal and community ecology*. PhD thesis. Bren School of Environmental Management and Science, University of California, Santa Barbara.

Boyce, R.R. (1963) "Myth versus reality in urban planning". *Land Economics,* 39 (3), pp. 241-251.

Breheny, M. (1997) "Urban compaction: Feasible and acceptable?" *Cities*, **14** (4), pp. 209-217.

Brueckner, J.K., Thisse J.F. and Zenou, Y. (1999) "Why is central Paris rich and downtown Detroit poor?: An amenity-based theory". *European Economic Review,* **43** (1), pp. 91-107.

Cadwallader, M. (1996) *Urban geography: An analytical approach*. Upper Saddle River, NJ: Prentice Hall.

Candau, J. (2000) "Visualizing modeled land cover change and related uncertainty". In *First International Conference on Geographic Information Science*. Savannah, GA, 28-31 October.

Candau, J. (2002) *Temporal calibration sensitivity of the SLEUTH urban growth model*. Master thesis. Department of Geography, University of California.

Candau, J. and Clarke, K.C. (2000) "Probabilistic land cover modeling using deltatrons". In *Proceedings of the 38th Annual Conference of the Urban Regional Information Systems Association*. Orlando, FL.

CEC (1999) *European spatial development perspective: towards balanced and sustainable development of the territory of the European Union*. Luxembourg: The European Commission.

CEC (2006a) *Urban sprawl in Europe: the ignored challenge, European Environmental Agency EEA Report No 10/2006*. Copenhagen: European Environment Agency (EEA).

CEC (2006b) *Thematic strategy on the urban environment*, *11 November, COM (2005) 718 final*. Brussels: The European Commission.

CEC (2010) *Declaration following the Informal ministerial meeting on urban development*. Commission of the European Communities, 22 June. Toledo, Spain, p.17.

CEC (2011) *Territorial Agenda of the European Union 2020: towards an inclusive, smart, and sustainable Europe of diverse regions, 19 May*. Hungary.

CGIS (2010) "*Urban Sprawl*". Towson University Center for Geographic Information Sciences, Available at http://chesapeake.towson.edu/landscape/urbansprawl [Last access 10 March 2015].

Chalkias, C., Petrakis, M., Psiloglou, B. and Lianou, M. (2006) "Modelling of light pollution in suburban areas using remotely sensed imagery and GIS". *Journal of Environmental Management* **79** (1), pp.57-63.

Chaudhuri, G. and Clarke, K. C. (2013) "The SLEUTH Land Use Change Model: A Review" *The International Journal of Environmental Resources Research* **1** (1), pp. 88-104.

Cheng, J. (2003) *Modeling spatial and temporal urban growth*. PhD thesis. Faculty of Geographical Sciences, Utrecht University.

Cheng, J. and Masser, I. (2003) "Urban growth pattern modeling: A case study of Wuhan city, PR China". *Landscape & Urban Planning*, **62** (4), pp. 199-217.

Chowdhury, A.M., and Faruqui, S. (1989) "Physical growth of Dhaka city". In: Ahmed S.U. (ed.) *Dhaka: Past, present and future*. Dhaka: The Asiatic Society of Bangladesh.
Claggett, P., Jantz, C.A., Goetz, S.J. and Bisland, C. (2004) "Assessing development pressure in the Chesapeake Bay watershed: An evaluation of two land-use change models". *Environmental Monitoring and Assessment*, **94** (1-3), pp. 129-46.

Clarke, K.C. (1997) "Land use modeling with deltatrons". In *NCGIA*. *The Land Use Modeling \workshop*. Sioux Falls, SD, 5-6 June. Available at http://www.ncgia.ucsb.edu/conf/landuse97 [Last access 12 March 2015].

Clarke, K.C., Hoppen, S., and Gaydos, L. (1997) "A self-modifying cellular automaton model of historical urbanization in the San Francisco Bay area". *Environment and Planning B: Planning & Design*, **24** (2), pp. 247-261.

Clarke, K.C., and Gaydos, L. (1998) "Loose-coupling a cellular automaton model and GIS: Long-term urban growth prediction for San Francisco and Washington/Baltimore". *International Journal of Geographic Information Science* **12** (7), pp. 699-714.

Clarke, K.C. and Couclelis, H.M. (1999) *Developing an integrated modeling environment for urban change research: Methodological and theoretical challenges*. Proposal submitted to 1998 US-NSF urban initiative solicitation. Santa Barbara: UCSB/NCGIA.

Cogan, C.B., Davis, F.W. and Clarke, K.C. (2001) *Application of urban growth models and wildlife habitat models to assess biodiversity losses*. Gap Analysis Program. University of California-Santa Barbara Institute for Computational Earth System Science, U.S. department of the Interior, US geological Survey, Biological Resources Division, Santa Barbara, CA.

Cohen, B. (2006) "Urbanization in developing countries: Current trends, future projections, and key challenges for sustainability". *Technology in Society*, **28** (1-2), pp. 63-68.

Collins, J.P., Kinzig, A., Grimm, N.B., Fagan, W.F., Hope, D., Wu, J. and Borer, E.T. (2000) "A new urban ecology". *American Scientist*, **88** (5), pp. 416-425.

Cornell University (2013) *The Game of Life, CS1114 Section 9,* Department of Computer Science, Cornell University. Available at http://www.cs.cornell.edu/courses/cs1114/2013sp/sections/S09_gameoflife.pdf   [Last access 4 March 2015].

Couclelis, H. (1985) "Cellular worlds: A framework for modeling micro-macro dynamics". *Environment and Planning A*, **17** (5), pp. 585-596.

Couclelis, H. (1989) "Macrostructure and microbehavior in a metropolitan area". *Environment and Planning B*, **16** (2), pp. 141-154.

Desai, V. and Potter, B.R. (2002) *The companion to development studies*. New York: Oxford University Press.

Dietzel, C.K., and Clarke, K.C. (2004) "Spatial differences in multi-resolution urban automata modeling". *Transactions in GIS*, **8** (4), pp. 479-492.

Dietzel, C., and Clarke, K.C. (2007) "Toward optimal calibration of the SLEUTH land use change model". *Transactions in GIS*, **11** (1), pp. 29-45.

Ewing, R. (1994) "Characteristics, causes and effects of sprawl: a literature review". In: J. Matzluff, et al., (eds) *Urban ecology: an international perspective on the interaction between humans and nature*. New York: Springer, pp. 519-535.

Ewing, R. (1997) "Is Los Angeles-style sprawl desirable?" *Journal of the American Planning Association*, Winter, **63** (1), pp.107-126.

Frenkel, A. and Ashkenazi, M. (2008) "Measuring urban sprawl: how can we deal with it?" *Environment and Planning B: Planning and Design*, **35** (1), pp. 56-79.

Fujita, M., Krugman, P.R. and Venables, A.J. (2001) *The spatial economy: Cities, regions and international trade*. Cambridge, MA: MIT Press.

Gardner, M. (1970) "Mathematical games – The fantastic combinations of John Conway's new solitaire game life." Scientific American, **223** (4), pp.120–123.

Garreau, J. (1991) *Edge city: Life on the new frontier*. New York: Doubleday.

Giuliano, G. (1989) "New directions for understanding transportation and land use". *Environment and Planning A*, **21** (2), pp.145-159.

Goldstein, N.C., Candau, J. and Moritz, M. (2000) "Burning Santa Barbara at both ends: A study of fire history and urban growth predictions". In *Proceedings of the 4th International Conference on Integrating GIS and Environmental Modeling: Problems, Prospects, and Research Needs)*. Banff, Alberta, Canada, 2-8 September.

Goldstein, C (2004) "Brains vs. Brawn: Comparative strategies for the calibration of a cellular automata-based urban growth model". In Atkinson, P., Foody, G.M., Darby, S.E. and Wu, F. (eds) *Geodynamics.* Boca Raton: CRC Press.

Goldstein, N.C., Candau, J. T. and Clarke, K. C. (2004) "Approaches to simulating the march of bricks and mortar". *Computers, Environment and Urban Systems*, **28** (1-2), pp. 125-147.

Gordon, P. and Richardson, H. (1997) "Are compact cities a desirable planning goal?" *Journal of the American Planning Association*, *winter,* **63** (1), pp. 95-106.

Grimm, N.B., Faeth, S.H., Golubiewski, N.E., Redman, C.L., Wu1, J., Bai, X. and Briggs, J.M. (2008) "Global change and the ecology of cities". *Science*, **319** (5864), pp. 756-760.

Guardian (2015) *The urbanist's guide to Dhaka, Bangladesh: 'an unplanned sprawl.* Available at http://www.theguardian.com/cities/2014/aug/19/an-urbanists-guide-to-dhaka-an-unplanned-urban-sprawl [Last access 2 March 2015].

Guth, D., Holz-Rau, C. and Maciolek, M. (2009) "Employment, suburbanization and commuter traffic in German city regions". In *9th Swiss Transport Research Conference.* Ascona, Switzerland, 9-11 September.

Haack, B.S., Guptill, S., Holz, R., Jampoler, S., Jensen, J. and Welch, R. (1997) "Urban analysis and planning". In: W.R. Philipson. (ed.) *Manual of photographic interpretation.* Bethesda, MD: Asprs.

Hall, P. (1999) "The future of cities". *Computers, Environment and Urban Systems,* **23** (3), pp. 173-185.

Herold, M., Goldstein, N.C. and Clarke, K.C. (2003) "The spatio-temporal form of urban growth: Measurement, analysis and modeling". *Remote Sensing of Environment,* **86** (3), pp. 286-302.

Islam, I. (2012) *Threats on the Existing Lakes/ Water Bodies in Dhaka.* Available at http://cseindia.org/userfiles/Ishrat%20Islam_BUET_E-Sept26-2012.pdf [Last access 12 January 2015].

Islam, N. (1999) "Urbanization, migration and development in Bangladesh: Recent trends and emerging issues". *CPD-UNFPA Series,* 1. Dhaka: Centre for Policy Dialogue.

Jackson, K. (1985) *Crabgrass frontier: The suburbanization of the United States*. Oxford: Oxford University Press.

Jantz, C.A., Goetz, S.J., and Shelley, M.K. (2003) "Using the SLEUTH urban growth model to simulate the impacts of future policy scenarios on urban land use in the Baltimore-Washington metropolitan area". *Environment and Planning B: Planning and Design*, **30** (2), pp. 251-271.

Japan International Cooperation Agency (JICA), (1992) *Feasibility study of Greater Dhaka Flood Protection Project, FAP 8A Interim and Main Reports*. Flood Plan Coordination Organization (presently WARPO), Dhaka, Bangladesh.

Kam, W.C. (1994) *Cities with invisible walls: Reinter presenting urbanization in post-1949 china*. Hong Kong: Oxford University Press.

Kasanko, M., Barredo J.I., Lavalle, C., McCormick, N., Demicheli, L., Sagris, V. and Brezger, A. (2006) "Are European cities becoming dispersed? A comparative analysis of 15 European urban areas". *Landscape and Urban Planning,* **77** (1-2), pp.111-130.

Kier, L.B., Seybold, P.G. and Cheng, C.K. (2005) *Modeling chemical systems using cellular automata*. Amsterdan: Springer.

Knox, P. (1995) *Urban social geography: An introduction*. London: Longman.

Leão, S., Bishop, I., and Evans, D. (2004) "Spatial-temporal model for demand allocation of waste landfills in growing urban regions". *Computers Environment and Urban Systems*, **28** (4), pp. 353-385.

Lin, Y.P., Lin, Y.B., Wang, Y.T. and Hong, N.M. (2008) "Monitoring and predicting land-use changes and the hydrology of the urbanized Paochiao watershed in Taiwan using remote sensing data, urban growth models and a hydrological model*". Sensors,* **8** (2), pp. 658-680.

Liu, X.H. and Andersson, C. (2004) "Assessing the impact of temporal dynamics onland-use change modeling". *Computers, Environment and Urban Systems,* **28** (1-2), pp. 107-124.

Lloyd-Jones, T. and Erickson, B. (1997) "Rule-based models as planning tools: Three prototypes". In: Sikdar, P.K., et al. (eds.) *Computers in urban planning and management*. New Delhi: Narosa Publishing House.

Malik, A. (1989) "Muslim cities, recent history and possible future". In Sardar, Z. (ed.) *An early cresent: The future of knowledge and the environment in Islam*. London: Mansell, pp. 198–220.

Mannan, M.S. and Karim, M.M. (2001) "Current State of the Mobility of the Urban Dwellers in Greater Dhaka". *Paper for Presentation for 94th Annual Conference and Exhibition of Air and Waste Management Association*. 24-28 June, 2001. Orlando, Florida, USA.

Maplandia.com (2005) *Bangladesh Google satellite map*. Available at http://www.maplandia.com/bangladesh. [Last access 10 March 2015].

Maerivoet, S. and Moor, B.D. (2005) "Cellular automata models of road traffic". *Physics Reports*, **419** (1), pp. 1-64.

Mills, E.S. (1972) *Studies in the structure of the urban economy*. Baltimore: John Hopkins Press.

Mills, E.S. and Luan, S.L. (1997) "Inner cities". *Journal of Economic Literature*, **35** (2), pp. 727-756.

Moeller, M.S. (2005) "Remote sensing for the monitoring of urban growth patterns". In *Joint Symposium URBAN-URS*. Tempe, AZ, USA, 14-15 March.

Muller, P.O. (1981) *Contemporary suburban America.* Englewood Cliffs, NJ: Prentice Hall.

Muth, R.F.(1969) *Cities and housing.* Chicago: The University of Chicago Press.

Myllyla, S. (2001) *Street environmentalism: Civic associations and environmental practices in the urban governance of Third World megacities.* PhD thesis. Department of Regional Studies and Environmental Policy, University of Tampre, Finland.

National Taiwan University (NTU), (2012) *Game of Life.* Network and Systems Laboratory, Department of Electrical Engineering, NTU, Taiwan.
Available at http://nslab.ee.ntu.edu.tw/~brian/introCS/homework/essay-2/p2-22-0518-1702.pdf. [Last access 5 February 2015].

Neuman, M. (2005) "The compact city fallacy". *Journal of Planning Education and Research*, **25**, pp.11-26.

Oguz, H., Klein, A. and Srinivasan, R. (2007) "Using the Sleuth urban growth model to simulate the impacts of future policy scenarios on urban land use in the Houston-Galveston-Brazoria CMSA". *Research Journal of Social* Sciences, **2**, pp. 72-82.

Osaragi, T. and Kurisaki, N. (2000) "Modeling of land use transition and its application". *Geographical & Environmental Modeling*, **4** (2), pp. 203-218.

O'Sullivan, A. (2002) *Urban economics*. New York: Irwin/McGraw-Hill.

O'Sullivan, D. and Torrens, P.M. (2000) "Cellular models of urban systems". *CASA Working Paper 22*. Centre for Advanced Spatial Analysis, University College London.

Patterson, Z. and Bierlaire, M. (2010) "Development of prototype UrbanSim models". *Environment and Planning B: Planning and Design* **37** (2), pp. 344- 366.

Perlman, J. (1990) "A dual strategy for deliberate social change in cities". *The International Journal of Urban Policy and Planning*, **7** (1), pp. 3-15.

Pijanowski, B.C., Brown, D.G., Shellitoc, B.A. and Manikd, G.A. (2002) "Using neural networks and GIS to forecast land use changes: A land transformation model". *Computers, Environment and Urban Systems*, **26** (6), pp. 553-575.

Project Gigalopolis (2014a) *Data Input.* Available at http://www.ncgia.ucsb.edu/projects/gig/About/dtInput.htm [Last access 15 March 2015].

Project Gigalopolis (2014b) *Edge growth.* Available at http://www.ncgia.ucsb.edu/projects/gig/About/gwEdge.htm [Last access 15 March 2015].

Project Gigalopolis (2014c) *New Spreading Center Growth.* Available at http://www.ncgia.ucsb.edu/projects/gig/About/gwNewCenter.htm [Last access 15 March 2015].

Project Gigalopolis (2014d) *Self Modification.* Available at http://www.ncgia.ucsb.edu/projects/gig/About/gwSelfMod.htm. [Last access 15 March 2015].

Project Gigalopolis (2014e) *SLEUTH Applications.* Available at *http://www.ncgia.ucsb.edu/projects/gig/Repository/SLEUTHapplications.htm.* [Last access 15 March 2015].

Project Gigalopolis (2014f) *Spontaneous growth.* Available at http://www.ncgia.ucsb.edu/projects/gig/About/gwSpontaneous.htm [Last access 15 March 2015].

Rana, M.M.P. (2010) "Urbanization and sustainability: Challenges and strategies for sustainable urban development in Bangladesh". *Environment, Development and Sustainability*, **13** (1), pp. 237-265.

Razin, E. and Rosentraub, M. (2000) "Are fragmentation and sprawl interlinked? North American evidence". *Urban Affairs Review*, **35** (6), pp. 821-836.

Sangawongse, S., Sun, C.H., and Tsai, B.W. (2005) "Urban growth and land cover change In Chiang Mai and Taipei: Results from the SLEUTH model". In: Zerger, A. and Argent, R.M. (eds.) *MODSIM 2005 International Congress on Modeling and Simulation*. Modeling and Simulation Society of Australia and New Zealand.

Santé, I., García, A.M., Miranda, D. and Crecente, R. (2010) "Cellular automata models for the simulation of real-world urban processes: A review and analysis". *Landscape and Urban Planning*, **96** (2), pp. 108-122.

Schneider, A. and Woodcock, C. (2008) "Compact, dispersed, fragmented, extensive? A comparison of urban growth in twenty-five global cities using remotely sensed data, pattern metrics and census information". *Urban Studies*, 45 (3), pp. 659-692.

Shankland Cox Partnership and Others (1981) *Dhaka metropolitan area integrated urban development project.* Dhaka: Planning Commission, Government of Bangladesh.

Shenghe, L. and Sylvia, P. (2002) "Spatial patterns and dynamic mechanisms of urban land use growth in China: Case study in Beijing and Shanghai". *IIASA Interim Report,* 02-005. Laxenburg: IIASA.

Siddiqui, M.Z., Everett, J.W. and Vieux, B.E. (1996) "Land fill siting using geographic information systems: A demonstration". *Journal of Urban Planning and Development,* **122** (6), pp. 515-523.

Silva, E.A. and Clarke, K.C. (2002) "Calibration of the SLEUTH urban growth model for Lisbon and Porto, Portugal". *Computers, Environment and Urban Systems*, **26** (6), pp. 525-552.

Singh, A.K. (2003) *Modelling land use land cover changes using cellular automata in a geo-spatial environment*. Master thesis. International Institution for Geo-Information and Earth Observation, Enschede, The Netherlands.

Smailes, A. (1966) *The geography of towns*. London: Hutchinson.

Soltani, A. (2004) "Towards modeling urban growth using cellular automata (CA) and GIS". *Research Report*. Adelaide: University of South Australia.

Stalker, P. (2000) *Handbook of the world*. New York: Oxford University Press.

Stathakis, D. and Vasilakos, A. (2006) "Comparison of several computational intelligence based classification techniques for remotely sensed optical image classification". *IEEE Transactions in Geoscience and Remote Sensing*, **8** (44), pp. 2305-2318.

Stathakis, D. (2009) "How many hidden layers and nodes?" *International Journal of Remote Sensing,* **8** (30), pp. 2133-2147.

Stathakis, D. and Tsilimigkas, G. (2014) "Measuring the compactness of European medium-sized cities by spatial metrics based on fused data sets". *International Journal of Image and Data Fusion.***6** (1), pp. 42-64.

Theobald, D.M. (2001) "Land-use dynamics beyond the American urban fringe". *Geographical Review,* **91** (3), pp. 544-564.

Tobler, W.R. (1970) "A computer movie simulating urban growth in the Detroit region". *Economic Geography*, **46** (2), pp. 234-240.

Tobler, W.R. (1979) "Cellular geography". In: Gale, S. and Olsson, G. (eds.) *Philosophy in geography*. Dordrecth: Reidel, pp. 339-346.

Torrens, P.M. (2000) "How cellular models of urban systems work". *CASA Working Paper 28*. Centre for Advanced Spatial Analysis, University College London.

Torrens, P. M. (2008) "A toolkit for measuring sprawl". *Applied Spatial Analysis and Policy*, **1**(1), pp. 5-36.

UIUC (2006) *Framework and methods: Analysis course lectures*. Department of Urban and Regional Planning, University of Illinois.

United Nations, Department of Economic and Social Affairs, Population Division (2014) "World urbanization prospects: The 2014 revision, methodology". *Working Paper,* No. ESA/P/WP.237.
USGS (2014) *EarthExplorer*. Available at http://www.ncgia.ucsb.edu/projects/gig/ [Last access 11 March 2015].

Veldkamp, A. and Lambin, E.F. (2001) "Editorial: Predicting land-use change". *Agriculture, Ecosystems and Environment,* **85** (1-3), pp. 1-6.

Waddell, P. (2002) 'UrbanSim: Modeling urban development for land use, transportation, and environmental planning', *Journal of the American Planning Association,* **68** (3), pp. 297-314.

Watanabe, H. (2012) *Monocentric city model*. Lecture slides. Economics Department, Washington University. Available at
http://d.umn.edu/~watanabe/econ460su12/docs/monoho.pdf [Last access 27 March 2015].

Wassmer, R. W. (2000) "Urban sprawl in a U.S. metropolitan area: ways to measure and a comparison of the Sacramento area to similar metropolitan areas in California and the U.S". *CSUS Public Policy and Administration Working Paper No. 2000–03*. Available at: http://papers.ssrn.com/sol3/papers.cfm?abstract_id=241975 [Last access 15 March 2015].

White, R. and Engelen, G. (1993) "Cellular automata and fractal urban form: A cellular modeling approach to the evolution of urban land-use patterns". *Environment and Planning A*, **25** (8), pp. 1175-1199.

Wilson, E. H., Hurd, J.D., Civco, D.L., Prisloe, M.P., and Arnold, C. (2003) "Development of a geospatial model to quantify, describe and map urban growth". *Remote Sensing of Environment*, **86**, pp. 275-285.

Wolfram, S. (1983) "Statistical mechanics of cellular automata". *Reviews of Modern Physics*, **55** (3), pp. 601-644.

World Bank (2007a) "Dhaka: Improving living conditions for the urban poor", Sustainable Development Unit, South Asia Region, Report No. 35824-BD. Available at
 http://siteresources.worldbank.org/BANGLADESHEXTN/Resources/295759-1182963268987/dhakaurbanreport.pdf [Last access 08 February 2015].

World Bank (2007b) "Dhaka metropolitan development plan: strategic environmental assessment", Washington DC: World Bank. Available at
http://documents.worldbank.org/curated/en/2007/07/17207304/dhaka-metropolitan-development-plan-strategic-environmental-assessment [Last access 3 March 2015].

Wu, F. (1996) "A linguistic cellular automata simulation approach for sustainable land development in a fast growing region". *Computers, Environment and Urban Systems*, **20** (6), pp. 367-837.

Wu, F. (2000) "A parameterised urban cellular model combining spontaneous and self-organizing growth". In Atkinson, P., and Martin, P. (eds) *GIS and Geocomputation: Innovations in GIS 7*. New York: Taylor and Francis, pp. 73-86.

Yang, X., and Lo, C.P. (2003) "Modelling urban growth and landscape change in the Atlanta metropolitan area". *International Journal of Geographical Information Science,* **17** (5), pp. 463-488.

Zhang, Q., Levin, N., Chalkias, C. and Letu, H. (forth.) "Nighttime light remote sensing: Monitoring human societies from outer space". In: Thenkabail, P.S. (ed.) *Remote sensing handbook*. London: CRC Press, Chapter 26.

Appendix A

Application of Sleuth Model in international Cities of the World

Geography		Research Group / Affiliation	Application
Country	**City**		
Australia	Sydney	The University of Southern Queensland	Urban Change
Brazil	Porto Alegre	The University of Melbourne.	Coupled Modeling
Cameroon	Yaounde	University of Melbourne, School of Anthropology	Urban Change
China	Chongqing	National University of Singapore	Urban change
	Changsha City	Central South University, China	Urban change
	Dianchi basin,	Nanjing University, China	Urban change
	Shenyang-Fushun	Chinese Academy of Science	Urban change
	Lanzhou	Lanzhou University, China	Urban change
	Nanjing	Suzhou University of Science and Technology, China	Urban change
	Hangzhou	Southwest University, China	Urban change
	Shenyang	Chinese Academy of Sciences	Urban change
	Xinxiang city	Suzhou University of Science and Technology, China.	Urban change
	Yingkou City	Chinese Academy of Sciences	Coupled Modeling
Egypt	Alexandria	Newcastle University	Urban Change
	Cairo	Cairo University	Urban Change
Finland	Helsinki	Polytechnic of Milan. Italy	Urban Change
	Helsinki-Turku	Tampere University of Technology	Urban Change
India	Hyderabad	University of Madras, India	Urban Change
	Pune	Bharati Vidyapeeth University	Urban Change
Italy	Palermo, Padova-Mestre	Polytechnic of Milan,	Urban Change
Iran	Mashad City	University of Tehran,	Urban Change
	Gorghan City	University of Agriculture and Natural Resources Sciences	Urban Change
Mexico	Tijuana	Université Paul Valéry	Urban Change
	Nogales-Sonora	US Geological Survey	Urban Change
	Mexico City	Paola Gomez, UCSB Bren School	Urban Change
Netherlands	Netherlands	Berlage Institute	Urban Change
Portugal	Lisbon	University of Massachusetts	Urban Change
	Porto	UCSB Geography	
Oman	Muscat	Sultan Qaboos University	Urban Change
Spain	Bilbao	Polytechnic of Milan	Urban Change
South Africa	Cape Town	Stellenbosch University, South Africa	Urban Change
Taiwan	Taipei	National Science Council of Taiwan	Urban Change
Thailand	Chiang Mai	National Science Council of Taiwan	Urban Change

Source: Adapted from Project Gigalopolis, 2014e

Application of Sleuth Model in international Cities of the World

Geography		Research Group / Affiliation	Application
Country	City		
USA	Atlanta, Georgia	Florida State University	Urban Change
USA	Austin, Texas	Tallahassee, Department of USGS/GD/RMMC*	Urban & Landuse Change
USA	Chester County, Pennsylvania	Penn State Meteorology and Atmospheric Science	Coupled Modeling
USA	Chicago, Illinois	USGS Urban Dynamics	Urban Change
USA	Colorado Frontrange	USGS/GD/RMMC*	Urban & Landuse Change
USA	Detroit, Michigon	USGS Eros Data Center	Urban Change
USA	Houston, Texas	Texas A&M University	Urban Change
USA	Albuquerque, New Mexico	USGS/GD/RMMC*	Urban Change
USA	Monterey Bay, California	UC Santa Cruz Environmental Studies / UCSB Geography	Biodiversity loss /model integration
USA	New York	Montclair State University	New York Climate and Health Project
USA	New York City	USGS/GD/RMMC*	Urban Change
USA	Oahu, Hawaii	University of Hawaii at Manoa	Urban Change
USA	Phoenix, Arizona	Arizona State University, School of Life Sciences	Urban Change
USA	San Antonio, Texas	USGS/GD/RMMC*	Urban & Landuse Change
USA	San Francisco, California	UCSB Geography / USGS Urban Dynamics	Urban Change
USA	San Joaquin Valley, California	UCSB Geography	Urban Change / Calibration testing
USA	Santa Barbara, California	UCSB Geography	Urban Change / Calibration testing
USA	Santa Monica Mountains, California	San Diego State University	Vegetation Succession
USA	Seattle Washington	USGS/GD/RMMC*	Urban Change
USA	Sioux Falls, South Dakota	UCSB Geography	development of GA
USA	Tampa, Florida	USGS/GD/RMMC*	Urban Change
USA	Washington, DC- Baltimore	University of Maryland, College Park, Department of Geography	Urban Change
USA	Washington	USGS/GD/RMMC* / UCSB Geography	Urban Change/ Change Visualization

Source: Adapted from Project Gigalopolis, 2014d

80

Appendix B

Photographs: Future urban sprawl will affect the following activities in urban fringe of Dhaka

A) Direct Use Values

Agriculture

Fisheries

Recreation

B) Indirect Use Values

Ground Water Recharge Function

Flood Control Function

Source: Islam, 2012

81

Appendix C

Photographs: Existing Traffic congestion in Dhaka city

Source: DEMOTIX, 2011

Appendix D

Installation instructions for the Sleuth

1. Installation of Cygwin
i. Download the Cygwin from www.cygwin.com/setup.exe
ii. It is better to put the installed files in the subfolder named Cygwin in C: / and not in another subfolder.

2. Files of Sleuth
i.Firstly, download the files (Sleuth3.0beta_p01 LINUX released 6/2005) from http://www.ncgia.ucsb.edu/projects/gig/Dnload/download.htm
ii. Save directly to a new folder in C:/ name Sleuth.

3. Import files
Slope – Land steepness
Land use - At least 2 years land coverage
Excluded – Restricted Areas where build up area is not developed.
Urban - At least 4 years urban land coverage.
Transport -At least 2 year road network.
Hill shade – Derived from Slope.

Images will follow three basic rules:
- Same limits

- Same projector

- Same resolution.

After preparing the above layers in GIS and Remote Sensing Software these images are converted into gray scale image format by using GIMP software. Here in case of urban layer 0 represent the non-built up area and 1 represent built up area. More information can be found at the site of the Sleuth model: http://www.ncgia.ucsb.edu/projects/gig/About/dtInput.html. The name of each file is of the form (area. layer name.gif)(for example, dhaka.excluded.gif or dhaka.urban.2000.gif).

4. Implementation of the Sleuth:
The Sleuth runs through Cygwin, so it will open with administrator privileges (right click --> Run as administrator - run as administrator)
The basic command is:
 "cd": Change Directory - Change folder
 "ls": List Files - Displays all files
 "cd .. ": goes to previous folder/directory
 "make clean" and
 "make"

5. Editing the files scenario:
n the folder (C: /Sleuth/Scenarios) the scenarios files are copied and pasted in the same folder with a different name. The name will be of the form scenario. (area)_(mode) (e.g. scenario.dhaka_predict. A very good free editor for files written in the language C is Netbeans, which can be download from http://netbeans.org/downloads/start.html. After download the netbeans and installed, we can start to work through the scenarios.

In detail the exact steps to be followed:
Open a Cygwin terminal with administrator rights
cd C: /
cd SLEUTH (to get the file of SLEUTH)
cd Whirlgif (---------- // ---------------------- of whirlgif)
make clean (I'll write the procedure, and after you finish continued)
make (----------------------------------- // ---------- ---)
cd .. (turns back to the file of the SLEUTH)
cd GD (to go to GD)
make clean
make

For the compilation/translation
" .. /grow.exe (one of the calibrate, predict, test) (the name of the scenario, e.g. scenario.dhaka_calibrate)

For the forecast the command would be
" .. /grow.exe predict scenario.demo200_predict"

6. Calibration of the model
After finishing the procedure for the compilation, calibration process is started. This process takes a long time and wants enough attention to implementation. The setting range of the above variables is via an output file which after examination shows changes these variables through statistics. One of the methods for setting variable is the OSM (Optimum SLEUTH Metric) and results outputs can be used to introduce the range of variables will have the best performance. Optimal coefficients for the model may be found through the process Lee-Salee Metric, for finding which followed a more time consuming process, but with more accurate results. These two these methods can determine optimal values for the process of forecasting (prediction best fit) after multiple tests.

Phase 1
In particular, for the application of the method followed 3 stages: coarse, fine and final calibration (Source: http://www.ncgia.ucsb.edu/projects/gig/Imp/imCalibrate.htm). For the purposes the first (coarse) stage, some elements of the scenario calibration (calibration) is changed as follows:
Monte Carlo Iterations: 4-5. All variables (Coefficients) to have the values:

◦ Start: 0
◦ Stop: 100
◦ Step: 25

Here detail is shown in http://www.ncgia.ucsb.edu/projects/gig/Imp/calCoarseSelect.htm [Last access 03 March 2015].

Phase 2
After run the scenario with the above data it is required to go to the directory C: / SLEUTH / Output / dhaka_cal and to open the file control_stats.log. Then, the data will be sorted by descending order based on OSM value. The first 10 parameter sets are taken as the best fit parameter combinations. From these values it is required to subtract the smaller and larger, which are placed as start and stop values respectively for the next phase of calibration. Furthermore, step as the value for the next phase of calibration should place a number which results from the difference between the start and stop value, by a number between 4-6. Here 7-8 Monte Carlo iterations were used.

Coefficient ranges	Coefficients				
	Diffusion	Breed	Spread	Slope	Road
Start	0	0	75	0	0
Step	5	20	5	5	20
_ Stop	20	100	100	25	100

For example, if the table shows that for the next phase of the domain is 0-20, then step will be 5. Here detail is shown in (http://www.ncgia.ucsb.edu/projects/gig/Imp/calFineSelect.htm).

Phase 3
After executing the second calibration phase (fine calibration), the file control_stats.log is opened. Again the first 10 parameter sets are taken as the best fit parameter combinations. From these values it is required to subtract the smaller and larger, which are placed as start and stop values respectively for the next phase of calibration. Furthermore, step as the value for the next phase of calibration should place a number which results from the difference between the start and stop value, by a number between 4-5. Here 8-10 Monte Carlo iterations were used

Coefficient ranges	Coefficients				
	Diffusion	Breed	Spread	Slope	Road
Start	0	20	80	0	40
_ Step	5	8	4	3	12
Stop	20	60	100	15	100

Here detail is shown in (http://www.ncgia.ucsb.edu/projects/gig/Imp/calFinalSelect.htm).

Phase 4
After executing the final calibration phase (final calibration), the file control_stats.log is opened. In this case only the first coefficient set is selected based on the performance of the OSM. Table 3.7 shows that for model diffusion value 1, breed value 28, spread value 96, slope resistance value 1 and road gravity of 52 produces the optimum OSM of 0.384. These are the starting coefficient values that produced the optimum goodness of fit to the control layers. But SLEUTH through its self-modification characteristics change these values. For deriving the forecasting coefficients, another calibration run was conducted with the data using these best fit coefficients (showed in Table 3.7) with 110 Monte Carlo iterations.

Coefficient ranges	Coefficients				
	Diffusion	Breed	Spread	Slope	Road
Start	1	28	96	1	52
Step	1	1	1	1	1
_ Stop	1	28	96	1	52

Here detail is shown in http://www.ncgia.ucsb.edu/projects/gig/Imp/calForecastSelect.htm).

Urban growth prediction
After executing the forecasting phase the file control_stats.log is opened. It shows that for model forecasting diffusion value 1, breed value 36, spread value 100, slope resistance value 1 and road gravity of 56. Best fit coefficients derived through the calibration process were applied for predicting future growth scenario of the study area. It is done through the prediction mode of the SLEUTH model. The scenario.log file was updated for this purpose where the calibrated forecasting coefficients were mentioned in the PREDICTION_*_BEST_FIT flag (where * indicate the name of the coefficient). 110 MONTE_CARLO_ITERATIONS were used for the prediction runs for getting the optimum result which was also indicated in the scenario.log file. Here detail is shown in (http://www.ncgia.ucsb.edu/projects/gig/Imp/imPredict.htm

85

Appendix E

Source code of Coarse calibration

```
FILE: 'scenario file' for SLEUTH land cover transition model
#      (UGM  v3.0)
#      Comments start with #
#
#  I. Path Name Variables
# II. Running Status (Echo)
# III. Output ASCII Files
# IV. Log File Preferences
#  V. Working Grids
# VI. Random Number Seed
# VII. Monte Carlo Iteration
#VIII. Coefficients
#     A. Coefficients and Growth Types
#     B. Modes and Coefficient Settings
# IX. Prediction Date Range
#  X. Input Images
# XI. Output Images
# XII. Colortable Settings
#     A. Date_Color
#     B. Non-Landuse Colortable
#     C. Land Cover Colortable
#     D. Growth Type Images
#     E. Deltatron Images
#XIII. Self Modification Parameters


# I.PATH NAME VARIABLES
#   INPUT_DIR: relative or absolute path where input image files and
#          (if modeling land cover) 'landuse.classes' file are
#          located.
#   OUTPUT_DIR: relative or absolute path where all output files will
#           be located.
#   WHIRLGIF_BINARY: relative path to 'whirlgif' gif animation program.
#            These must be compiled before execution.
INPUT_DIR=../Input/dhaka/
OUTPUT_DIR=../Output/dhakacoarse/
WHIRLGIF_BINARY=../Whirlgif/whirlgif


# II. RUNNING STATUS (ECHO)
#  Status of model run, monte carlo iteration, and year will be
#  printed to the screen during model execution.
ECHO(YES/NO)=yes


# III. Output Files
# INDICATE TYPES OF ASCII DATA FILES TO BE WRITTEN TO OUTPUT_DIRECTORY.
#
#   COEFF_FILE: contains coefficient values for every run, monte carlo
#          iteration and year.
#   AVG_FILE: contains measured values of simulated data averaged over
#         monte carlo iterations for every run and control year.
#   STD_DEV_FILE: contains standard diviation of averaged values
#          in the AVG_FILE.
#   MEMORY_MAP: logs memory map to file 'memory.log'
#   LOGGING: will create a 'LOG_#' file where # signifies the processor
#        number that created the file if running code in parallel.
#        Otherwise, # will be 0. Contents of the LOG file may be
#        described below.
WRITE_COEFF_FILE(YES/NO)=yes
WRITE_AVG_FILE(YES/NO)=yes
WRITE_STD_DEV_FILE(YES/NO)=yes
WRITE_MEMORY_MAP(YES/NO)=no
LOGGING(YES/NO)=YES


# IV. Log File Preferences
# INDICATE CONTENT OF LOG_# FILE (IF LOGGING == ON).
#   LANDCLASS_SUMMARY: (if landuse is being modeled) summary of input
#             from 'landuse.classes' file
#   SLOPE_WEIGHTS(YES/NO): annual slope weight values as effected
#               by slope_coeff
#   READS(YES/NO)= notes if a file is read in
#   WRITES(YES/NO)= notes if a file is written
```

```
#   COLORTABLES(YES/NO)= rgb lookup tables for all colortables generated
#   PROCESSING_STATUS(0:off/1:low verbosity/2:high verbosity)=
#   TRANSITION_MATRIX(YES/NO)= pixel count and annual probability of
#               land class transitions
#   URBANIZATION_ATTEMPTS(YES/NO)= number of times an attempt to urbanize
#                   a pixel occurred
#   INITIAL_COEFFICIENTS(YES/NO)= initial coefficient values for
#                   each monte carlo
#   BASE_STATISTICS(YES/NO)= measurements of urban control year data
#   DEBUG(YES/NO)= data dump of igrid object and grid pointers
#   TIMINGS(0:off/1:low verbosity/2:high verbosity)= time spent within
#   each module. If running in parallel, LOG_0 will contain timing for
#   complete job.
LOG_LANDCLASS_SUMMARY(YES/NO)=yes
LOG_SLOPE_WEIGHTS(YES/NO)=no
LOG_READS(YES/NO)=no
LOG_WRITES(YES/NO)=no
LOG_COLORTABLES(YES/NO)=no
LOG_PROCESSING_STATUS(0:off/1:low verbosity/2:high verbosity)=1
LOG_TRANSITION_MATRIX(YES/NO)=yes
LOG_URBANIZATION_ATTEMPTS(YES/NO)=no
LOG_INITIAL_COEFFICIENTS(YES/NO)=no
LOG_BASE_STATISTICS(YES/NO)=yes
LOG_DEBUG(YES/NO)= yes
LOG_TIMINGS(0:off/1:low verbosity/2:high verbosity)=1


# V. WORKING GRIDS
# The number of working grids needed from memory during model execution is

# designated up front. This number may change depending upon modes. If
# NUM_WORKING_GRIDS needs to be increased, the execution will be exited
# and an error message will be written to the screen and to 'ERROR_LOG'
# in the OUTPUT_DIRECTORY. If the number may be decreased an optimal
# number will be written to the end of the LOG_0 file.
NUM_WORKING_GRIDS=4


# VI. RANDOM NUMBER SEED
# This number initializes the random number generator. This seed will be
# used to initialize each model run.
RANDOM_SEED=1


# VII. MONTE CARLO ITERATIONS
# Each model run may be completed in a monte carlo fashion.
# For CALIBRATION or TEST mode measurements of simulated data will be
# taken for years of known data, and averaged over the number of monte
# carlo iterations. These averages are written to the AVG_FILE, and
# the associated standard diviation is written to the STD_DEV_FILE.
# The averaged values are compared to the known data, and a Pearson
# correlation coefficient measure is calculated and written to the
# control_stats.log file. The input per run may be associated across
# files using the 'index' number in the files' first column.
#
MONTE_CARLO_ITERATIONS=5


# VIII. COEFFICIENTS
# The coefficients effect how the growth rules are applied to the data.
# Setting requirements:
#   *_START values >= *_STOP values
#   *_STEP values > 0
#   if no coefficient increment is desired:
#   *_START == *_STOP
#   *_STEP == 1
# For additional information about how these values affect simulated
# land cover change see our publications and PROJECT GIGALOPOLIS
# site: (www.ncgia.ucsb.edu/project/gig/About/abGrowth.htm).
# A. COEFFICIENTS AND GROWTH TYPES
#   DIFFUSION: affects SPONTANEOUS GROWTH and search distance along the
#           road network as part of ROAD INFLUENCED GROWTH.
#   BREED: NEW SPREADING CENTER probability and affects number of ROAD
#       INFLUENCED GROWTH attempts.
#   SPREAD: the probabilty of ORGANIC GROWTH from established urban
#       pixels occuring.
#   SLOPE_RESISTANCE: affects the influence of slope to urbanization. As
#               value increases, the ability to urbanize
#               ever steepening slopes decreases.
#   ROAD_GRAVITY: affects the outward distance from a selected pixel for
```

```
#            which a road pixel will be searched for as part of
#            ROAD INFLUENCED GROWTH.
#
#  B. MODES AND COEFFICIENT SETTINGS
#    TEST: TEST mode will perform a single run through the historical
#       data using the CALIBRATION_*_START values to initialize
#       growth, complete the MONTE_CARLO_ITERATIONS, and then conclude
#       execution. GIF images of the simulated urban growth will be
#       written to the OUTPUT_DIRECTORY.
#    CALIBRATE: CALIBRATE will perform monte carlo runs through the
#          historical data using every combination of the
#          coefficient values indicated. The CALIBRATION_*_START
#          coefficient values will initialize the first run. A
#          coefficient will then be increased by its *_STEP value,
#          and another run performed. This will be repeated for all
#          possible permutations of given ranges and increments.
#    PREDICTION: PREDICTION will perform a single run, in monte carlo
#          fashion, using the PREDICTION_*_BEST_FIT values
#          for initialization.
```

CALIBRATION_DIFFUSION_START= 0
CALIBRATION_DIFFUSION_STEP= 25
CALIBRATION_DIFFUSION_STOP= 100

CALIBRATION_BREED_START=   0
CALIBRATION_BREED_STEP=   25
CALIBRATION_BREED_STOP=   100

CALIBRATION_SPREAD_START=   0
CALIBRATION_SPREAD_STEP=   25
CALIBRATION_SPREAD_STOP=   100

CALIBRATION_SLOPE_START=   0
CALIBRATION_SLOPE_STEP=   25
CALIBRATION_SLOPE_STOP=   100

CALIBRATION_ROAD_START=   0
CALIBRATION_ROAD_STEP=   25
CALIBRATION_ROAD_STOP=   100

PREDICTION_DIFFUSION_BEST_FIT= 20
PREDICTION_BREED_BEST_FIT= 20
PREDICTION_SPREAD_BEST_FIT= 20
PREDICTION_SLOPE_BEST_FIT= 20
PREDICTION_ROAD_BEST_FIT= 20

```
# IX. PREDICTION DATE RANGE
# The urban and road images used to initialize growth during
# prediction are those with dates equal to, or greater than,
# the PREDICTION_START_DATE. If the PREDICTION_START_DATE is greater
# than any of the urban dates, the last urban file on the list will be
# used. Similarly, if the PREDICTION_START_DATE is greater
# than any of the road dates, the last road file on the list will be
# used. The prediction run will terminate at PREDICTION_STOP_DATE.
#
```
PREDICTION_START_DATE=2014
PREDICTION_STOP_DATE=2030

```
# X. INPUT IMAGES
# The model expects grayscale, GIF image files with file name
# format as described below. For more information see our
# PROJECT GIGALOPOLIS web site:
# (www.ncgia.ucsb.edu/project/gig/About/dtInput.htm).
#
# IF LAND COVER IS NOT BEING MODELED: Remove or comment out
# the LANDUSE_DATA data input flags below.
#
#   < > = user selected fields
#  [< >] = optional fields
#
# Urban data GIFs
#  format:  <location>.urban.<date>.[<user info>].gif
#
#
```
URBAN_DATA= dhaka.urban.1989.gif
URBAN_DATA= dhaka.urban.1999.gif

URBAN_DATA= dhaka.urban.2009.gif
URBAN_DATA= dhaka.urban.2014.gif
#
Road data GIFs
format: <location>.roads.<date>.[<user info>].gif
#
ROAD_DATA= dhaka.roads.1989.gif
ROAD_DATA= dhaka.roads.1999.gif
ROAD_DATA= dhaka.roads.2009.gif
ROAD_DATA= dhaka.roads.2014.gif
#
Landuse data GIFs
format: <location>.landuse.<date>.[<user info>].gif
#
LANDUSE_DATA= dhaka.landuse.1989.gif
LANDUSE_DATA= dhaka.landuse.2014.gif
#
Excluded data GIF
format: <location>.excluded.[<user info>].gif
#
EXCLUDED_DATA= dhaka.excluded.gif
#
Slope data GIF
format: <location>.slope.[<user info>].gif
#
SLOPE_DATA= dhaka.slope.gif
#
Background data GIF
format: <location> hillshade.[<user info>].gif
#
#BACKGROUND_DATA= dhaka.hillshade.gif
BACKGROUND_DATA= dhaka.hillshade.water.gif

XI. OUTPUT IMAGES
WRITE_COLOR_KEY_IMAGES: Creates image maps of each colortable.
File name format: 'key_[type]_COLORMAP'
where [type] represents the colortable.
ECHO_IMAGE_FILES: Creates GIF of each input file used in that job.
File names format: 'echo_of_[input_filename]'
where [input_filename] represents the input name.
ANIMATION: if whirlgif has been compiled, and the WHIRLGIF_BINARY
path has been defined, animated gifs begining with the
file name 'animated' will be created in PREDICT mode.
WRITE_COLOR_KEY_IMAGES(YES/NO)=yes
ECHO_IMAGE_FILES(YES/NO)=yes
ANIMATION(YES/NO)= yes

XII. COLORTABLE SETTINGS
A. DATE COLOR SETTING
The date will automatically be placed in the lower left corner
of output images. DATE_COLOR may be designated in with red, green,
and blue values (format: <red_value, green_value, blue_value>)
or with hexadecimal begining with '0X' (format: <0X######>).
#default DATE_COLOR= 0XFFFFFF white
DATE_COLOR=   0XFFFFFF #white

B. URBAN (NON-LANDUSE) COLORTABLE SETTINGS
1. URBAN MODE OUTPUTS
TEST mode: Annual images of simulated urban growth will be
created using SEED_COLOR to indicate urbanized areas.

CALIBRATE mode: Images will not be created.
PREDICT mode: Annual probability images of simulated urban
growth will be created using the PROBABILITY
_COLORTABLE. The initializing urban data will be
indicated by SEED_COLOR.
#
2. COLORTABLE SETTINGS
SEED_COLOR: initializing and extrapolated historic urban extent

WATER_COLOR: BACKGROUND_DATA is used as a backdrop for

simulated urban growth. If pixels in this file
contain the value zero (0), they will be filled
with the color value in WATER_COLOR. In this way,
major water bodies in a study area may be included

```
#                in output images.
#SEED_COLOR= 0XFFFF00 #yellow
SEED_COLOR= 249, 209, 110 #pale yellow
#WATER_COLOR= 0X0000FF # blue
WATER_COLOR= 20, 52, 214 # royal blue


#   3. PROBABILITY COLORTABLE FOR URBAN GROWTH
#     For PREDICTION, annual probability images of urban growth
#     will be created using the monte carlo iterations. In these
#     images, the higher the value the more likely urbanizaion is.
#     In order to interpret these 'continuous' values more easily
#     they may be color classified by range.
#
#     If 'hex' is not present then the range is transparent.
#     The transparent range must be the first on the list.
#     The max number of entries is 100.
#      PROBABILITY_COLOR: a color value in hexadecimal that indicates
#                a probability range.
#        low/upper: indicate the boundaries of the range.
#
#          low, upper, hex, (Optional Name)
PROBABILITY_COLOR= 0,  50,      , #transparent
PROBABILITY_COLOR= 50, 60, 0X005A00, #0, 90,0 dark green
PROBABILITY_COLOR= 60, 70, 0X008200, #0,130,0
PROBABILITY_COLOR= 70, 80, 0X00AA00, #0,170,0
PROBABILITY_COLOR= 80, 90, 0X00D200, #0,210,0
PROBABILITY_COLOR= 90, 95, 0X00FF00, #0,255,0 light green
PROBABILITY_COLOR= 95, 100, 0X8B0000, #dark red


# C. LAND COVER COLORTABLE
# Land cover input images should be in grayscale GIF image format.
# The 'pix' value indicates a land class grayscale pixel value in
# the image. If desired, the model will create color classified
# land cover output. The output colortable is designated by the
# 'hex/rgb' values.
#   pix: input land class pixel value
#   name: text string indicating land class
#   flag: special case land classes
#      URB - urban class (area is included in urban input data
#         and will not be transitioned by deltatron)
#      UNC - unclass (NODATA areas in image)
#      EXC - excluded (land class will be ignored by deltatron)
#   hex/rgb: hexidecimal or rgb (red, green, blue) output colors
#
#        pix, name,    flag,  hex/rgb, #comment
LANDUSE_CLASS= 0, Unclass , UNC  , 0X000000
LANDUSE_CLASS= 1, Urban  , URB  , 0X8b2323 #dark red
LANDUSE_CLASS= 2, Agric  ,      , 0Xffec8b #pale yellow
LANDUSE_CLASS= 3, Range  ,      , 0Xee9a49 #tan
LANDUSE_CLASS= 4, Forest ,      , 0X006400
LANDUSE_CLASS= 5, Water  , EXC  , 0X104e8b
LANDUSE_CLASS= 6, Wetland ,     , 0X483d8b
LANDUSE_CLASS= 7, Barren ,      , 0Xeec591


# D. GROWTH TYPE IMAGE OUTPUT CONTROL AND COLORTABLE
#
# From here you can control the output of the Z grid
# (urban growth) just after it is returned from the spr_spread()
# function. In this way it is possible to see the different types
# of growth that have occured for a particular growth cycle.
#
# VIEW_GROWTH_TYPES(YES/NO) provides an on/off
# toggle to control whether the images are generated.
#
# GROWTH_TYPE_PRINT_WINDOW provides a print window
# to control the amount of images created.
# format: <start_run>,<end_run>,<start_monte_carlo>,
#       <end_monte_carlo>,<start_year>,<end_year>
# for example:
# GROWTH_TYPE_PRINT_WINDOW=run1,run2,mc1,mc2,year1,year2
# so images are only created when
# run1<= current run <=run2 AND
# mc1 <= current monte carlo <= mc2 AND
# year1 <= currrent year <= year2
#
# 0 == first
```

```
VIEW_GROWTH_TYPES(YES/NO)=NO
GROWTH_TYPE_PRINT_WINDOW=0,0,0,0,1995,2020
PHASE0G_GROWTH_COLOR= 0xff0000 # seed urban area
PHASE1G_GROWTH_COLOR= 0X00ff00 # diffusion growth
PHASE2G_GROWTH_COLOR= 0X0000ff # NOT USED
PHASE3G_GROWTH_COLOR= 0Xffff00 # breed growth
PHASE4G_GROWTH_COLOR= 0Xffffff # spread growth
PHASE5G_GROWTH_COLOR= 0X00ffff # road influenced growth


#***********************************************************
#
# E. DELTATRON AGING SECTION
#
# From here you can control the output of the deltatron grid
# just before they are aged
#
# VIEW_DELTATRON_AGING(YES/NO) provides an on/off
# toggle to control whether the images are generated.
#
# DELTATRON_PRINT_WINDOW provides a print window
# to control the amount of images created.
# format:  <start_run>,<end_run>,<start_monte_carlo>,
#        <end_monte_carlo>,<start_year>,<end_year>
# for example:
# DELTATRON_PRINT_WINDOW=run1,run2,mc1,mc2,year1,year2
# so images are only created when
# run1<= current run <=run2 AND
# mc1 <= current monte carlo <= mc2 AND
# year1 <= currrent year <= year2
#
# 0 == first
VIEW_DELTATRON_AGING(YES/NO)=NO
DELTATRON_PRINT_WINDOW=0,0,0,0,1930,2020
DELTATRON_COLOR= 0x000000 # index 0 No or dead deltatron
DELTATRON_COLOR= 0X00FF00 # index 1 age = 1 year
DELTATRON_COLOR= 0X00D200 # index 2 age = 2 year
DELTATRON_COLOR= 0X00AA00 # index 3 age = 3 year
DELTATRON_COLOR= 0X008200 # index 4 age = 4 year
DELTATRON_COLOR= 0X005A00 # index 5 age = 5 year

# XIII. SELF-MODIFICATION PARAMETERS
#     SLEUTH is a self-modifying cellular automata. For more
#     information see our PROJECT GIGALOPOLIS web site
#     (www.ncgia.ucsb.edu/project/gig/About/abGrowth.htm)
#     and publications (and/or grep 'self modification' in code).
ROAD_GRAV_SENSITIVITY=0.01
SLOPE_SENSITIVITY=0.1
CRITICAL_LOW=0.97
CRITICAL_HIGH=1.3
#CRITICAL_LOW=0.0
#CRITICAL_HIGH=10000000000000.0
CRITICAL_SLOPE=21.0
BOOM=1.01
BUST=0.9
```

Source code of Fine calibration

```
# FILE: 'scenario file' for SLEUTH land cover transition model
#     (UGM  v3.0)
#      Comments start with #
#
#  I. Path Name Variables
# II. Running Status (Echo)
# III. Output ASCII Files
# IV. Log File Preferences
#  V. Working Grids
#  VI. Random Number Seed
# VII. Monte Carlo Iteration
#VIII. Coefficients
#     A. Coefficients and Growth Types
#     B. Modes and Coefficient Settings
# IX. Prediction Date Range
#  X. Input Images
# XI. Output Images
# XII. Colortable Settings
#     A. Date_Color
#     B. Non-Landuse Colortable
#     C. Land Cover Colortable
#     D. Growth Type Images
#     E. Deltatron Images
#XIII. Self Modification Parameters


# I.PATH NAME VARIABLES
#  INPUT_DIR: relative or absolute path where input image files and
#         (if modeling land cover) 'landuse.classes' file are
#         located.
#  OUTPUT_DIR: relative or absolute path where all output files will
#          be located.
#  WHIRLGIF_BINARY: relative path to 'whirlgif' gif animation program.
#          These must be compiled before execution.
INPUT_DIR=../Input/dhaka/
OUTPUT_DIR=../Output/dhakafine/
WHIRLGIF_BINARY=../Whirlgif/whirlgif


# II. RUNNING STATUS (ECHO)
#  Status of model run, monte carlo iteration, and year will be
#  printed to the screen during model execution.
ECHO(YES/NO)=yes


# III. Output Files
# INDICATE TYPES OF ASCII DATA FILES TO BE WRITTEN TO OUTPUT_DIRECTORY.
#
#  COEFF_FILE: contains coefficient values for every run, monte carlo
#         iteration and year.
#  AVG_FILE: contains measured values of simulated data averaged over
#         monte carlo iterations for every run and control year.
#  STD_DEV_FILE: contains standard diviation of averaged values
#         in the AVG_FILE.
#  MEMORY_MAP: logs memory map to file 'memory.log'
#  LOGGING: will create a 'LOG_#' file where # signifies the processor
#         number that created the file if running code in parallel.
#         Otherwise, # will be 0. Contents of the LOG file may be
#         described below.
WRITE_COEFF_FILE(YES/NO)=yes
WRITE_AVG_FILE(YES/NO)=yes
WRITE_STD_DEV_FILE(YES/NO)=yes
WRITE_MEMORY_MAP(YES/NO)=no
LOGGING(YES/NO)=YES


# IV. Log File Preferences
# INDICATE CONTENT OF LOG_# FILE (IF LOGGING == ON).
#  LANDCLASS_SUMMARY: (if landuse is being modeled) summary of input
#              from 'landuse.classes' file
#  SLOPE_WEIGHTS(YES/NO): annual slope weight values as effected
#                 by slope_coeff
#  READS(YES/NO)= notes if a file is read in
#  WRITES(YES/NO)= notes if a file is written
#  COLORTABLES(YES/NO)= rgb lookup tables for all colortables generated
#  PROCESSING_STATUS(0:off/1:low verbosity/2:high verbosity)=
```

92

```
#   TRANSITION_MATRIX(YES/NO)= pixel count and annual probability of
#                 land class transitions
#   URBANIZATION_ATTEMPTS(YES/NO)= number of times an attempt to urbanize
#                     a pixel occurred
#   INITIAL_COEFFICIENTS(YES/NO)= initial coefficient values for
#                     each monte carlo
#   BASE_STATISTICS(YES/NO)= measurements of urban control year data
#   DEBUG(YES/NO)= data dump of igrid object and grid pointers
#   TIMINGS(0:off/1:low verbosity/2:high verbosity)= time spent within
#     each module. If running in parallel, LOG_0 will contain timing for
#     complete job.
LOG_LANDCLASS_SUMMARY(YES/NO)=yes
LOG_SLOPE_WEIGHTS(YES/NO)=no
LOG_READS(YES/NO)=no
LOG_WRITES(YES/NO)=no
LOG_COLORTABLES(YES/NO)=no
LOG_PROCESSING_STATUS(0:off/1:low verbosity/2:high verbosity)=1
LOG_TRANSITION_MATRIX(YES/NO)=yes
LOG_URBANIZATION_ATTEMPTS(YES/NO)=no
LOG_INITIAL_COEFFICIENTS(YES/NO)=no
LOG_BASE_STATISTICS(YES/NO)=yes
LOG_DEBUG(YES/NO)= yes
LOG_TIMINGS(0:off/1:low verbosity/2:high verbosity)=1


# V. WORKING GRIDS
# The number of working grids needed from memory during model execution is

# designated up front. This number may change depending upon modes. If
# NUM_WORKING_GRIDS needs to be increased, the execution will be exited
# and an error message will be written to the screen and to 'ERROR_LOG'
# in the OUTPUT_DIRECTORY. If the number may be decreased an optimal
# number will be written to the end of the LOG_0 file.
NUM_WORKING_GRIDS=4


# VI. RANDOM NUMBER SEED
# This number initializes the random number generator. This seed will be
# used to initialize each model run.
RANDOM_SEED=1


# VII. MONTE CARLO ITERATIONS
# Each model run may be completed in a monte carlo fashion.
# For CALIBRATION or TEST mode measurements of simulated data will be
# taken for years of known data, and averaged over the number of monte
# carlo iterations. These averages are written to the AVG_FILE, and
# the associated standard diviation is written to the STD_DEV_FILE.
# The averaged values are compared to the known data, and a Pearson
# correlation coefficient measure is calculated and written to the
# control_stats.log file. The input per run may be associated across
# files using the 'index' number in the files' first column.
#
MONTE_CARLO_ITERATIONS= 8

# VIII. COEFFICIENTS
# The coefficients effect how the growth rules are applied to the data.
# Setting requirements:
#   *_START values >= *_STOP values
#   *_STEP values > 0
#   if no coefficient increment is desired:
#   *_START == *_STOP
#   *_STEP == 1
# For additional information about how these values affect simulated
# land cover change see our publications and PROJECT GIGALOPOLIS
# site: (www.ncgia.ucsb.edu/project/gig/About/abGrowth.htm).
# A. COEFFICIENTS AND GROWTH TYPES
#   DIFFUSION: affects SPONTANEOUS GROWTH and search distance along the
#           road network as part of ROAD INFLUENCED GROWTH.
#   BREED: NEW SPREADING CENTER probability and affects number of ROAD
#           INFLUENCED GROWTH attempts.
#   SPREAD: the probabilty of ORGANIC GROWTH from established urban
#           pixels occuring.
#   SLOPE_RESISTANCE: affects the influence of slope to urbanization. As
#               value increases, the ability to urbanize
#               ever steepening slopes decreases.
#   ROAD_GRAVITY: affects the outward distance from a selected pixel for
#           which a road pixel will be searched for as part of
#           ROAD INFLUENCED GROWTH.
```

93

```
#
# B. MODES AND COEFFICIENT SETTINGS
#   TEST: TEST mode will perform a single run through the historical
#       data using the CALIBRATION_*_START values to initialize
#       growth, complete the MONTE_CARLO_ITERATIONS, and then conclude
#       execution. GIF images of the simulated urban growth will be
#       written to the OUTPUT_DIRECTORY.
#   CALIBRATE: CALIBRATE will perform monte carlo runs through the
#           historical data using every combination of the
#           coefficient values indicated. The CALIBRATION_*_START
#           coefficient values will initialize the first run. A
#           coefficient will then be increased by its *_STEP value,
#           and another run performed. This will be repeated for all
#           possible permutations of given ranges and increments.
#   PREDICTION: PREDICTION will perform a single run, in monte carlo
#            fashion, using the PREDICTION_*_BEST_FIT values
#            for initialization.
```

CALIBRATION_DIFFUSION_START= 0
CALIBRATION_DIFFUSION_STEP= 5
CALIBRATION_DIFFUSION_STOP= 20

CALIBRATION_BREED_START=   0
CALIBRATION_BREED_STEP=   20
CALIBRATION_BREED_STOP=   100

CALIBRATION_SPREAD_START=   75
CALIBRATION_SPREAD_STEP=   5
CALIBRATION_SPREAD_STOP=   100

CALIBRATION_SLOPE_START=   0
CALIBRATION_SLOPE_STEP=   5
CALIBRATION_SLOPE_STOP=   25

CALIBRATION_ROAD_START=   0
CALIBRATION_ROAD_STEP=   20
CALIBRATION_ROAD_STOP=   100

```
PREDICTION_DIFFUSION_BEST_FIT= 20
PREDICTION_BREED_BEST_FIT= 20
PREDICTION_SPREAD_BEST_FIT= 20
PREDICTION_SLOPE_BEST_FIT= 20
PREDICTION_ROAD_BEST_FIT= 20

# IX. PREDICTION DATE RANGE
# The urban and road images used to initialize growth during
# prediction are those with dates equal to, or greater than,
# the PREDICTION_START_DATE. If the PREDICTION_START_DATE is greater
# than any of the urban dates, the last urban file on the list will be
# used. Similarly, if the PREDICTION_START_DATE is greater
# than any of the road dates, the last road file on the list will be
# used. The prediction run will terminate at PREDICTION_STOP_DATE.
#
```
PREDICTION_START_DATE=2014
PREDICTION_STOP_DATE=2030

```
# X. INPUT IMAGES
# The model expects grayscale, GIF image files with file name
# format as described below. For more information see our
# PROJECT GIGALOPOLIS web site:
# (www.ncgia.ucsb.edu/project/gig/About/dtInput.htm).
#
# IF LAND COVER IS NOT BEING MODELED: Remove or comment out
# the LANDUSE_DATA data input flags below.
#
#   < > = user selected fields
#   [< >] = optional fields
#
# Urban data GIFs
# format:  <location>.urban.<date>.[<user info>].gif
#
#
```
URBAN_DATA= dhaka.urban.1989.gif
URBAN_DATA= dhaka.urban.1999.gif
URBAN_DATA= dhaka.urban.2009.gif
URBAN_DATA= dhaka.urban.2014.gif
```
#
# Road data GIFs
```

94

```
# format: <location>.roads.<date>.[<user info>].gif
#
ROAD_DATA= dhaka.roads.1989.gif
ROAD_DATA= dhaka.roads.1999.gif
ROAD_DATA= dhaka.roads.2009.gif
ROAD_DATA= dhaka.roads.2014.gif
#
# Landuse data GIFs
# format: <location>.landuse.<date>.[<user info>].gif
#
LANDUSE_DATA= dhaka.landuse.1989.gif
LANDUSE_DATA= dhaka.landuse.2014.gif
#
# Excluded data GIF
# format: <location>.excluded.[<user info>].gif
#
EXCLUDED_DATA= dhaka.excluded.gif
#
# Slope data GIF
# format: <location>.slope.[<user info>].gif
#
SLOPE_DATA= dhaka.slope.gif
#
# Background data GIF
# format:  <location> hillshade.[<user info>].gif
#
#BACKGROUND_DATA= dhaka.hillshade.gif
BACKGROUND_DATA= dhaka.hillshade.water.gif

# XI. OUTPUT IMAGES
#  WRITE_COLOR_KEY_IMAGES: Creates image maps of each colortable.
#               File name format: 'key_[type]_COLORMAP'
#                 where [type] represents the colortable.
#  ECHO_IMAGE_FILES: Creates GIF of each input file used in that job.
#            File names format: 'echo_of_[input_filename]'
#            where [input_filename] represents the input name.
#  ANIMATION: if whirlgif has been compiled, and the WHIRLGIF_BINARY
#        path has been defined, animated gifs begining with the
#        file name 'animated' will be created in PREDICT mode.
WRITE_COLOR_KEY_IMAGES(YES/NO)=yes
ECHO_IMAGE_FILES(YES/NO)=yes
ANIMATION(YES/NO)= yes

# XII. COLORTABLE SETTINGS
#  A. DATE COLOR SETTING
#    The date will automatically be placed in the lower left corner
#    of output images. DATE_COLOR may be designated in with red, green,
#    and blue values (format: <red_value, green_value, blue_value> )
#    or with hexadecimal begining with '0X' (format: <0X######> ).
#default DATE_COLOR= 0XFFFFFF white
DATE_COLOR=    0XFFFFFF #white

#  B. URBAN (NON-LANDUSE) COLORTABLE SETTINGS
#   1. URBAN MODE OUTPUTS
#     TEST mode: Annual images of simulated urban growth will be
#            created using SEED_COLOR to indicate urbanized areas.

#     CALIBRATE mode: Images will not be created.
#     PREDICT mode: Annual probability images of simulated urban
#            growth will be created using the PROBABILITY
#            _COLORTABLE. The initializing urban data will be
#            indicated by SEED_COLOR.
#
#   2. COLORTABLE SETTINGS
#      SEED_COLOR: initializing and extrapolated historic urban extent

#       WATER_COLOR: BACKGROUND_DATA is used as a backdrop for

#            simulated urban growth. If pixels in this file
#            contain the value zero (0), they will be filled
#            with the color value in WATER_COLOR. In this way,
#            major water bodies in a study area may be included
#            in output images.
#SEED_COLOR= 0XFFFF00 #yellow
SEED_COLOR=  249, 209, 110 #pale yellow
#WATER_COLOR=  0X0000FF # blue
```

95

WATER_COLOR= 20, 52, 214 # royal blue

```
#    3. PROBABILITY COLORTABLE FOR URBAN GROWTH
#    For PREDICTION, annual probability images of urban growth
#    will be created using the monte carlo iterations. In these
#    images, the higher the value the more likely urbanizaion is.
#    In order to interpret these 'continuous' values more easily
#    they may be color classified by range.
#
#    If 'hex' is not present then the range is transparent.
#    The transparent range must be the first on the list.
#    The max number of entries is 100.
#     PROBABILITY_COLOR: a color value in hexadecimal that indicates
#             a probability range.
#       low/upper: indicate the boundaries of the range.
#
#           low,  upper,  hex,  (Optional Name)
PROBABILITY_COLOR=  0,   50,        , #transparent
PROBABILITY_COLOR=  50,  60, 0X005A00, #0, 90,0 dark green
PROBABILITY_COLOR=  60,  70, 0X008200, #0,130,0
PROBABILITY_COLOR=  70,  80, 0X00AA00, #0,170,0
PROBABILITY_COLOR=  80,  90, 0X00D200, #0,210,0
PROBABILITY_COLOR=  90,  95, 0X00FF00, #0,255,0 light green
PROBABILITY_COLOR=  95, 100, 0X8B0000, #dark red


# C. LAND COVER COLORTABLE
# Land cover input images should be in grayscale GIF image format.
# The 'pix' value indicates a land class grayscale pixel value in
# the image. If desired, the model will create color classified
# land cover output. The output colortable is designated by the
# 'hex/rgb' values.
#   pix: input land class pixel value
#   name: text string indicating land class
#   flag: special case land classes
#       URB - urban class (area is included in urban input data
#           and will not be transitioned by deltatron)
#       UNC - unclass (NODATA areas in image)
#       EXC - excluded (land class will be ignored by deltatron)
#   hex/rgb: hexidecimal or rgb (red, green, blue) output colors
#
#          pix, name,    flag,  hex/rgb, #comment
LANDUSE_CLASS= 0, Unclass , UNC  , 0X000000
LANDUSE_CLASS= 1, Urban   , URB  , 0X8b2323 #dark red
LANDUSE_CLASS= 2, Agric   ,      , 0Xffec8b #pale yellow
LANDUSE_CLASS= 3, Range   ,      , 0Xee9a49 #tan
LANDUSE_CLASS= 4, Forest  ,      , 0X006400
LANDUSE_CLASS= 5, Water   , EXC  , 0X104e8b
LANDUSE_CLASS= 6, Wetland ,      , 0X483d8b
LANDUSE_CLASS= 7, Barren  ,      , 0Xeec591


# D. GROWTH TYPE IMAGE OUTPUT CONTROL AND COLORTABLE
#
# From here you can control the output of the Z grid
# (urban growth) just after it is returned from the spr_spread()
# function. In this way it is possible to see the different types
# of growth that have occured for a particular growth cycle.
#
# VIEW_GROWTH_TYPES(YES/NO) provides an on/off
# toggle to control whether the images are generated.
#
# GROWTH_TYPE_PRINT_WINDOW provides a print window
# to control the amount of images created.
# format:  <start_run>,<end_run>,<start_monte_carlo>,
#       <end_monte_carlo>,<start_year>,<end_year>
# for example:
# GROWTH_TYPE_PRINT_WINDOW=run1,run2,mc1,mc2,year1,year2
# so images are only created when
# run1<= current run <=run2 AND
# mc1 <= current monte carlo <= mc2 AND
# year1 <= currrent year <= year2
#
# 0 == first
VIEW_GROWTH_TYPES(YES/NO)=NO
GROWTH_TYPE_PRINT_WINDOW=0,0,0,0,1995,2020
PHASE0G_GROWTH_COLOR=  0xff0000 # seed urban area
PHASE1G_GROWTH_COLOR=  0X00ff00 # diffusion growth
```

96

```
PHASE2G_GROWTH_COLOR= 0X0000ff # NOT USED
PHASE3G_GROWTH_COLOR= 0Xffff00 # breed growth
PHASE4G_GROWTH_COLOR= 0Xffffff # spread growth
PHASE5G_GROWTH_COLOR= 0X00ffff # road influenced growth


#*********************************************************
#
# E. DELTATRON AGING SECTION
#
# From here you can control the output of the deltatron grid
# just before they are aged
#
# VIEW_DELTATRON_AGING(YES/NO) provides an on/off
# toggle to control whether the images are generated.
#
# DELTATRON_PRINT_WINDOW provides a print window
# to control the amount of images created.
# format:  <start_run>,<end_run>,<start_monte_carlo>,
#        <end_monte_carlo>,<start_year>,<end_year>
# for example:
# DELTATRON_PRINT_WINDOW=run1,run2,mc1,mc2,year1,year2
# so images are only created when
# run1<= current run <=run2 AND
# mc1 <= current monte carlo <= mc2 AND
# year1 <= currrent year <= year2
#
#  0 == first
VIEW_DELTATRON_AGING(YES/NO)=NO
DELTATRON_PRINT_WINDOW=0,0,0,0,1930,2020
DELTATRON_COLOR= 0x000000 # index 0 No or dead deltatron
DELTATRON_COLOR= 0X00FF00 # index 1 age = 1 year
DELTATRON_COLOR= 0X00D200 # index 2 age = 2 year
DELTATRON_COLOR= 0X00AA00 # index 3 age = 3 year
DELTATRON_COLOR= 0X008200 # index 4 age = 4 year
DELTATRON_COLOR= 0X005A00 # index 5 age = 5 year


# XIII. SELF-MODIFICATION PARAMETERS
#      SLEUTH is a self-modifying cellular automata. For more
#      information see our PROJECT GIGALOPOLIS web site
#      (www.ncgia.ucsb.edu/project/gig/About/abGrowth.htm)
#      and publications (and/or grep 'self modification' in code).
ROAD_GRAV_SENSITIVITY=0.01
SLOPE_SENSITIVITY=0.1
CRITICAL_LOW=0.97
CRITICAL_HIGH=1.3
#CRITICAL_LOW=0.0
#CRITICAL_HIGH=10000000000000.0
CRITICAL_SLOPE=21.0
BOOM=1.01
BUST=0.9
```

97

Source code of Final calibration

```
# FILE: 'scenario file' for SLEUTH land cover transition model
#      (UGM  v3.0)
#      Comments start with #
#
#  I. Path Name Variables
#  II. Running Status (Echo)
# III. Output ASCII Files
#  IV. Log File Preferences
#   V. Working Grids
#  VI. Random Number Seed
# VII. Monte Carlo Iteration
#VIII. Coefficients
#     A. Coefficients and Growth Types
#     B. Modes and Coefficient Settings
#  IX. Prediction Date Range
#   X. Input Images
#  XI. Output Images
# XII. Colortable Settings
#     A. Date_Color
#     B. Non-Landuse Colortable
#     C. Land Cover Colortable
#     D. Growth Type Images
#     E. Deltatron Images
#XIII. Self Modification Parameters


# I.PATH NAME VARIABLES
#  INPUT_DIR: relative or absolute path where input image files and
#        (if modeling land cover) 'landuse.classes' file are
#        located.
#  OUTPUT_DIR: relative or absolute path where all output files will
#        be located.
#  WHIRLGIF_BINARY: relative path to 'whirlgif' gif animation program.
#             These must be compiled before execution.
INPUT_DIR=../Input/dhaka/
OUTPUT_DIR=../Output/dhakafinal/
WHIRLGIF_BINARY=../Whirlgif/whirlgif


# II. RUNNING STATUS (ECHO)
# Status of model run, monte carlo iteration, and year will be
# printed to the screen during model execution.
ECHO(YES/NO)=yes


# III. Output Files
# INDICATE TYPES OF ASCII DATA FILES TO BE WRITTEN TO OUTPUT_DIRECTORY.
#
#  COEFF_FILE: contains coefficient values for every run, monte carlo
#        iteration and year.
#  AVG_FILE: contains measured values of simulated data averaged over
#        monte carlo iterations for every run and control year.
#  STD_DEV_FILE: contains standard diviation of averaged values
#        in the AVG_FILE.
#  MEMORY_MAP: logs memory map to file 'memory.log'
#  LOGGING: will create a 'LOG_#' file where # signifies the processor
#        number that created the file if running code in parallel.
#        Otherwise, # will be 0. Contents of the LOG file may be
#        described below.
WRITE_COEFF_FILE(YES/NO)=yes
WRITE_AVG_FILE(YES/NO)=yes
WRITE_STD_DEV_FILE(YES/NO)=yes
WRITE_MEMORY_MAP(YES/NO)=no
LOGGING(YES/NO)=YES


# IV. Log File Preferences
# INDICATE CONTENT OF LOG_# FILE (IF LOGGING == ON).
#  LANDCLASS_SUMMARY: (if landuse is being modeled) summary of input
#             from 'landuse.classes' file
#  SLOPE_WEIGHTS(YES/NO): annual slope weight values as effected
#             by slope_coeff
#  READS(YES/NO)= notes if a file is read in
#  WRITES(YES/NO)= notes if a file is written
#  COLORTABLES(YES/NO)= rgb lookup tables for all colortables generated
#  PROCESSING_STATUS(0:off/1:low verbosity/2:high verbosity)=
```

98

```
#   TRANSITION_MATRIX(YES/NO)= pixel count and annual probability of
#                   land class transitions
#   URBANIZATION_ATTEMPTS(YES/NO)= number of times an attempt to urbanize
#                    a pixel occurred
#   INITIAL_COEFFICIENTS(YES/NO)= initial coefficient values for
#                   each monte carlo
#   BASE_STATISTICS(YES/NO)= measurements of urban control year data
#   DEBUG(YES/NO)= data dump of igrid object and grid pointers
#   TIMINGS(0:off/1:low verbosity/2:high verbosity)= time spent within
#    each module. If running in parallel, LOG_0 will contain timing for
#    complete job.
LOG_LANDCLASS_SUMMARY(YES/NO)=yes
LOG_SLOPE_WEIGHTS(YES/NO)=no
LOG_READS(YES/NO)=no
LOG_WRITES(YES/NO)=no
LOG_COLORTABLES(YES/NO)=no
LOG_PROCESSING_STATUS(0:off/1:low verbosity/2:high verbosity)=1
LOG_TRANSITION_MATRIX(YES/NO)=yes
LOG_URBANIZATION_ATTEMPTS(YES/NO)=no
LOG_INITIAL_COEFFICIENTS(YES/NO)=no
LOG_BASE_STATISTICS(YES/NO)=yes
LOG_DEBUG(YES/NO)= yes
LOG_TIMINGS(0:off/1:low verbosity/2:high verbosity)=1


# V. WORKING GRIDS
# The number of working grids needed from memory during model execution is

# designated up front. This number may change depending upon modes. If
# NUM_WORKING_GRIDS needs to be increased, the execution will be exited
# and an error message will be written to the screen and to 'ERROR_LOG'
# in the OUTPUT_DIRECTORY. If the number may be decreased an optimal
# number will be written to the end of the LOG_0 file.
NUM_WORKING_GRIDS=4


# VI. RANDOM NUMBER SEED
# This number initializes the random number generator. This seed will be
# used to initialize each model run.
RANDOM_SEED=1


# VII. MONTE CARLO ITERATIONS
# Each model run may be completed in a monte carlo fashion.
# For CALIBRATION or TEST mode measurements of simulated data will be
# taken for years of known data, and averaged over the number of monte
# carlo iterations. These averages are written to the AVG_FILE, and
# the associated standard diviation is written to the STD_DEV_FILE.
# The averaged values are compared to the known data, and a Pearson
# correlation coefficient measure is calculated and written to the
# control_stats.log file. The input per run may be associated across
# files using the 'index' number in the files' first column.
#
MONTE_CARLO_ITERATIONS=10
# VIII. COEFFICIENTS
# The coefficients effect how the growth rules are applied to the data.
# Setting requirements:
#   *_START values >= *_STOP values
#   *_STEP values > 0
#   if no coefficient increment is desired:
#   *_START == *_STOP
#   *_STEP == 1
# For additional information about how these values affect simulated
# land cover change see our publications and PROJECT GIGALOPOLIS
# site: (www.ncgia.ucsb.edu/project/gig/About/abGrowth.htm).
# A. COEFFICIENTS AND GROWTH TYPES
#   DIFFUSION: affects SPONTANEOUS GROWTH and search distance along the
#           road network as part of ROAD INFLUENCED GROWTH.
#   BREED: NEW SPREADING CENTER probability and affects number of ROAD
#           INFLUENCED GROWTH attempts.
#   SPREAD: the probabilty of ORGANIC GROWTH from established urban
#           pixels occuring.
#   SLOPE_RESISTANCE: affects the influence of slope to urbanization. As
#               value increases, the ability to urbanize
#               ever steepening slopes decreases.
#   ROAD_GRAVITY: affects the outward distance from a selected pixel for
#           which a road pixel will be searched for as part of
#           ROAD INFLUENCED GROWTH.
```

99

```
#
# B. MODES AND COEFFICIENT SETTINGS
#   TEST: TEST mode will perform a single run through the historical
#       data using the CALIBRATION_*_START values to initialize
#       growth, complete the MONTE_CARLO_ITERATIONS, and then conclude
#       execution. GIF images of the simulated urban growth will be
#       written to the OUTPUT_DIRECTORY.
#   CALIBRATE: CALIBRATE will perform monte carlo runs through the
#           historical data using every combination of the
#           coefficient values indicated. The CALIBRATION_*_START
#           coefficient values will initialize the first run. A
#           coefficient will then be increased by its *_STEP value,
#           and another run performed. This will be repeated for all
#           possible permutations of given ranges and increments.
#   PREDICTION: PREDICTION will perform a single run, in monte carlo
#            fashion, using the PREDICTION_*_BEST_FIT values
#             for initialization.
```

CALIBRATION_DIFFUSION_START= 0
CALIBRATION_DIFFUSION_STEP= 5
CALIBRATION_DIFFUSION_STOP= 20

CALIBRATION_BREED_START=   20
CALIBRATION_BREED_STEP=   8
CALIBRATION_BREED_STOP=   60

CALIBRATION_SPREAD_START= 80
CALIBRATION_SPREAD_STEP=   4
CALIBRATION_SPREAD_STOP=   100

CALIBRATION_SLOPE_START=   0
CALIBRATION_SLOPE_STEP=   3
CALIBRATION_SLOPE_STOP=   15

CALIBRATION_ROAD_START=   40
CALIBRATION_ROAD_STEP=   12
CALIBRATION_ROAD_STOP=   100

```
PREDICTION_DIFFUSION_BEST_FIT= 20
PREDICTION_BREED_BEST_FIT= 20
PREDICTION_SPREAD_BEST_FIT= 20
PREDICTION_SLOPE_BEST_FIT= 20
PREDICTION_ROAD_BEST_FIT= 20

# IX. PREDICTION DATE RANGE
# The urban and road images used to initialize growth during
# prediction are those with dates equal to, or greater than,
# the PREDICTION_START_DATE. If the PREDICTION_START_DATE is greater
# than any of the urban dates, the last urban file on the list will be
# used. Similarly, if the PREDICTION_START_DATE is greater
# than any of the road dates, the last road file on the list will be
# used. The prediction run will terminate at PREDICTION_STOP_DATE.
#
```
PREDICTION_START_DATE=2014
PREDICTION_STOP_DATE=2030

```
# X. INPUT IMAGES
# The model expects grayscale, GIF image files with file name
# format as described below. For more information see our
# PROJECT GIGALOPOLIS web site:
# (www.ncgia.ucsb.edu/project/gig/About/dtInput.htm).
#
# IF LAND COVER IS NOT BEING MODELED: Remove or comment out
# the LANDUSE_DATA data input flags below.
#
#   < > = user selected fields
#   [< >] = optional fields
#
# Urban data GIFs
# format:  <location>.urban.<date>.[<user info>].gif
#
#
```
URBAN_DATA= dhaka.urban.1989.gif
URBAN_DATA= dhaka.urban.1999.gif
URBAN_DATA= dhaka.urban.2009.gif
URBAN_DATA= dhaka.urban.2014.gif

100

```
#
# Road data GIFs
# format: <location>.roads.<date>.[<user info>].gif
#
ROAD_DATA= dhaka.roads.1989.gif
ROAD_DATA= dhaka.roads.1999.gif
ROAD_DATA= dhaka.roads.2009.gif
ROAD_DATA= dhaka.roads.2014.gif
#
# Landuse data GIFs
# format: <location>.landuse.<date>.[<user info>].gif
#
LANDUSE_DATA= dhaka.landuse.1989.gif
LANDUSE_DATA= dhaka.landuse.2014.gif
#
# Excluded data GIF
# format: <location>.excluded.[<user info>].gif
#
EXCLUDED_DATA= dhaka.excluded.gif
#
# Slope data GIF
# format: <location>.slope.[<user info>].gif
#
SLOPE_DATA= dhaka.slope.gif
#
# Background data GIF
# format:  <location> hillshade.[<user info>].gif
#
#BACKGROUND_DATA= dhaka.hillshade.gif
BACKGROUND_DATA= dhaka.hillshade.water.gif

# XI. OUTPUT IMAGES
#  WRITE_COLOR_KEY_IMAGES: Creates image maps of each colortable.
#            File name format: 'key_[type]_COLORMAP'
#               where [type] represents the colortable.
#  ECHO_IMAGE_FILES: Creates GIF of each input file used in that job.
#            File names format: 'echo_of_[input_filename]'
#               where [input_filename] represents the input name.
#  ANIMATION: if whirlgif has been compiled, and the WHIRLGIF_BINARY
#        path has been defined, animated gifs begining with the
#        file name 'animated' will be created in PREDICT mode.
WRITE_COLOR_KEY_IMAGES(YES/NO)=yes
ECHO_IMAGE_FILES(YES/NO)=yes
ANIMATION(YES/NO)= yes

# XII. COLORTABLE SETTINGS
#  A. DATE COLOR SETTING
#    The date will automatically be placed in the lower left corner
#    of output images. DATE_COLOR may be designated in with red, green,
#    and blue values (format: <red_value, green_value, blue_value> )
#    or with hexadecimal begining with '0X' (format: <0X######> ).
#default DATE_COLOR= 0XFFFFFF white
DATE_COLOR=    0XFFFFFF #white

# B. URBAN (NON-LANDUSE) COLORTABLE SETTINGS
#    1. URBAN MODE OUTPUTS
#      TEST mode: Annual images of simulated urban growth will be
#             created using SEED_COLOR to indicate urbanized areas.

#      CALIBRATE mode: Images will not be created.
#      PREDICT mode: Annual probability images of simulated urban
#             growth will be created using the PROBABILITY
#             _COLORTABLE. The initializing urban data will be
#             indicated by SEED_COLOR.
#
#    2. COLORTABLE SETTINGS
#       SEED_COLOR: initializing and extrapolated historic urban extent

#       WATER_COLOR: BACKGROUND_DATA is used as a backdrop for

#             simulated urban growth. If pixels in this file
#             contain the value zero (0), they will be filled
#             with the color value in WATER_COLOR. In this way,
#             major water bodies in a study area may be included
#             in output images.
#SEED_COLOR= 0XFFFF00 #yellow
```

```
SEED_COLOR= 249, 209, 110 #pale yellow
#WATER_COLOR= 0X0000FF # blue
WATER_COLOR= 20, 52, 214 # royal blue


#    3. PROBABILITY COLORTABLE FOR URBAN GROWTH
#      For PREDICTION, annual probability images of urban growth
#      will be created using the monte carlo iterations. In these
#      images, the higher the value the more likely urbanizaion is.
#      In order to interpret these 'continuous' values more easily
#      they may be color classified by range.
#
#      If 'hex' is not present then the range is transparent.
#      The transparent range must be the first on the list.
#      The max number of entries is 100.
#       PROBABILITY_COLOR: a color value in hexadecimal that indicates
#                a probability range.
#         low/upper: indicate the boundaries of the range.
#
#            low, upper, hex, (Optional Name)
PROBABILITY_COLOR= 0,   50,       , #transparent
PROBABILITY_COLOR= 50,  60, 0X005A00, #0, 90,0 dark green
PROBABILITY_COLOR= 60,  70, 0X008200, #0,130,0
PROBABILITY_COLOR= 70,  80, 0X00AA00, #0,170,0
PROBABILITY_COLOR= 80,  90, 0X00D200, #0,210,0
PROBABILITY_COLOR= 90,  95, 0X00FF00, #0,255,0 light green
PROBABILITY_COLOR= 95, 100, 0X8B0000, #dark red


# C. LAND COVER COLORTABLE
# Land cover input images should be in grayscale GIF image format.
# The 'pix' value indicates a land class grayscale pixel value in
# the image. If desired, the model will create color classified
# land cover output. The output colortable is designated by the
# 'hex/rgb' values.
#   pix: input land class pixel value
#   name: text string indicating land class
#   flag: special case land classes
#      URB - urban class (area is included in urban input data
#         and will not be transitioned by deltatron)
#      UNC - unclass (NODATA areas in image)
#      EXC - excluded (land class will be ignored by deltatron)
#   hex/rgb: hexidecimal or rgb (red, green, blue) output colors
#
#          pix, name,    flag,  hex/rgb, #comment
LANDUSE_CLASS= 0, Unclass , UNC  , 0X000000
LANDUSE_CLASS= 1, Urban  , URB  , 0X8b2323 #dark red
LANDUSE_CLASS= 2, Agric  ,      , 0Xffec8b #pale yellow
LANDUSE_CLASS= 3, Range  ,      , 0Xee9a49 #tan
LANDUSE_CLASS= 4, Forest ,      , 0X006400
LANDUSE_CLASS= 5, Water  , EXC  , 0X104e8b
LANDUSE_CLASS= 6, Wetland ,     , 0X483d8b
LANDUSE_CLASS= 7, Barren ,      , 0Xeec591


# D. GROWTH TYPE IMAGE OUTPUT CONTROL AND COLORTABLE
#
# From here you can control the output of the Z grid
# (urban growth) just after it is returned from the spr_spread()
# function. In this way it is possible to see the different types
# of growth that have occured for a particular growth cycle.
#
# VIEW_GROWTH_TYPES(YES/NO) provides an on/off
# toggle to control whether the images are generated.
#
# GROWTH_TYPE_PRINT_WINDOW provides a print window
# to control the amount of images created.
# format: <start_run>,<end_run>,<start_monte_carlo>,
#       <end_monte_carlo>,<start_year>,<end_year>
# for example:
# GROWTH_TYPE_PRINT_WINDOW=run1,run2,mc1,mc2,year1,year2
# so images are only created when
# run1<= current run <=run2 AND
# mc1 <= current monte carlo <= mc2 AND
# year1 <= currrent year <= year2
#
# 0 == first
VIEW_GROWTH_TYPES(YES/NO)=NO
GROWTH_TYPE_PRINT_WINDOW=0,0,0,0,1995,2020
```

```
PHASE0G_GROWTH_COLOR= 0xff0000 # seed urban area
PHASE1G_GROWTH_COLOR= 0X00ff00 # diffusion growth
PHASE2G_GROWTH_COLOR= 0X0000ff # NOT USED
PHASE3G_GROWTH_COLOR= 0Xffff00 # breed growth
PHASE4G_GROWTH_COLOR= 0Xffffff # spread growth
PHASE5G_GROWTH_COLOR= 0X00ffff # road influenced growth

#*********************************************************
#
# E. DELTATRON AGING SECTION
#
# From here you can control the output of the deltatron grid
# just before they are aged
#
# VIEW_DELTATRON_AGING(YES/NO) provides an on/off
# toggle to control whether the images are generated.
#
# DELTATRON_PRINT_WINDOW provides a print window
# to control the amount of images created.
# format:  <start_run>,<end_run>,<start_monte_carlo>,
#          <end_monte_carlo>,<start_year>,<end_year>
# for example:
# DELTATRON_PRINT_WINDOW=run1,run2,mc1,mc2,year1,year2
# so images are only created when
# run1<= current run <=run2 AND
# mc1 <= current monte carlo <= mc2 AND
# year1 <= currrent year <= year2
#
# 0 == first
VIEW_DELTATRON_AGING(YES/NO)=NO
DELTATRON_PRINT_WINDOW=0,0,0,0,1930,2020
DELTATRON_COLOR= 0x000000 # index 0 No or dead deltatron
DELTATRON_COLOR= 0X00FF00 # index 1 age = 1 year
DELTATRON_COLOR= 0X00D200 # index 2 age = 2 year
DELTATRON_COLOR= 0X00AA00 # index 3 age = 3 year
DELTATRON_COLOR= 0X008200 # index 4 age = 4 year
DELTATRON_COLOR= 0X005A00 # index 5 age = 5 year


# XIII. SELF-MODIFICATION PARAMETERS
#     SLEUTH is a self-modifying cellular automata. For more
#     information see our PROJECT GIGALOPOLIS web site
#     (www.ncgia.ucsb.edu/project/gig/About/abGrowth.htm)
#     and publications (and/or grep 'self modification' in code).
ROAD_GRAV_SENSITIVITY=0.01
SLOPE_SENSITIVITY=0.1
CRITICAL_LOW=0.97
CRITICAL_HIGH=1.3
#CRITICAL_LOW=0.0
#CRITICAL_HIGH=10000000000000.0
CRITICAL_SLOPE=21.0
BOOM=1.01
BUST=0.9
```

Source code of Prediction

```
# FILE: 'scenario file' for SLEUTH land cover transition model
#     (UGM  v3.0)
#     Comments start with #
#
#  I. Path Name Variables
# II. Running Status (Echo)
# III. Output ASCII Files
# IV. Log File Preferences
#  V. Working Grids
#  VI. Random Number Seed
# VII. Monte Carlo Iteration
#VIII. Coefficients
#    A. Coefficients and Growth Types
#    B. Modes and Coefficient Settings
# IX. Prediction Date Range
#  X. Input Images
# XI. Output Images
# XII. Colortable Settings
#    A. Date_Color
#    B. Non-Landuse Colortable
#    C. Land Cover Colortable
#    D. Growth Type Images
#    E. Deltatron Images
#XIII. Self Modification Parameters


# I.PATH NAME VARIABLES
#  INPUT_DIR: relative or absolute path where input image files and
#        (if modeling land cover) 'landuse.classes' file are
#        located.
#  OUTPUT_DIR: relative or absolute path where all output files will
#         be located.
#  WHIRLGIF_BINARY: relative path to 'whirlgif' gif animation program.
#          These must be compiled before execution.
INPUT_DIR=../Input/dhaka/
OUTPUT_DIR=../Output/dhaka_pre/
WHIRLGIF_BINARY=../Whirlgif/whirlgif


# II. RUNNING STATUS (ECHO)
#  Status of model run, monte carlo iteration, and year will be
#  printed to the screen during model execution.
ECHO(YES/NO)=yes


# III. Output Files
# INDICATE TYPES OF ASCII DATA FILES TO BE WRITTEN TO OUTPUT_DIRECTORY.
#
#  COEFF_FILE: contains coefficient values for every run, monte carlo
#         iteration and year.
#  AVG_FILE: contains measured values of simulated data averaged over
#         monte carlo iterations for every run and control year.
#  STD_DEV_FILE: contains standard diviation of averaged values
#          in the AVG_FILE.
#  MEMORY_MAP: logs memory map to file 'memory.log'
#  LOGGING: will create a 'LOG_#' file where # signifies the processor
#        number that created the file if running code in parallel.
#        Otherwise, # will be 0. Contents of the LOG file may be
#        described below.
WRITE_COEFF_FILE(YES/NO)=yes
WRITE_AVG_FILE(YES/NO)=yes
WRITE_STD_DEV_FILE(YES/NO)=yes
WRITE_MEMORY_MAP(YES/NO)=no
LOGGING(YES/NO)=YES


# IV. Log File Preferences
# INDICATE CONTENT OF LOG_# FILE (IF LOGGING == ON).
#  LANDCLASS_SUMMARY: (if landuse is being modeled) summary of input
#             from 'landuse.classes' file
#  SLOPE_WEIGHTS(YES/NO): annual slope weight values as effected
#             by slope_coeff
#  READS(YES/NO)= notes if a file is read in
#  WRITES(YES/NO)= notes if a file is written
#  COLORTABLES(YES/NO)= rgb lookup tables for all colortables generated
#  PROCESSING_STATUS(0:off/1:low verbosity/2:high verbosity)=
```

```
#   TRANSITION_MATRIX(YES/NO)= pixel count and annual probability of
#                  land class transitions
#   URBANIZATION_ATTEMPTS(YES/NO)= number of times an attempt to urbanize
#                     a pixel occurred
#   INITIAL_COEFFICIENTS(YES/NO)= initial coefficient values for
#                  each monte carlo
#   BASE_STATISTICS(YES/NO)= measurements of urban control year data
#   DEBUG(YES/NO)= data dump of igrid object and grid pointers
#   TIMINGS(0:off/1:low verbosity/2:high verbosity)= time spent within
#    each module. If running in parallel, LOG_0 will contain timing for
#    complete job.
LOG_LANDCLASS_SUMMARY(YES/NO)=yes
LOG_SLOPE_WEIGHTS(YES/NO)=no
LOG_READS(YES/NO)=no
LOG_WRITES(YES/NO)=no
LOG_COLORTABLES(YES/NO)=no
LOG_PROCESSING_STATUS(0:off/1:low verbosity/2:high verbosity)=1
LOG_TRANSITION_MATRIX(YES/NO)=yes
LOG_URBANIZATION_ATTEMPTS(YES/NO)=no
LOG_INITIAL_COEFFICIENTS(YES/NO)=no
LOG_BASE_STATISTICS(YES/NO)=yes
LOG_DEBUG(YES/NO)= yes
LOG_TIMINGS(0:off/1:low verbosity/2:high verbosity)=1


# V. WORKING GRIDS
# The number of working grids needed from memory during model execution is

# designated up front. This number may change depending upon modes. If
# NUM_WORKING_GRIDS needs to be increased, the execution will be exited
# and an error message will be written to the screen and to 'ERROR_LOG'
# in the OUTPUT_DIRECTORY. If the number may be decreased an optimal
# number will be written to the end of the LOG_0 file.
NUM_WORKING_GRIDS=4


# VI. RANDOM NUMBER SEED
# This number initializes the random number generator. This seed will be
# used to initialize each model run.
RANDOM_SEED=1


# VII. MONTE CARLO ITERATIONS
# Each model run may be completed in a monte carlo fashion.
# For CALIBRATION or TEST mode measurements of simulated data will be
# taken for years of known data, and averaged over the number of monte
# carlo iterations. These averages are written to the AVG_FILE, and
# the associated standard diviation is written to the STD_DEV_FILE.
# The averaged values are compared to the known data, and a Pearson
# correlation coefficient measure is calculated and written to the
# control_stats.log file. The input per run may be associated across
# files using the 'index' number in the files' first column.
#
MONTE_CARLO_ITERATIONS=110


# VIII. COEFFICIENTS
# The coefficients effect how the growth rules are applied to the data.
# Setting requirements:
#   *_START values >= *_STOP values
#   *_STEP values > 0
#   if no coefficient increment is desired:
#   *_START == *_STOP
#   *_STEP == 1
# For additional information about how these values affect simulated
# land cover change see our publications and PROJECT GIGALOPOLIS
# site: (www.ncgia.ucsb.edu/project/gig/About/abGrowth.htm).
# A. COEFFICIENTS AND GROWTH TYPES
#   DIFFUSION: affects SPONTANEOUS GROWTH and search distance along the
#         road network as part of ROAD INFLUENCED GROWTH.
#   BREED: NEW SPREADING CENTER probability and affects number of ROAD
#        INFLUENCED GROWTH attempts.
#   SPREAD: the probabilty of ORGANIC GROWTH from established urban
#        pixels occuring.
#   SLOPE_RESISTANCE: affects the influence of slope to urbanization. As
#             value increases, the ability to urbanize
#             ever steepening slopes decreases.
#   ROAD_GRAVITY: affects the outward distance from a selected pixel for
#            which a road pixel will be searched for as part of
#            ROAD INFLUENCED GROWTH.
```

105

```
#
# B. MODES AND COEFFICIENT SETTINGS
#    TEST: TEST mode will perform a single run through the historical
#        data using the CALIBRATION_*_START values to initialize
#        growth, complete the MONTE_CARLO_ITERATIONS, and then conclude
#        execution. GIF images of the simulated urban growth will be
#        written to the OUTPUT_DIRECTORY.
#    CALIBRATE: CALIBRATE will perform monte carlo runs through the
#        historical data using every combination of the
#        coefficient values indicated. The CALIBRATION_*_START
#        coefficient values will initialize the first run. A
#        coefficient will then be increased by its *_STEP value,
#        and another run performed. This will be repeated for all
#        possible permutations of given ranges and increments.
#    PREDICTION: PREDICTION will perform a single run, in monte carlo
#        fashion, using the PREDICTION_*_BEST_FIT values
#        for initialization.
```

CALIBRATION_DIFFUSION_START= 1
CALIBRATION_DIFFUSION_STEP= 1
CALIBRATION_DIFFUSION_STOP= 1

CALIBRATION_BREED_START=   36
CALIBRATION_BREED_STEP=   1
CALIBRATION_BREED_STOP=   36

CALIBRATION_SPREAD_START= 100
CALIBRATION_SPREAD_STEP=   1
CALIBRATION_SPREAD_STOP=   100

CALIBRATION_SLOPE_START=   1
CALIBRATION_SLOPE_STEP=   1
CALIBRATION_SLOPE_STOP=   1

CALIBRATION_ROAD_START=   56
CALIBRATION_ROAD_STEP=   1
CALIBRATION_ROAD_STOP=   56

PREDICTION_DIFFUSION_BEST_FIT= 1
PREDICTION_BREED_BEST_FIT= 36
PREDICTION_SPREAD_BEST_FIT= 100
PREDICTION_SLOPE_BEST_FIT= 1
PREDICTION_ROAD_BEST_FIT= 56

```
# IX. PREDICTION DATE RANGE
# The urban and road images used to initialize growth during
# prediction are those with dates equal to, or greater than,
# the PREDICTION_START_DATE. If the PREDICTION_START_DATE is greater
# than any of the urban dates, the last urban file on the list will be
# used. Similarly, if the PREDICTION_START_DATE is greater
# than any of the road dates, the last road file on the list will be
# used. The prediction run will terminate at PREDICTION_STOP_DATE.
#
```
PREDICTION_START_DATE=2014
PREDICTION_STOP_DATE=2030

```
# X. INPUT IMAGES
# The model expects grayscale, GIF image files with file name
# format as described below. For more information see our
# PROJECT GIGALOPOLIS web site:
# (www.ncgia.ucsb.edu/project/gig/About/dtInput.htm).
#
# IF LAND COVER IS NOT BEING MODELED: Remove or comment out
# the LANDUSE_DATA data input flags below.
#
#   < > = user selected fields
#   [< >] = optional fields
#
# Urban data GIFs
#  format:  <location>.urban.<date>.[<user info>].gif
#
#
```
URBAN_DATA= dhaka.urban.1989.gif
URBAN_DATA= dhaka.urban.1999.gif
URBAN_DATA= dhaka.urban.2009.gif
URBAN_DATA= dhaka.urban.2014.gif

```
#
# Road data GIFs
# format: <location>.roads.<date>.[<user info>].gif
#
ROAD_DATA= dhaka.roads.1989.gif
ROAD_DATA= dhaka.roads.1999.gif
ROAD_DATA= dhaka.roads.2009.gif
ROAD_DATA= dhaka.roads.2014.gif
#
# Landuse data GIFs
# format: <location>.landuse.<date>.[<user info>].gif
#
LANDUSE_DATA= dhaka.landuse.1989.gif
LANDUSE_DATA= dhaka.landuse.2014.gif
#
# Excluded data GIF
# format: <location>.excluded.[<user info>].gif
#
EXCLUDED_DATA= dhaka.excluded.gif
#
# Slope data GIF
# format: <location>.slope.[<user info>].gif
#
SLOPE_DATA= dhaka.slope.gif
#
# Background data GIF
# format:  <location> hillshade.[<user info>].gif
#
#BACKGROUND_DATA= dhaka.hillshade.gif
BACKGROUND_DATA= dhaka.hillshade.water.gif

# XI. OUTPUT IMAGES
#  WRITE_COLOR_KEY_IMAGES: Creates image maps of each colortable.
#              File name format: 'key_[type]_COLORMAP'
#                    where [type] represents the colortable.
#  ECHO_IMAGE_FILES: Creates GIF of each input file used in that job.
#          File names format: 'echo_of_[input_filename]'
#              where [input_filename] represents the input name.
#  ANIMATION: if whirlgif has been compiled, and the WHIRLGIF_BINARY
#          path has been defined, animated gifs begining with the
#          file name 'animated' will be created in PREDICT mode.
WRITE_COLOR_KEY_IMAGES(YES/NO)=yes
ECHO_IMAGE_FILES(YES/NO)=yes
ANIMATION(YES/NO)= yes

# XII. COLORTABLE SETTINGS
#  A. DATE COLOR SETTING
#    The date will automatically be placed in the lower left corner
#    of output images. DATE_COLOR may be designated in with red, green,
#    and blue values (format: <red_value, green_value, blue_value> )
#    or with hexadecimal begining with '0X' (format: <0X######> ).
#default DATE_COLOR= 0XFFFFFF white
DATE_COLOR=    0XFFFFFF #white

# B. URBAN (NON-LANDUSE) COLORTABLE SETTINGS
#    1. URBAN MODE OUTPUTS
#      TEST mode: Annual images of simulated urban growth will be
#              created using SEED_COLOR to indicate urbanized areas.

#      CALIBRATE mode: Images will not be created.
#      PREDICT mode: Annual probability images of simulated urban
#              growth will be created using the PROBABILITY
#              _COLORTABLE. The initializing urban data will be
#              indicated by SEED_COLOR.
#
#   2. COLORTABLE SETTINGS
#      SEED_COLOR: initializing and extrapolated historic urban extent

#      WATER_COLOR: BACKGROUND_DATA is used as a backdrop for

#              simulated urban growth. If pixels in this file
#              contain the value zero (0), they will be filled
#              with the color value in WATER_COLOR. In this way,
#              major water bodies in a study area may be included
#              in output images.
#SEED_COLOR= 0XFFFF00 #yellow
```

107

```
SEED_COLOR= 249, 209, 110 #pale yellow
#WATER_COLOR= 0X0000FF # blue
WATER_COLOR= 20, 52, 214 # royal blue


#   3. PROBABILITY COLORTABLE FOR URBAN GROWTH
#     For PREDICTION, annual probability images of urban growth
#     will be created using the monte carlo iterations. In these
#     images, the higher the value the more likely urbanizaion is.
#     In order to interpret these 'continuous' values more easily
#     they may be color classified by range.
#
#     If 'hex' is not present then the range is transparent.
#     The transparent range must be the first on the list.
#     The max number of entries is 100.
#      PROBABILITY_COLOR: a color value in hexadecimal that indicates
#                a probability range.
#        low/upper: indicate the boundaries of the range.
#
#           low, upper,  hex,  (Optional Name)
PROBABILITY_COLOR= 0,    50,       , #transparent
PROBABILITY_COLOR=  50,   60, 0X005A00, #0, 90,0 dark green
PROBABILITY_COLOR=  60,   70, 0X008200, #0,130,0
PROBABILITY_COLOR=  70,   80, 0X00AA00, #0,170,0
PROBABILITY_COLOR=  80,   90, 0X00D200, #0,210,0
PROBABILITY_COLOR=  90,   95, 0X00FF00, #0,255,0 light green
PROBABILITY_COLOR=  95, 100, 0X8B0000, #dark red


# C. LAND COVER COLORTABLE
# Land cover input images should be in grayscale GIF image format.
# The 'pix' value indicates a land class grayscale pixel value in
# the image. If desired, the model will create color classified
# land cover output. The output colortable is designated by the
# 'hex/rgb' values.
#   pix: input land class pixel value
#   name: text string indicating land class
#   flag: special case land classes
#       URB - urban class (area is included in urban input data
#           and will not be transitioned by deltatron)
#       UNC - unclass (NODATA areas in image)
#       EXC - excluded (land class will be ignored by deltatron)
#   hex/rgb: hexidecimal or rgb (red, green, blue) output colors
#
#         pix, name,    flag,  hex/rgb, #comment
LANDUSE_CLASS= 0, Unclass , UNC  , 0X000000
LANDUSE_CLASS= 1, Urban  , URB  , 0X8b2323 #dark red
LANDUSE_CLASS= 2, Agric  ,      , 0Xffec8b #pale yellow
LANDUSE_CLASS= 3, Range  ,      , 0Xee9a49 #tan
LANDUSE_CLASS= 4, Forest ,      , 0X006400
LANDUSE_CLASS= 5, Water  , EXC  , 0X104e8b
LANDUSE_CLASS= 6, Wetland ,     , 0X483d8b
LANDUSE_CLASS= 7, Barren ,      , 0Xeec591


# D. GROWTH TYPE IMAGE OUTPUT CONTROL AND COLORTABLE
#
# From here you can control the output of the Z grid
# (urban growth) just after it is returned from the spr_spread()
# function. In this way it is possible to see the different types
# of growth that have occured for a particular growth cycle.
#
# VIEW_GROWTH_TYPES(YES/NO) provides an on/off
# toggle to control whether the images are generated.
#
# GROWTH_TYPE_PRINT_WINDOW provides a print window
# to control the amount of images created.
# format:  <start_run>,<end_run>,<start_monte_carlo>,
#        <end_monte_carlo>,<start_year>,<end_year>
# for example:
# GROWTH_TYPE_PRINT_WINDOW=run1,run2,mc1,mc2,year1,year2
# so images are only created when
# run1<= current run <=run2 AND
# mc1 <= current monte carlo <= mc2 AND
# year1 <= currrent year <= year2
#
# 0 == first
VIEW_GROWTH_TYPES(YES/NO)=NO
GROWTH_TYPE_PRINT_WINDOW=0,0,0,0,1995,2020
```

```
PHASE0G_GROWTH_COLOR= 0xff0000 # seed urban area
PHASE1G_GROWTH_COLOR= 0X00ff00 # diffusion growth
PHASE2G_GROWTH_COLOR= 0X0000ff # NOT USED
PHASE3G_GROWTH_COLOR= 0Xffff00 # breed growth
PHASE4G_GROWTH_COLOR= 0Xffffff # spread growth
PHASE5G_GROWTH_COLOR= 0X00ffff # road influenced growth


#*********************************************************
#
# E. DELTATRON AGING SECTION
#
# From here you can control the output of the deltatron grid
# just before they are aged
#
# VIEW_DELTATRON_AGING(YES/NO) provides an on/off
# toggle to control whether the images are generated.
#
# DELTATRON_PRINT_WINDOW provides a print window
# to control the amount of images created.
# format: <start_run>,<end_run>,<start_monte_carlo>,
#        <end_monte_carlo>,<start_year>,<end_year>
# for example:
# DELTATRON_PRINT_WINDOW=run1,run2,mc1,mc2,year1,year2
# so images are only created when
# run1<= current run <=run2 AND
# mc1 <= current monte carlo <= mc2 AND
# year1 <= currrent year <= year2
#
# 0 == first
VIEW_DELTATRON_AGING(YES/NO)=NO
DELTATRON_PRINT_WINDOW=0,0,0,0,1930,2020
DELTATRON_COLOR= 0x000000 # index 0 No or dead deltatron
DELTATRON_COLOR= 0X00FF00 # index 1 age = 1 year
DELTATRON_COLOR= 0X00D200 # index 2 age = 2 year
DELTATRON_COLOR= 0X00AA00 # index 3 age = 3 year
DELTATRON_COLOR= 0X008200 # index 4 age = 4 year
DELTATRON_COLOR= 0X005A00 # index 5 age = 5 year


# XIII. SELF-MODIFICATION PARAMETERS
#       SLEUTH is a self-modifying cellular automata. For more
#       information see our PROJECT GIGALOPOLIS web site
#       (www.ncgia.ucsb.edu/project/gig/About/abGrowth.htm)
#       and publications (and/or grep 'self modification' in code).
ROAD_GRAV_SENSITIVITY=0.01
SLOPE_SENSITIVITY=0.1
CRITICAL_LOW=0.97
CRITICAL_HIGH=1.3
#CRITICAL_LOW=0.0
#CRITICAL_HIGH=10000000000000.0
CRITICAL_SLOPE=21.0
BOOM=1.01
BUST=0.9
```

--------------- x-----------------

109